The Dynamic Cutting of Metals.

Dissertation submitted to the University of Cambridge for the Degree of Doctor of Philosophy.

by

J.D. Smith.

St. Johns. July 1962.

Preface.

The work described in this dissertation was designed to resolve apparent discrepancies in previously published work on vibrating cutting forces. It was also intended to clarify ideas on the cutting process preparatory to measurements on the effect of vibration on tool wear.

The experiments were carried out at the Engineering Laboratory of the University of Cambridge, the Mechanical Engineering Department of Birmingham University and the Staveley Research Department under the supervision of Professor S.A. Tobias.

Thanks are due to the Department of Scientific and Industrial Research and the Staveley Research Department for their support of this project, to Professor Tobias for his guidance and help, and to the staff at Cambridge, Birmingham and Staveley for their advice and assistance.

The material presented in this dissertation is original except where reference has been made to the work of others. None of it has been, or is being concurrently, presented to any other University.

I hereby give permission for a copy of this dissertation, or any part of it, to be made for any applicant at any time provided that the applicant make suitable acknowledgment of any use he may make of it.

CONTENTS.

Figures.

1. Apparatus used by Doi and Kato.
2. Forces observed by Doi and Kato.
3. Derived time lags of cutting forces by Doi and Kato.
4. Forces observed by Tashlickii.
5. Forces observed by Holken.
6. Stability band envelope.
7. Experimentally determined stability chart (after Tobias).
8. Sketch of experimental rig.
9. Sketch of Dynamometer.
10. View of Dynamometer.
11. Torsional vibration plot.
12. Machine dynamic response.
13. Plot of force against chip thickness for the steady state.
14. Diagrams showing type of cut.
15. Actual test record - low frequency.
16. Actual test record - high frequency.

FIGS. 17-26 Test Results.

17. 50 ft./min. .135" x .005". Carbide tool. 10° rake.
18. " " " x .010" " "
19. 120ft./min. .075" x .005" " "
20. " " " x .015" " "

41. Individual phase angles at 30 c.p.s., 60ft./min.

42. " " " " 25 " "

43. " " " " 135 " 300ft./min.

44. Ratio of peak to mean cutting forces.

45. Time constants for force stabilisation.

46. Cutting force diagram after Merchant.

47. Plot of γ and sec. γ.

48. Qualitative sketch of temperature effect.

49. Diagram for built-up edge effect.

50. Torsional response of machine.

51. Qualitative lag effects due to torsion.

52. Phase measurement diagram.

53. Lissajous figure phase measurement.

54. Diagram for viscosity effect.

55. Sketch of built-up edge.

56. Relaxation grid.

57. Temperature varations in tool.

1. Summary.

Prediction of regenerative machine tool chatter requires a knowledge of the cutting forces existing under vibration conditions. Previous direct experimental work has been very limited in its range and has given results which contradicted those derived from observations on regenerative chatter.

A description of suitable experimental rigs and the results obtained from these rigs are given. The results show that there are large phase changes of cutting force relative to chip thickness when vibrating. A simplified criterion is given for assessing machining stability and it is shown that the observed phase changes will greatly affect machining stability; in some cases machining will be stable regardless of machine damping.

The requirements for machining stability contradict those for long cutting tool life so a compromise must be reached in practical cases.

The cutting process is not, in general, amenable to quantitative analysis but theories have been put forward to explain the observed force phase and amplitude changes. There is a reasonable qualitative correlation between experiment and theory for most of the experimental range.

Temperature estimates involved in phase change estimates show that there are large tool temperature variations under chatter or milling conditions. These temperature variations and the consequent thermal stresses are likely to cause tool failure with brittle materials such as carbides.

The results obtained under steady cutting conditions such as lathe turning have been extended to intermittent cuts as encountered in milling. The tests show that there is no fundamental difference between steady and intermittent cuts.

Suggestions are put forward for the large amount of further work required to clarify the mechanisms of the cutting process and to extend cutting force knowledge for chatter prevention.

2. Introduction.

Metal cutting processes on conventional machine tools are subject to two types of vibration, forced and self excited. The forced vibrations are usually of fairly small amplitude; they are excited by unbalance of shafts, irregular gears or the engagement of individual cutter teeth. The causes of this type of vibration are well known and the cures are relatively easy to apply, either by reduction of the exciting force or separation of the relevant machine resonant frequency from the exciting frequency.

The self-excited vibrations are much more troublesome. The amplitudes built up are large, of the order of ten thousandths of an inch rather than of one tenth of a "thou" and instability cannot be prevented in general simply by altering frequencies.

There are two main types of self-excited vibrations, usually called "chatter". The simple type depends on a mechanism basically similar to the stick-slip mechanism encountered with dry friction; this type usually occurs at fairly high frequencies of the order of a kilocycle per second. Arnold (1) investigated this type of chatter which is not usually of industrial importance since it is relatively

easy to cure and does not generate sufficient force to break a machine tool through it may ruin a brittle carbide cutter.

The important chatter is the type usually called regenerative machine tool chatter. This type occurs at low frequencies, typically 20-100 c/s. with large amplitudes. In addition to cutter breakage and possibly machine breakage, this type of chatter leaves deep patterns on the workpiece which is then scrap.

The simplest type of regenerative chatter occurs with one degree of freedom only, as indicated in Figure 14(a), in which the workpiece is considered as vibration-free while the tool can vibrate only perpendicular to the workpiece velocity. Tool vibration thus gives as change in chip thickness but no change in cutting velocity.

It is only comparatively recently that there has been understanding of the basic mechanism of regenerative chatter following the work of Tobias and Fishwick (2) in Britain and Tlusty and Polacek (3) in Czechoslovakia: Appendix I gives a simplified analysis of the effect; this approach to the analysis gives a physical picture of the mechanism, showing how the wave left on the workpiece surface by the previous cut, forces the machine system at the resonant frequency, leaving a wave on the

freshly cut surface.

Solution of chatter problems, whether carried out analytically (2 & 3), graphically (4) or by analogue computer is basically the solution of a differential equation in which the force on the machine is equated to the cutting force. The force on the machine, in terms of machine displacement, can be determined experimentally by straightforward vibration tests but very little is known about dynamic cutting forces since their experimental measurement is very difficult and there is no reliable theory to predict cutting forces.

The work described in this thesis is an attempt to determine dynamic forces and to understand the mechanisms which give observed effects.

3. Previous Work.

3.1 Classification.

The research on dynamic cutting forces falls into two categories.

(i) Direct measurement of the cutting forces.

(ii) Indirect evidence derived from regenerative chatter results.

3.2 Direct Measurements.

The original experiments to measure the cutting forces directly were made by Doi and Kato (5); a sketch of their apparatus is shown in Figure 1. The workpiece is attached to a long flexible shaft held in a chuck and supported at the free end by a steady which prevents vertical motion of the workpiece but allows a rotating cam to oscillate the workpiece horizontally. The fixed cutting tool then cuts a chip with an approximately sinusoidal thickness variation. The surface cutting speed for these tests was 3.4 ft./min. The cam oscillated the workpiece and hence varied the chip thickness at 1.4 c/s. The small elastic deflections of the tool were measured optically to give the normal and tangential cutting forces.

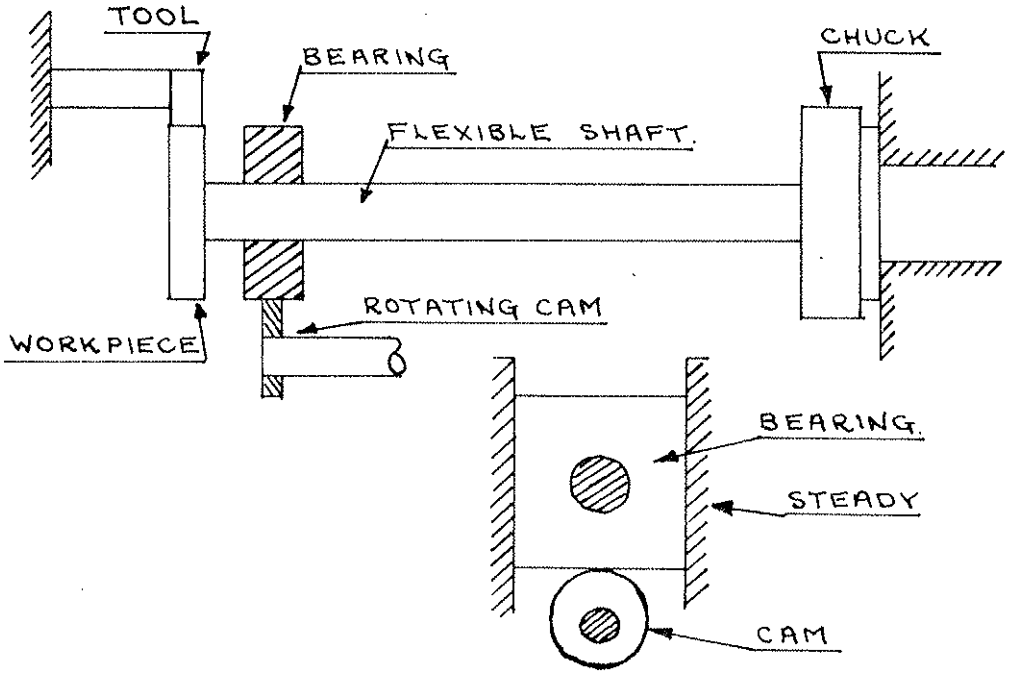

FIG. 1. SKETCH OF APPARATUS USED BY DOI AND KATO (5).

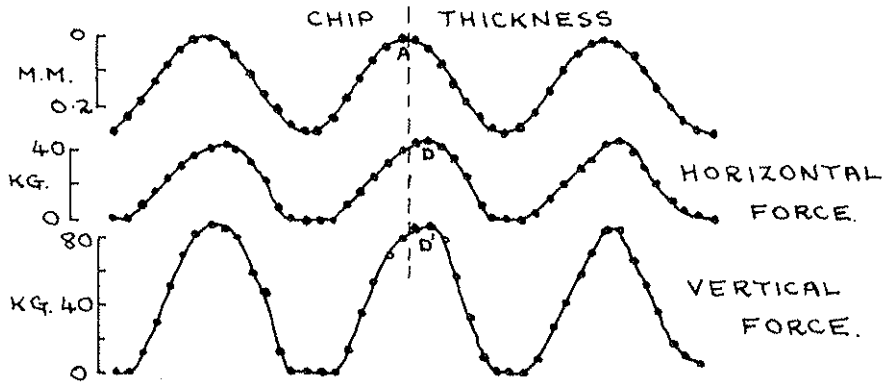

FIG. 2. WORKPIECE OSCILLATIONS AND RESULTING CUTTING FORCES, AFTER DOI AND KATO (5).

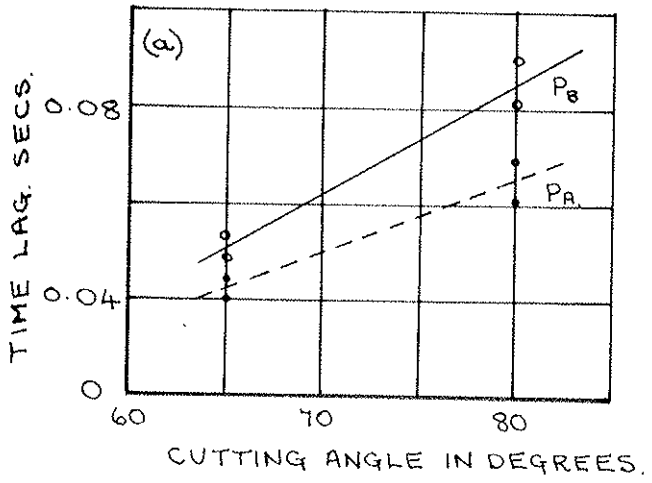

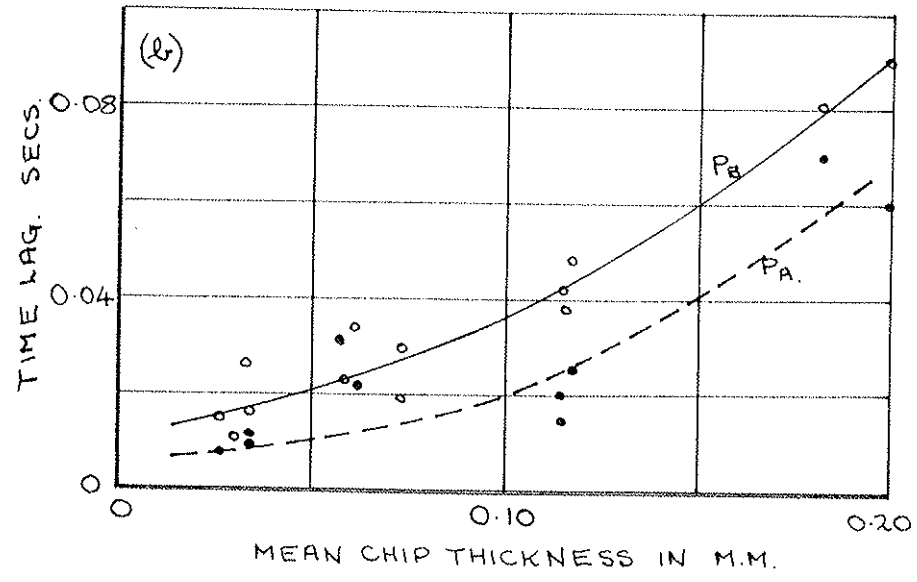

FIG. 3 LAG OF CUTTING FORCES BEHIND CHIP THICKNESS AS A FUNCTION OF CUTTING ANGLE AND CHIP THICKNESS. AFTER DOI & KATO (5)

P_A NORMAL THRUST P_B TANGENTIAL THRUST.

Results obtained from this rig are given in Figure 2, which shows a record of the chip thickness, the normal cutting force and the tangential cutting force variations while oscillating the workpiece. The figure indicates that the maximum values of the forces at points D and D' do not occur at the same time as the maximum value of chip thickness at point A. The time interval between A and D or D' is referred to as the inherent time lag of the normal or tangential cutting force respectively.

The derived values for this inherent time lag are given in Figures 3(a) and (b), plotted as functions of the cutting angle and the chip thickness. The observed time lag increases with chip thickness and cutting angle.

Similar Russian work by N.I. Tashlickii (6) was carried out at higher cutting speeds but low frequencies using a rigidly mounted tool and an eccentrically mounted workpiece. Results obtained from this rig are shown in Figure 4 which is again a plot of the cutting forces and chip thickness during vibration.

A typical result obtained by W. Hölken (7) is shown in Figure 5. The figure represents the variations of chip thickness, normal force and tangential force as a function of time. These results, like those of Tashlickii, confirm Doi and Kato's observations of a time lag of force relative to chip thickness.

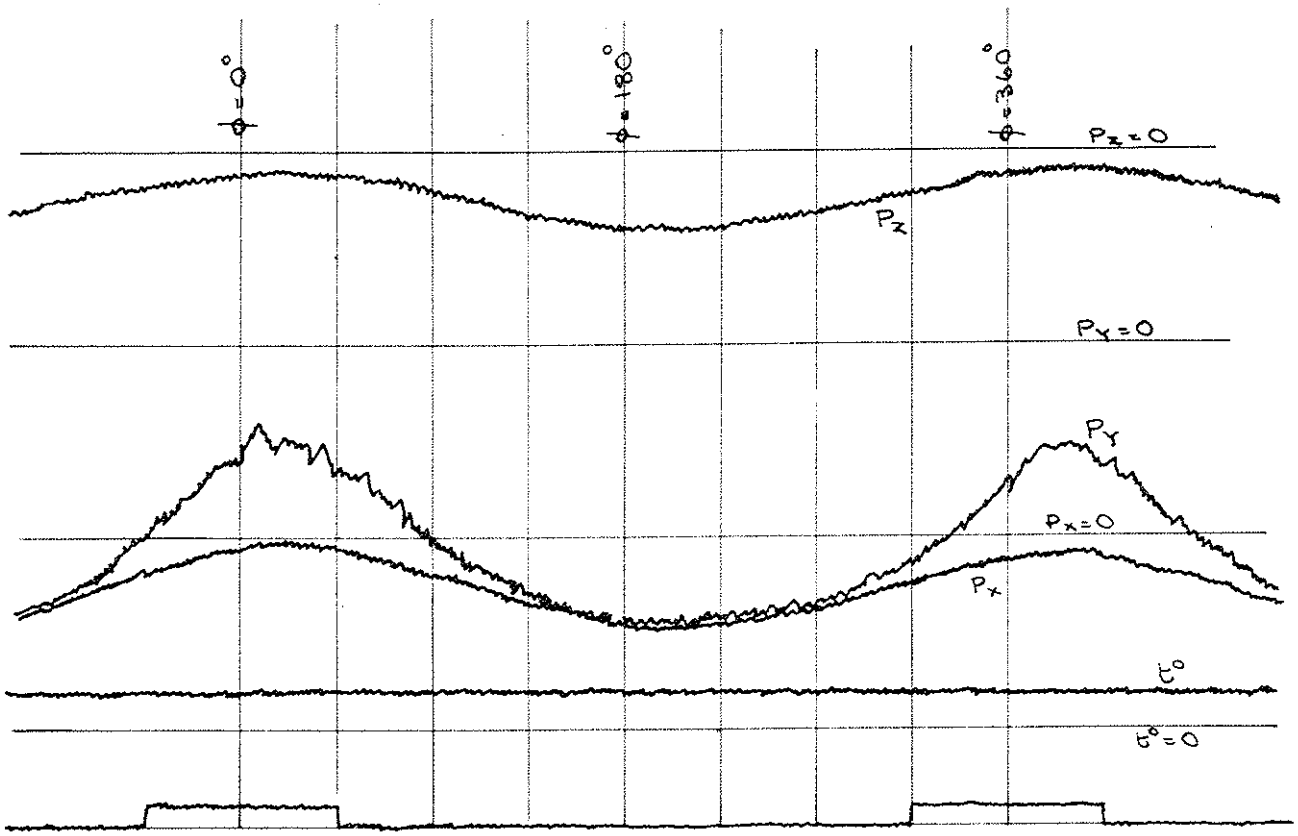

FIG. 4. LAG OF CUTTING FORCES BEHIND CHIP THICKNESS.

AN ECCENTRIC WORKPIECE WAS USED. THE LOWER TRACE GIVES THE POSITION OF MINIMUM CHIP THICKNESS. THE TANGENTIAL THRUST P_z, THE NORMAL THRUST P_Y AND THE FEED THRUST P_x ARE SHOWN DURING ONE CYCLE. THE TOOL-CHIP INTERFACE TEMPERATURE t° DID NOT VARY. AFTER TASHLICKII (6).

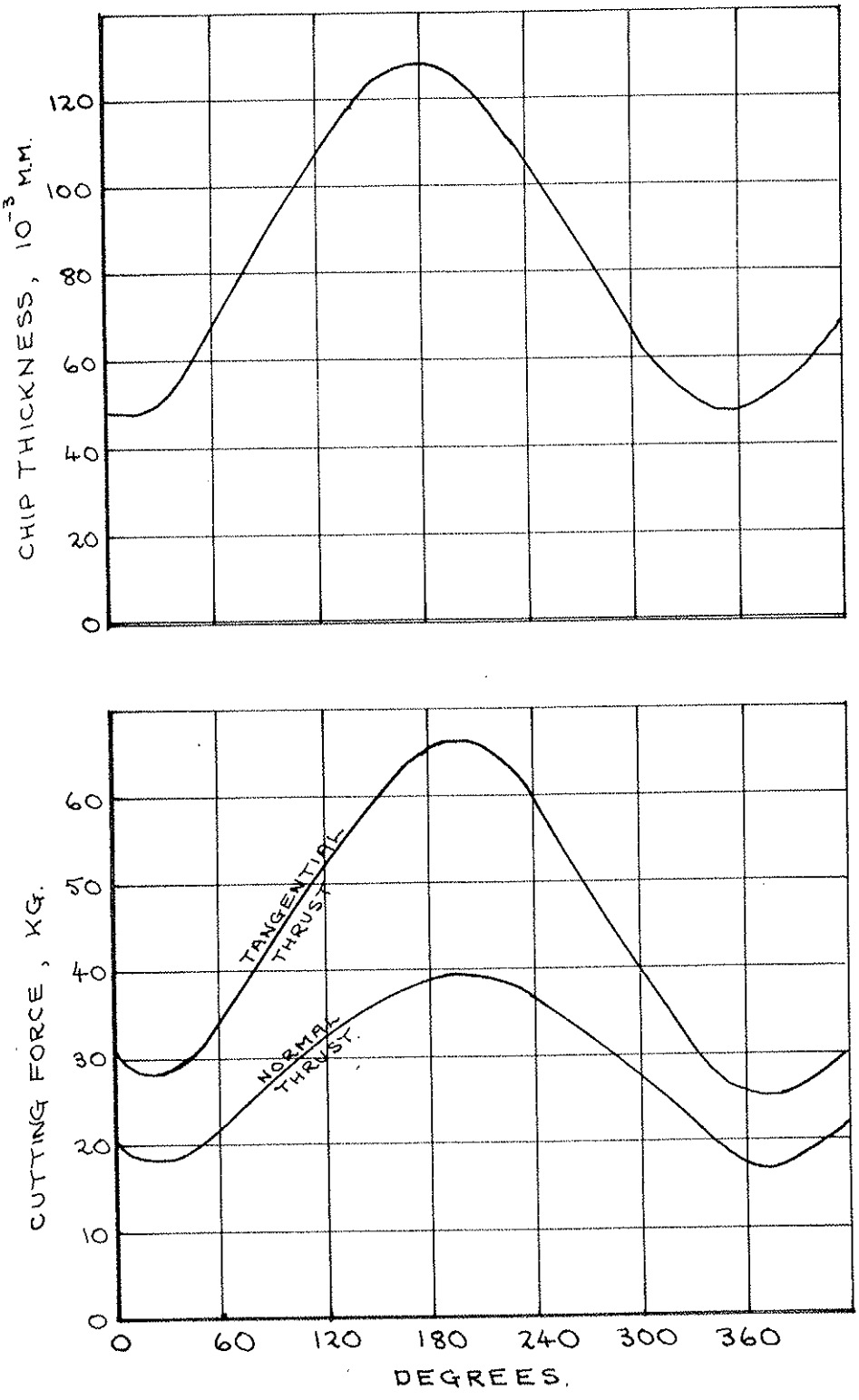

FIG. 5. CUTTING FORCE LAGS, AFTER HOLKEN (7).

THE TOP FIGURE SHOWS THE CHIP THICKNESS WHILE THE LOWER FIGURE SHOWS THE CORRESPONDING FORCES.

3.3 Indirect Evidence.

In their work on regenerative chatter S.A.Tobias and W.Fishwick (2) treat phase effects in a completely different manner. Their theory is based on the assumption that the cutting force is a function of feed velocity as well as of chip thickness, and it is easily shown that this is mathematically equivalent to postulating a lag or lead of force relative to displacement.

Evidence concerning the sign of the phase angle between chip thickness and thrust variations is derived from the form of stability charts, describing the stability of, say, a face milling process (Tobias 8). A chart of this type shows those speed ranges at which a certain depth of cut (or chip width) is stable or unstable. It can be obtained experimentally or theoretically and its form for drilling and face milling is well established. The stability chart is divided into two regions by the stability band envelope. For values of chip width less than the value given by this envelope the cutting process is unconditionally stable. In the region above the envelope the cutting process may be stable or unstable, depending on the rotational speed of the tool.

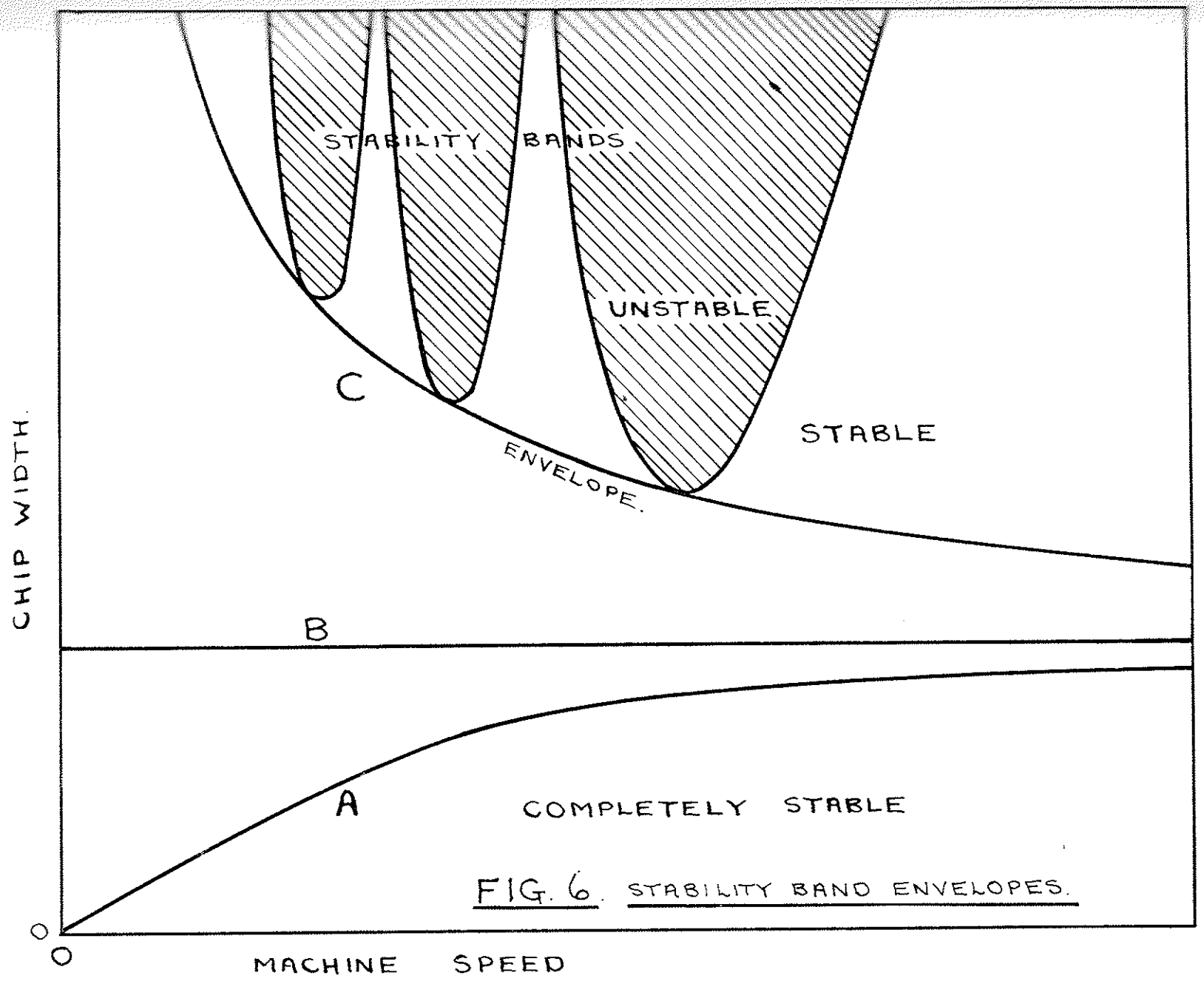

FIG. 6. STABILITY BAND ENVELOPES.

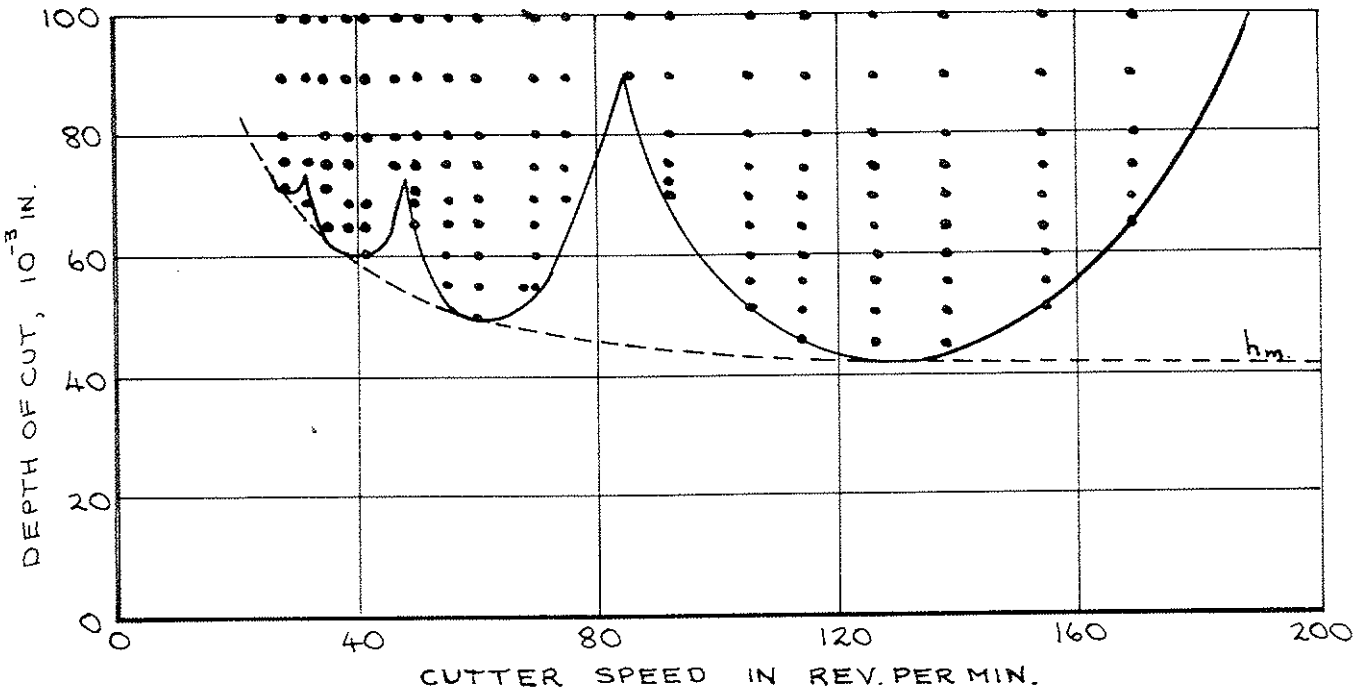

FIG. 7. EXPERIMENTALLY DETERMINED STABILITY CHART.

THE POINTS MARKED CORRESPOND TO CONDITIONS WHERE CHATTER AROSE. THE POINTS FALL INTO BANDS LYING ABOVE THE ENVELOPE h_m. AFTER TOBIAS. (8)

It can be shown that the shape of the stability envelope is an indication of the phase relationship between cutting force and chip thickness variation. When the cutting force lags the displacement (in accordance with Doi and Kato's observation) then the shape of the envelope is of the form indicated by curve A in Figure 6. A leading cutting force results in an envelope of the type of curve C, curve B being the transitional case when force and displacement are in phase.

An experimentally determined stability chart is shown in Figure 7. In that figure unstable combinations of the depth of cut and the rotational speed are marked by dots. Comparing this figure with Figure 6, it is clear that the form of the stability envelope leads to the conclusion that the cutting force must have been leading the dynamic displacement.

3.4 Correlation.

These two groups of tests have led to conflicting results; the first group measured a force lag while the regenerative chatter tests deduced a force lead. Since this phase effect can be of dominating importance in machine tool chatter it is necessary that more should be learnt with a view to improving chatter prediction and machine performance.

4. Main Tests.

4.1 Apparatus.

Previous experiments on dynamic forces have been restricted to a narrow range of cutting conditions and oscillation frequencies. To obtain a clear picture of the mechanisms involved it was necessary to experiment over a wide range of conditions and frequencies; the rig sketched in Figure 8 was designed for this.

Although lathe turning was being investigated it was found more convenient to carry out the tests by mounting specimens on the arbor of a rigid knee type horizontal milling machine while the cutting tool, with its associated suspension, damping, excitation and measuring systems, was mounted on the miller table. This set-up gave high machine rigidity and ample room on the table for apparatus.

The cutting tool was held on the dynamometer by straps which for clarity are not shown in the sketch. The dynamometer was supported by vertical leaf springs which allowed it to move horizontally but not vertically so that tool movement gave chip thickness variation but no change in surface cutting speed. Under these conditions, since mechanical damping in the leaf springs was very low, violent chatter occurred at nearly all cutting conditions. It was found in practice impossible to use

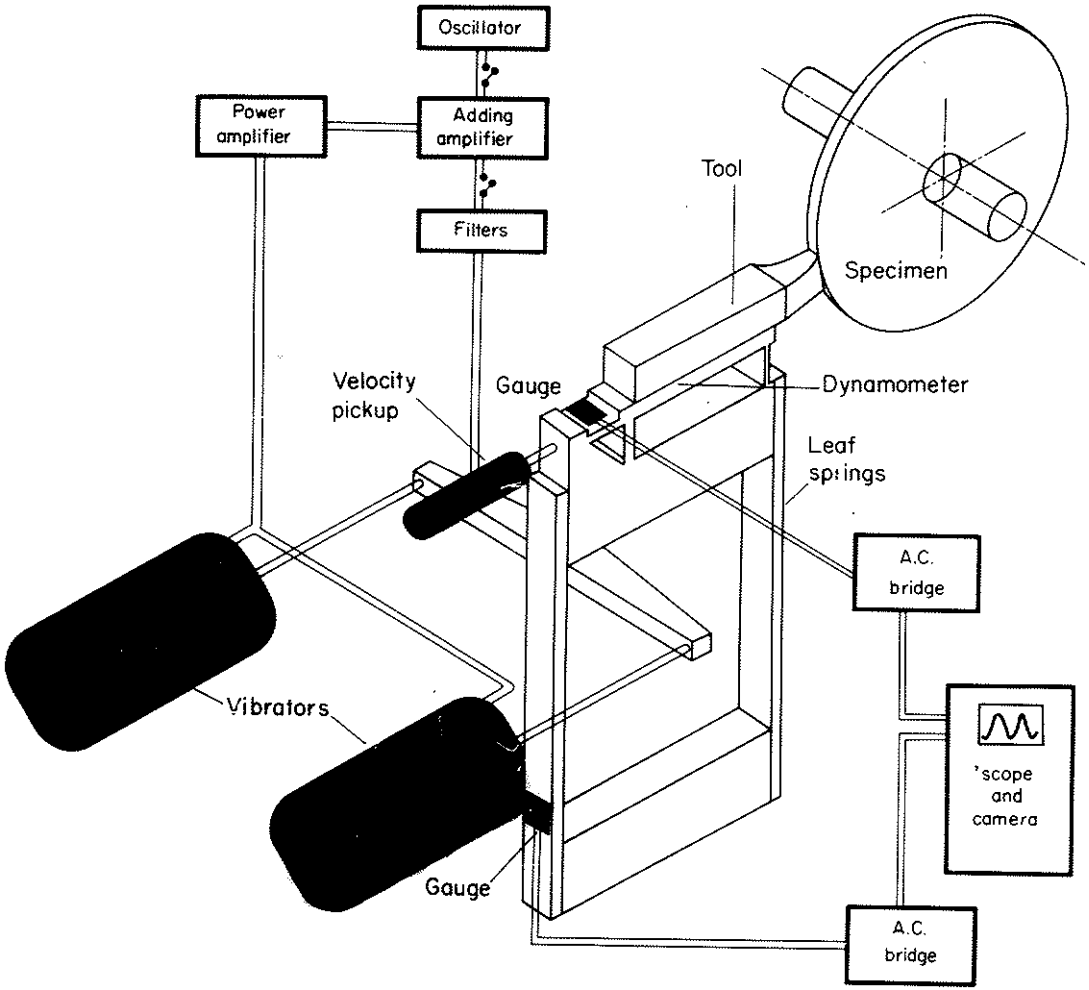

FIG. 8. EXPERIMENTAL RIG.

any passive damping system such as dashpot, rotary silicone damper or eddy current method since the combination of high frequency, low amplitude and large forces made any passive system inoperative. An active system was finally adopted, using a standard velocity pick-up whose signal was amplified and fed into electromagnetic vibrators arranged to oppose the motion. An additional signal from a separate oscillator was added to force the test vibration required; this composite system in which the vibration generators both damp out chatter and force the required oscillations, required far less power than two separate systems. Under normal experimental conditions the generators can excite vibrations of over 20 "thou" peak to peak amplitude over a frequency range from 5 to 400 cycles per second; this range can easily be extended. The circuits are arranged so that any level of damping can be switched in or out instantaneously during a test run and the required oscillation can similarly be switched during a run.

The damping circuit forms a closed servo power loop in which instability is likely unless suitable filters are inserted; in practice instability at high frequencies limits the damping to about half critical damping at the dynamometer resonance at 170 cycles per second.

For the majority of the tests a two-dimensional light-weight strut dynamometer was used; Figure 9 gives details of the dynamometer while Figure 10 gives a view of the dynamometer in situ. The cutting forces act on short struts in compression: two vertical struts take the tangential cutting force and the single horizontal strut carries the horizontal or normal cutting force. The combination of a tool and support of low mass with struts of high stiffness of 2×10^6 lb./inch, gives a natural frequency of above 6000 c/s.

This type of dynamometer was chosen for the tests because it has a low total mass, high rigidity, low frontal area, low inertia corrections and easy damping control by use of the side plates, which in addition to carrying the electrical connections and protecting the strain gauges give friction damping of the head. This type of dynamometer is not suitable for steady state force determination as heat from the cutting process slowly raises the temperature of the live gauges and gives a zero drift.

4.2 Measurements.

The vertical and horizontal forces were measured using conventional wire strain gauges on the dynamometer struts while the horizontal displacement of the tool was measured using similar

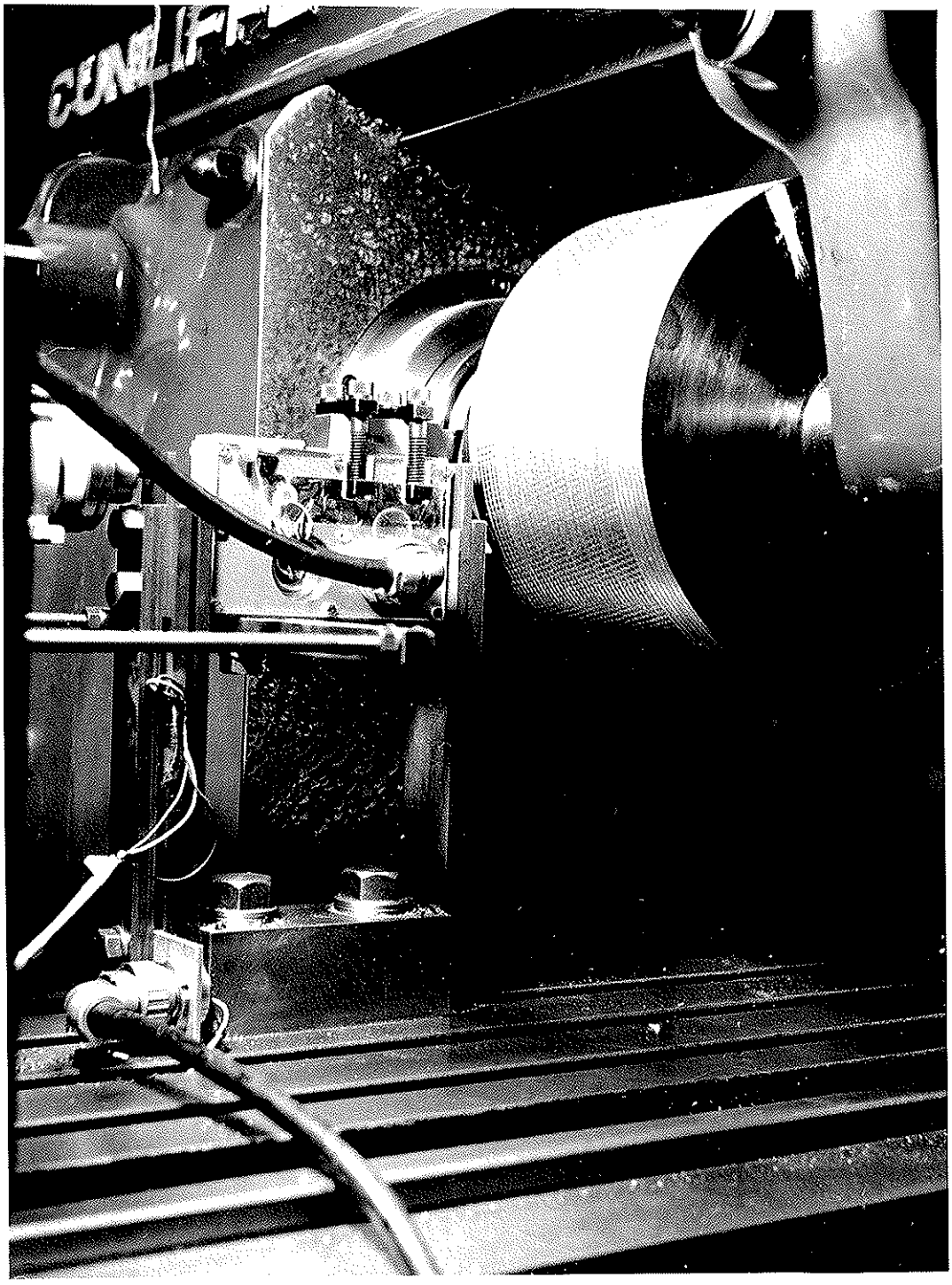

FIG. 10. VIEW OF DYNAMOMETER.

strain gauges on the vertical leaf springs. The gauge strains were measured using standard sensitive alternating current strain gauge bridges. The carrier frequency of 6 kilocycles per second, allowed measurement up to frequencies of 1 kilocycle; the sensitivity range allowed measurement of forces as low as 1 pound and deflections of one hundredth of a thou; the maximum capacity of the dynamometer was approximately one ton and deflections up to 20 thou. could be measured.

A standard seismic torsional pick-up attached to the end of the arbor gave continuous monitoring of any torsional vibrations in the workpiece. Figure 11 shows a torsional output curve for the machine when running without load; each peak corresponds to excitation at a gearshaft frequency. When experimenting, the frequencies corresponding to these peaks were avoided.

Similarly Figure 12 gives the machine response to horizontal excitation. Machine resonances, i.e. the peaks on this curve, were avoided; away from resonances it was possible to correct the observed test results by allowing for the machine deflections.

The outputs from the gauge bridges were fed either directly to an oscilloscope or via a band pass filter. Since the output from a band pass filter can vary in phase and amplitude relative to the input signal, whenever the frequency changed the phase and

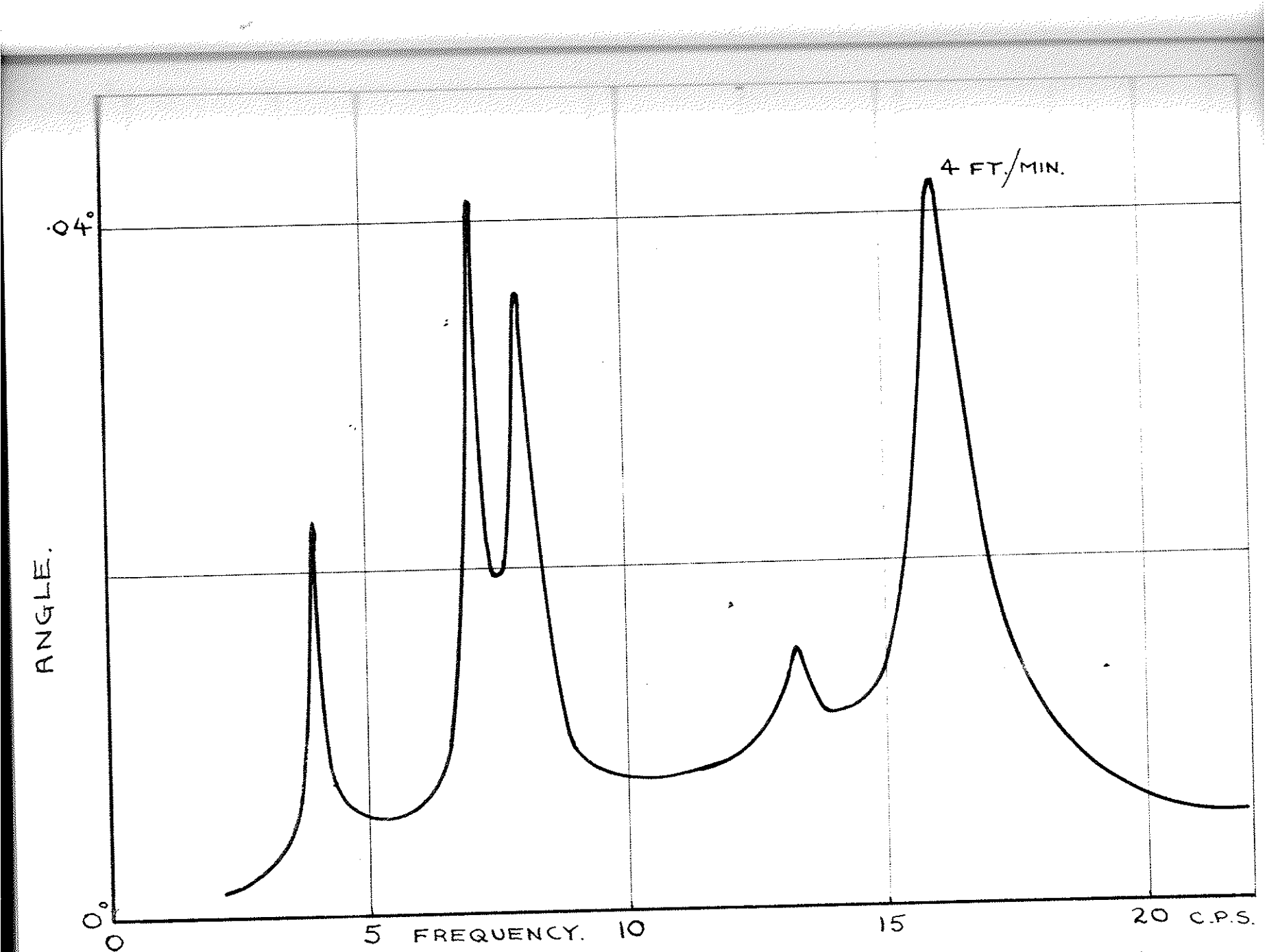

TORSIONAL VIBRATION. FIG. 11.

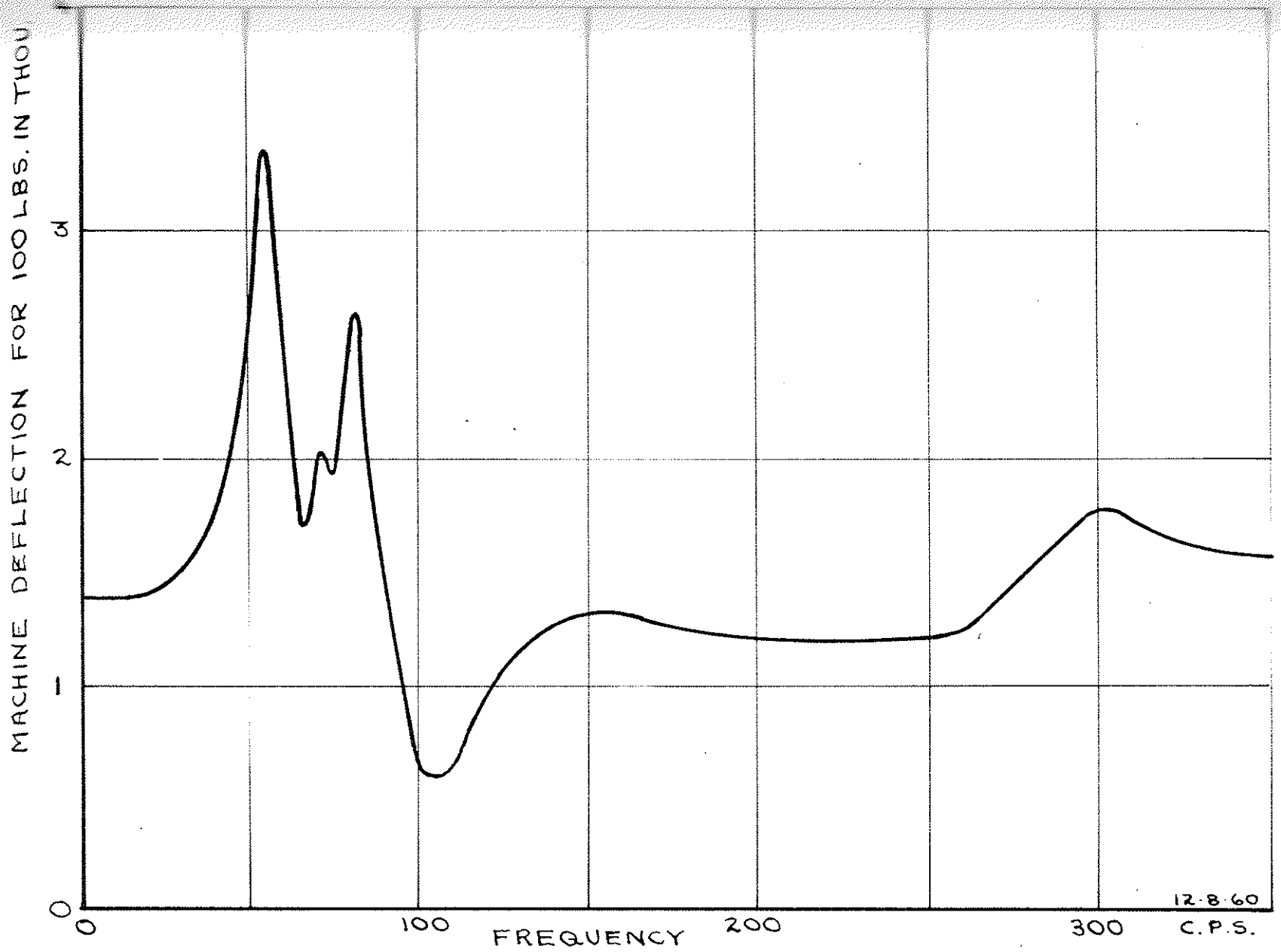

HORIZONTAL RESONANCE TEST. FIG. 12.

amplitude were reset to give a 1:1 amplitude ratio and exactly 180° phase change.

Since cutting forces vary greatly in amplitude and phase and have high noise levels, standard phasemeters cannot be used, particularly since some tests must last less than a tenth of a second. It was necessary to film the test results from the oscilloscope screen and analyse them later. At low frequencies the force and displacement traces were filmed on a base of time while at high frequencies the force was displayed on the X-axis and the displacement on the Y-axis, giving a Lissajous ellipse. Appendix 2 gives the methods used to measure the phase angles from the traces.

For some tests it was possible to determine curves of mean force against chip thickness; a typical curve is shown in Figure 13; the slope of this curve at the relevant chip thickness gives the stiffness corresponding to a zero frequency oscillation.

When testing, conditions were allowed to stabilise for at least five seconds. This ensures that the chip thickness is at the correct value and that tool temperatures are fairly stable since temperature stabilisation takes up to a second. The camera was then started and the forcing oscillation switched on.

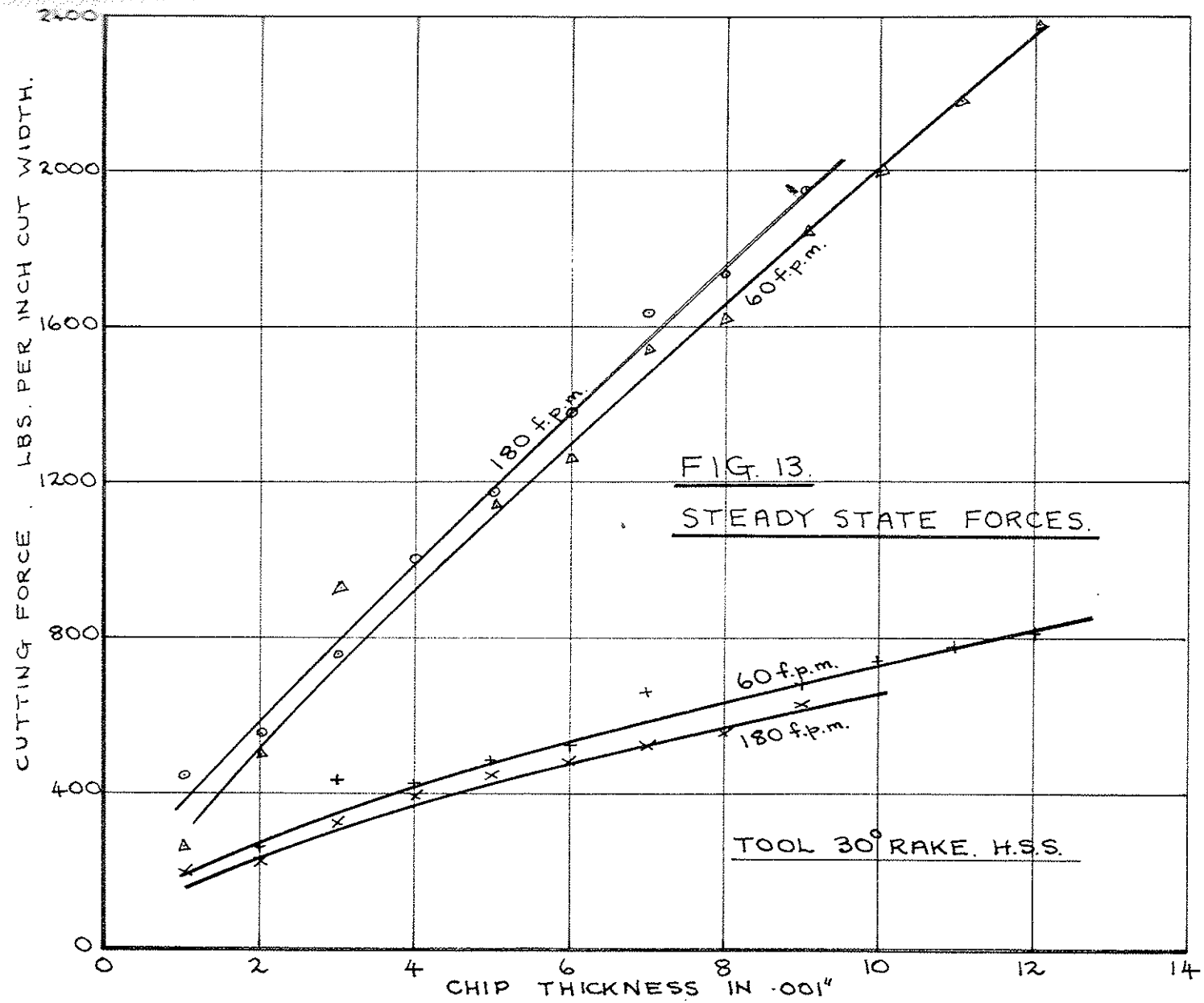

FIG. 13.

STEADY STATE FORCES.

For several cutting conditions it was not possible to obtain results. In some cases at high cutting speeds this was due to chatter involving the whole machine structure; this could not be controlled by the servo loop since this merely prevents the chatter involving motion of the tool relative to the bed. Chip instability at medium speeds prevented the establishment of steady conditions; instead of separating smoothly the chip appeared to collapse intermittently giving an irregular chip section and large force fluctuations. While collapsing the semi-plastic chip accumulates on the tip of the tool then separates suddenly. At low cutting speeds, particularly with heavy cuts, there is a large built up edge, giving low horizontal force amplitudes and high noise levels. Even using filters, the random fluctuations are so large relative to the fundamental force that measurements are not possible.

4.3 Experimental Results.

Although Doi and Kato expressed their results in the form of a lag of force behind displacement in terms of time, i.e. as a fraction of a second, this method of presentation is not suitable when a wide range of frequencies is under consideration. These test results have been plotted in terms of the phase angle between force and displacement.

The results have been given as a plot of relative phase angle between force and displacement against oscillating frequency for the normal and tangential forces. Similarly the amplitudes of the cutting forces have been plotted against frequency. The results are given in terms of a dynamic cutting stress which is the ratio of the increase of force to the increase of chip area. Though tangential i.e. vertical forces are not of primary interest in regenerative chatter, recording of these forces leads to a better understanding of the mechanisms of phase change.

For some of the tests, particularly the low surface speed tests, two curves of force amplitude are given. The higher stress value corresponds to Figure 14(a) when an initially smooth surface is being cut by an oscillating tool; the lower value corresponds to Figure 14(b) where the surface generated by 14(a) is removed by a stationary tool. It was not possible to measure phase of force relative to chip thickness in case 14(b).

A standard commercial grade mild steel in the as received condition was used for all tests; no coolant was used.

In all these tests there was no observed change in the mean force level when the oscillation was switched on.

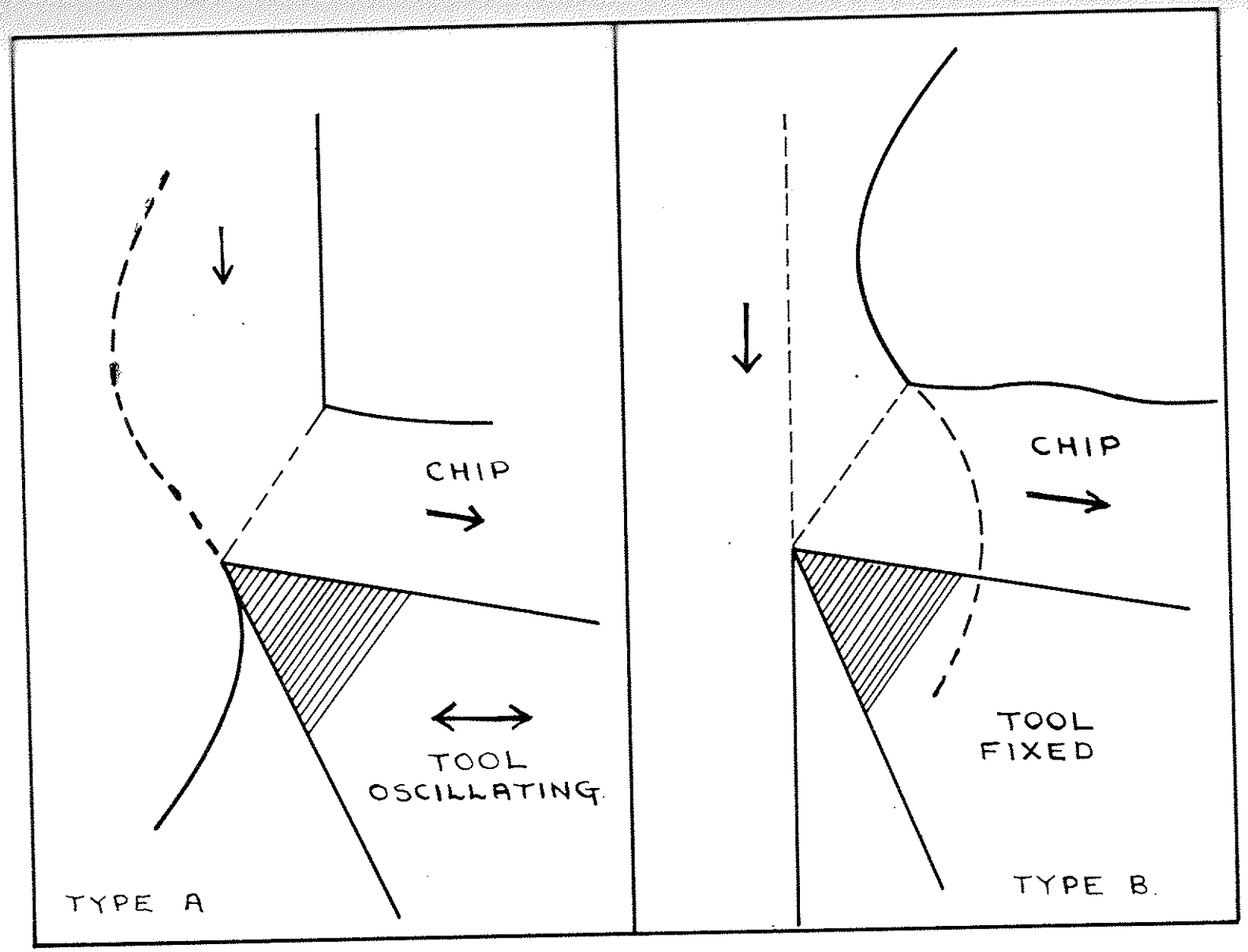

FIG. 14. TYPES OF CHIP THICKNESS VARIATION.

For analysis of results the values of the shear plane angle and the effective rake angle are required. The effective rake angle can only be measured by taking microsections of the chip and built-up edge after instantaneous stopping, as in Reference 11; the necessary apparatus and experience were not available so no estimates could be made. The shear plane angle can be measured rather elegantly by vibrating the tool at a known frequency, giving a chip thickness variation; the wave spacing on the chip will then give an accurate measure of the chip velocity. Comparison of the chip velocity and the cutting velocity gives an accurate value for the shear plane angle; see Shaw (14). This method was used on some tests but it was found that the shear angle varied widely for no apparent reason so no further chip measurements were made.

Figures 15 and 16 show typical test traces as recorded on the 35 mm. oscilloscope camera. The derived results from such traces are shown in Figures 17-25; Figure 26 was extracted from the preceding figures to allow comparison of the effects of change of cutting speed and chip size.

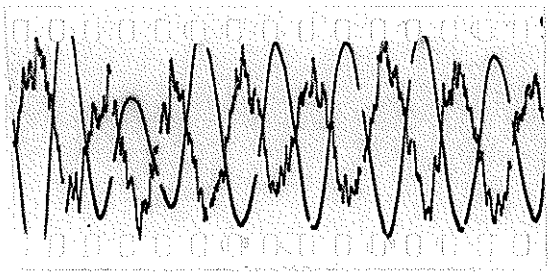

VERTICAL FORCE - FILTERED TRACE

DISPLACEMENT - UNFILTERED TRACE.

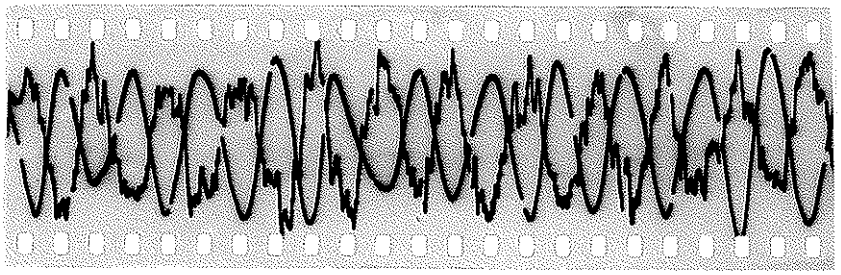

HORIZONTAL FORCE - FILTERED TRACE.

DISPLACEMENT - UNFILTERED TRACE.

FREQUENCY 7½ C/S. TOOL. CARBIDE 10° RAKE

CUT SPEED 50 FT/MIN. CUT .010" x .135"

LOW FREQUENCY CUTTING TRACES.

FIG. 15.

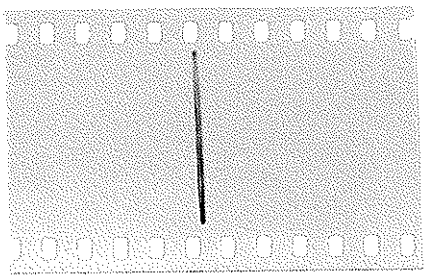

DISPLACEMENT AGAINST VERTICAL FORCE.

NO CUT

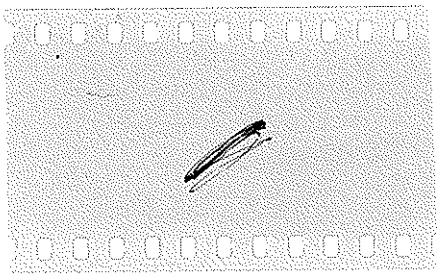

CUTTING.

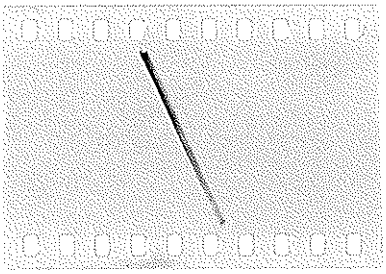

DISPLACEMENT AGAINST HORIZONTAL FORCE

NO CUT.

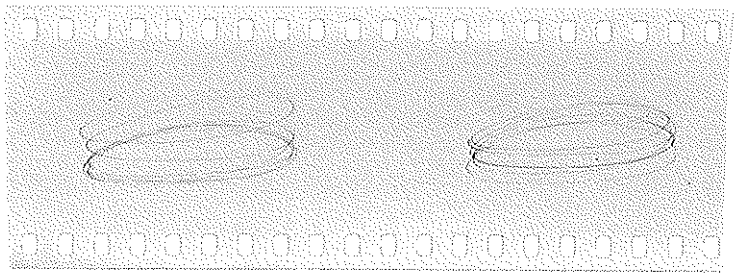

CUTTING.

FREQUENCY 220 c/s. TOOL. CARBIDE 10° RAKE.

CUT SPEED 50 FT./MIN. CUT .010" x .135".

HIGH FREQUENCY CUTTING TRACES

FIG. 16.

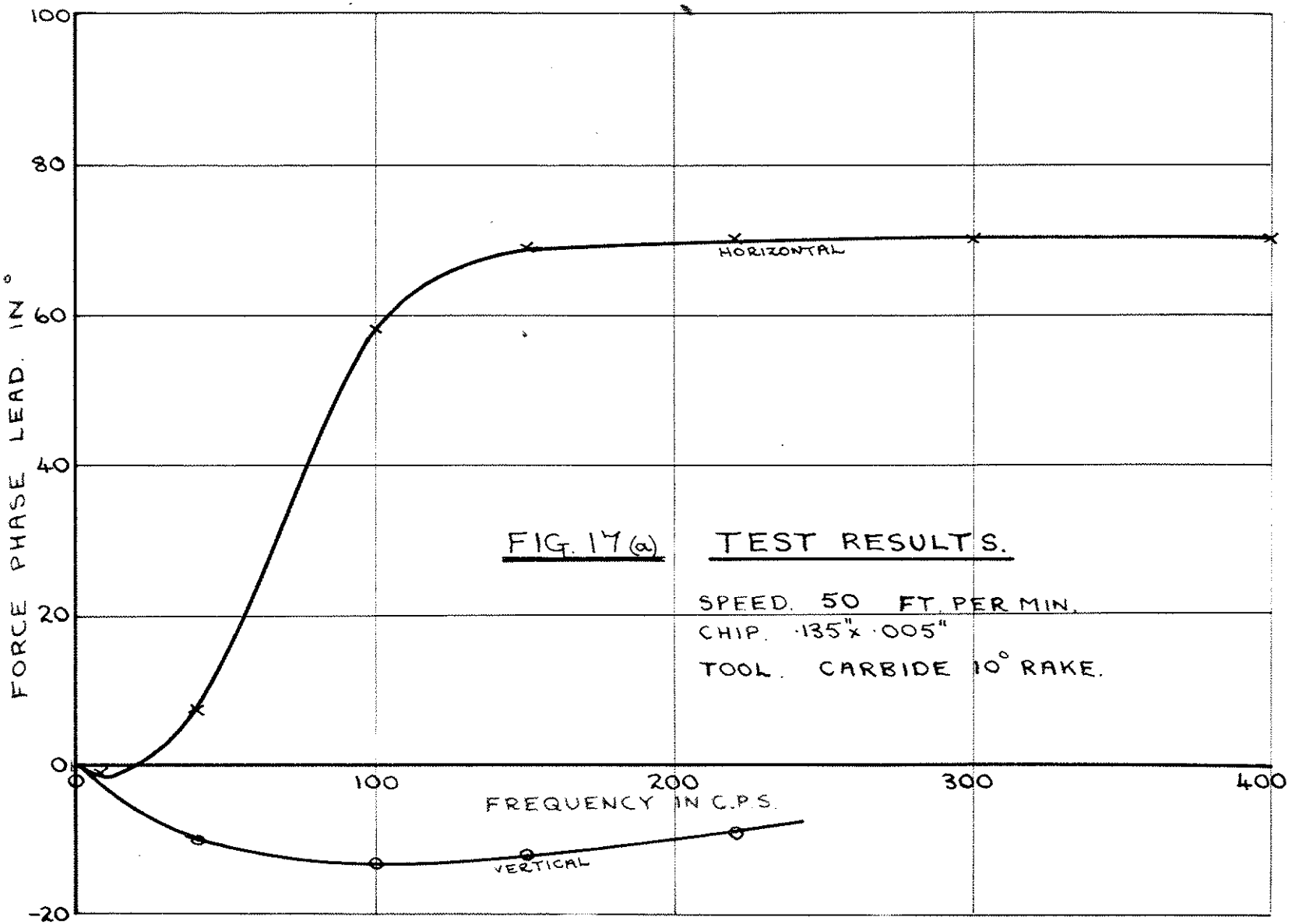

FIG. 17(a) TEST RESULTS.

SPEED. 50 FT. PER MIN.
CHIP. ·135" x ·005"
TOOL. CARBIDE 10° RAKE.

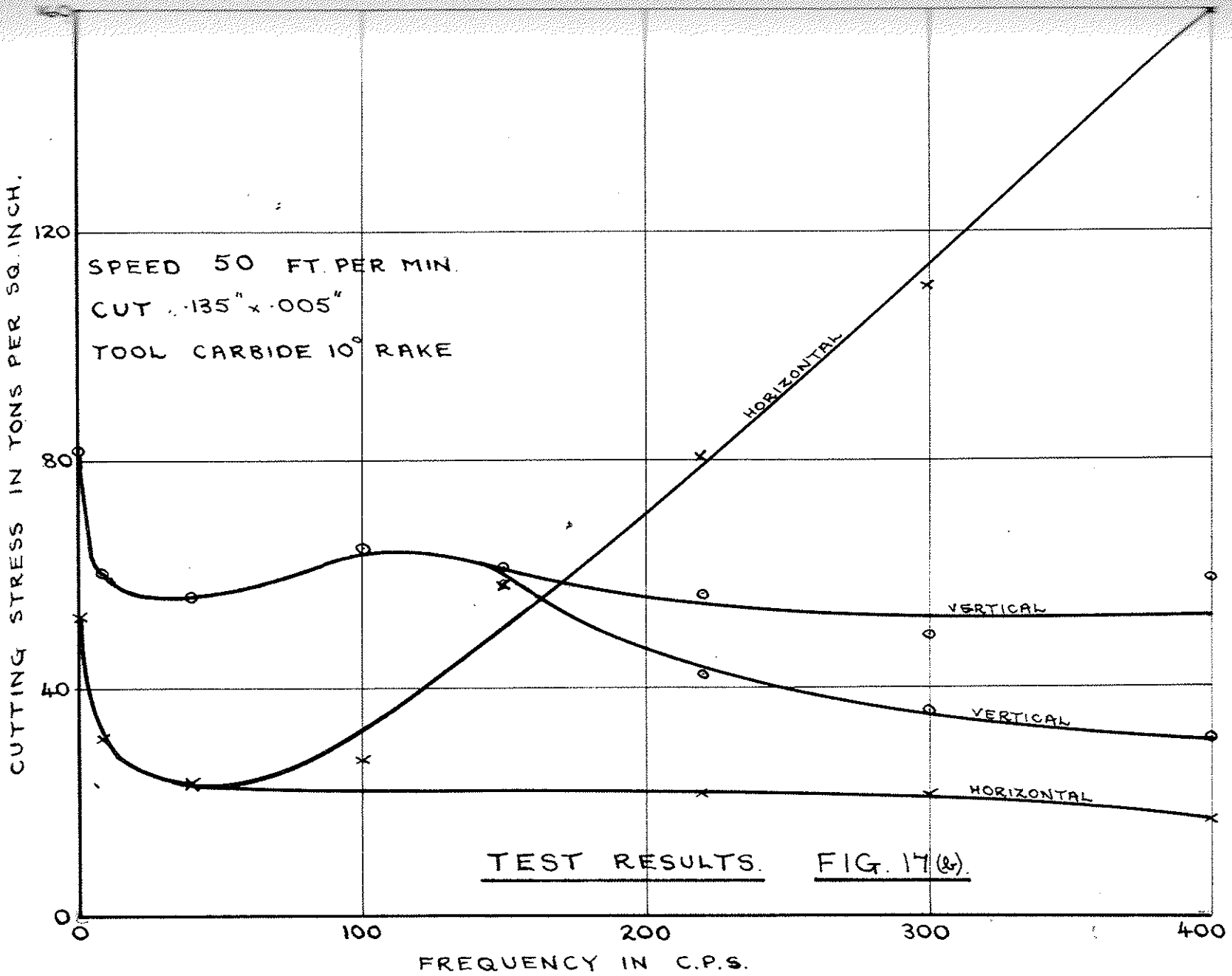

TEST RESULTS. FIG. 17 (a).

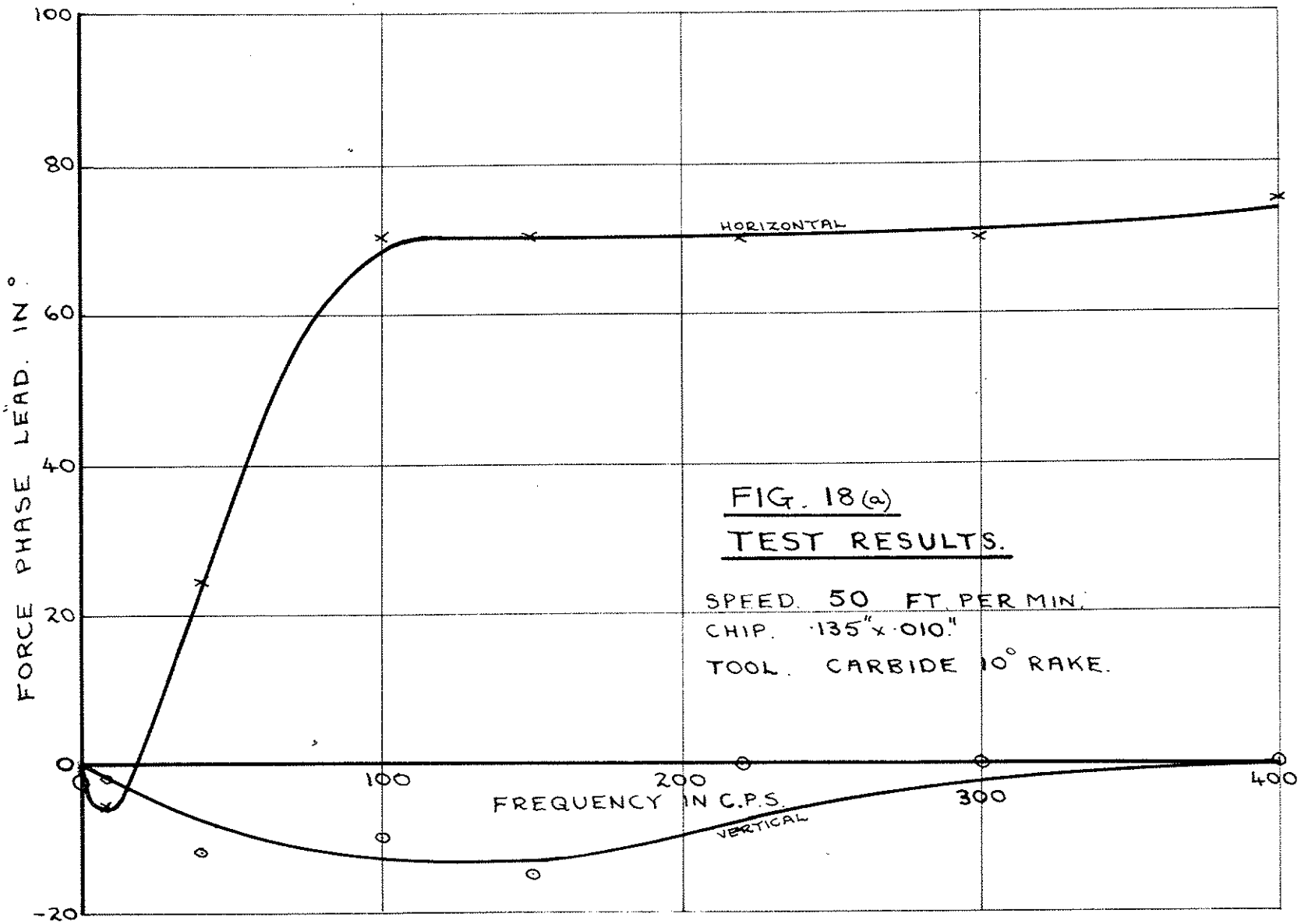

FIG. 18(a)

TEST RESULTS.

SPEED. 50 FT PER MIN.

CHIP. ·135" x ·010"

TOOL. CARBIDE 10° RAKE.

FIG 18 (b).

TEST RESULTS.

SPEED 50 FT. PER MIN

CUT ·135" x ·010"

TOOL CARBIDE 10° RAKE

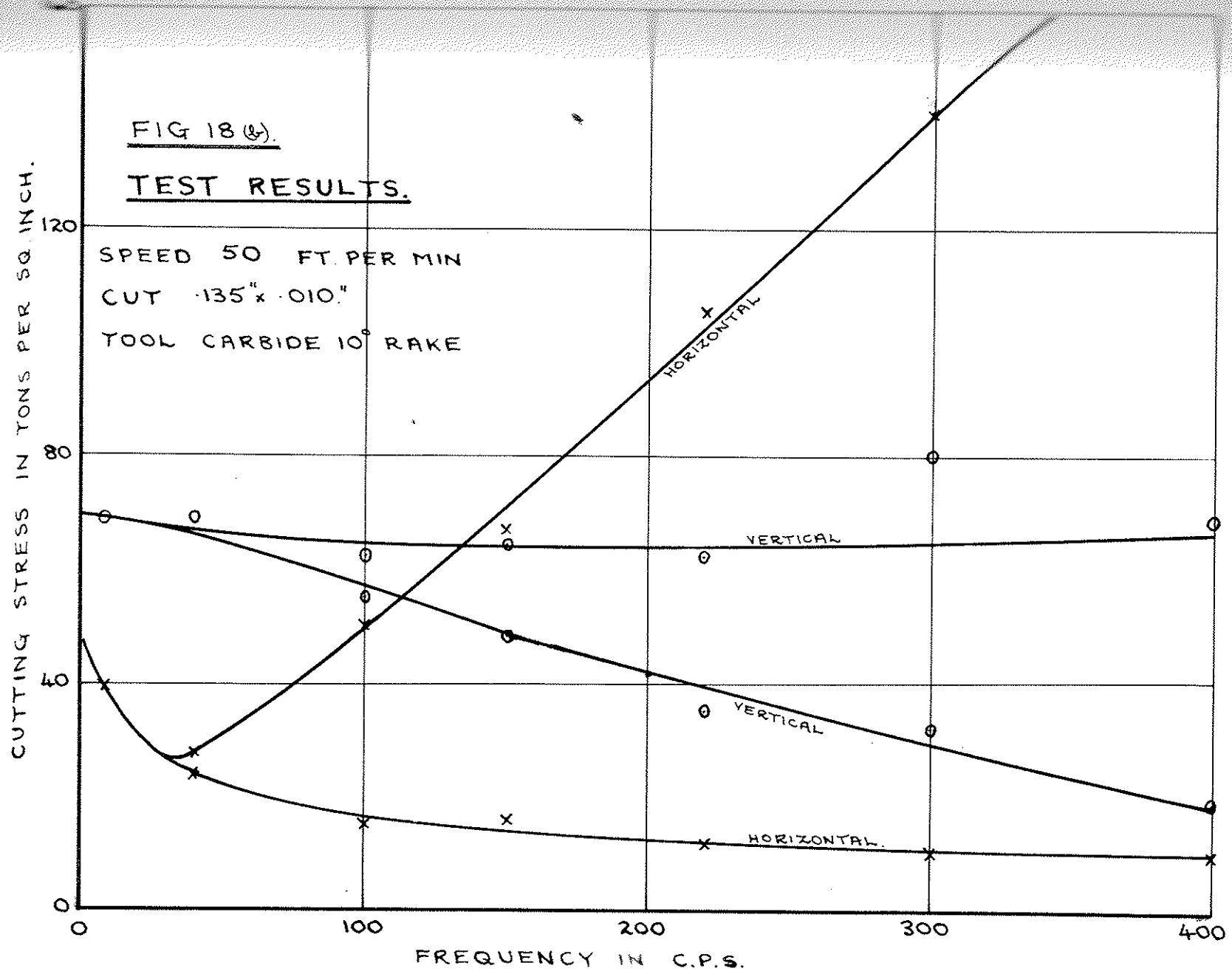

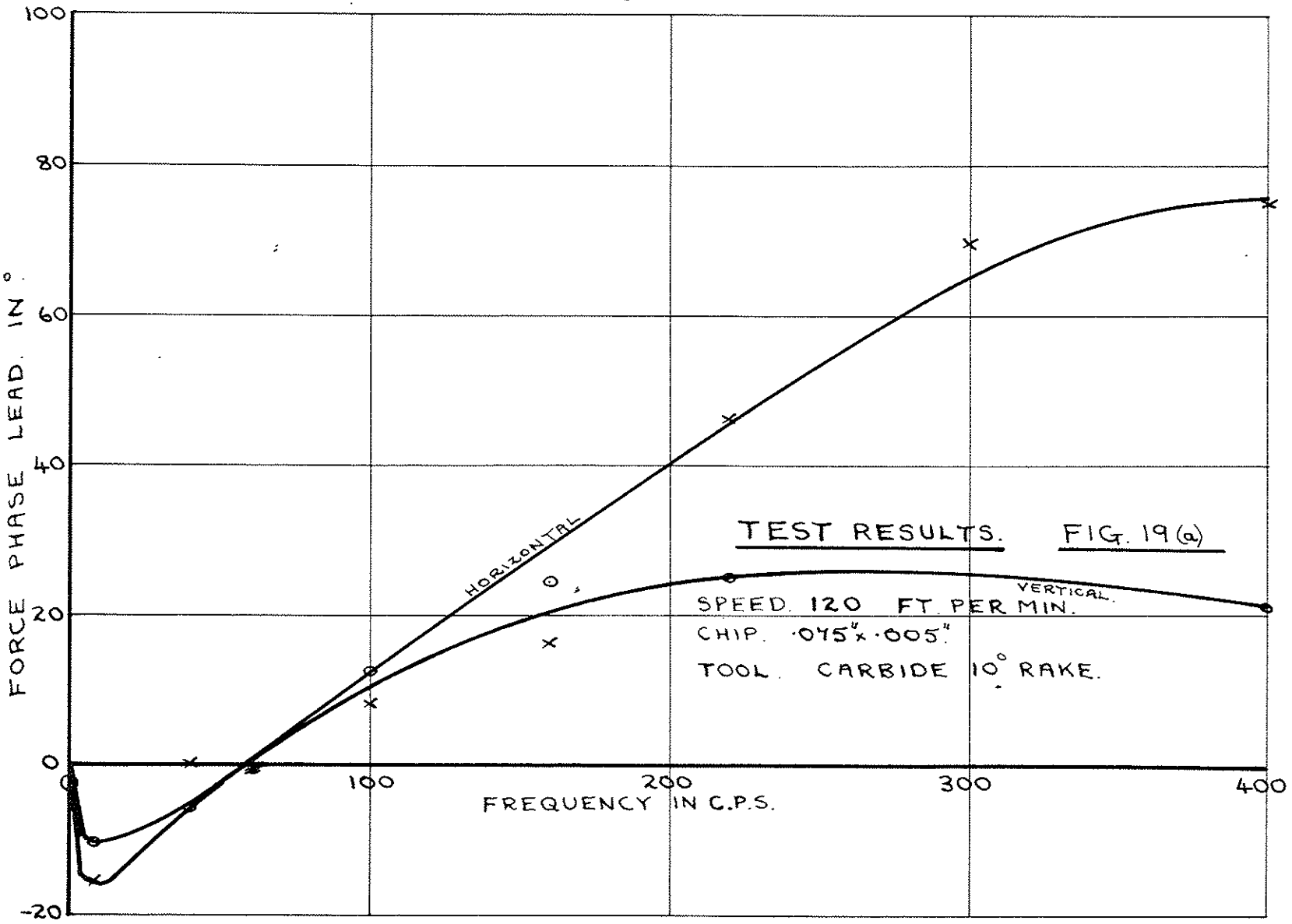
100
80
60
40
20
0
-20
FORCE PHASE LEAD. IN °.
0
100
200
300
400
FREQUENCY IN C.P.S.
HORIZONTAL
VERTICAL.
TEST RESULTS. FIG. 19(a)
SPEED. 120 FT. PER MIN.
CHIP. ·075" x ·005".
TOOL. CARBIDE 10° RAKE.

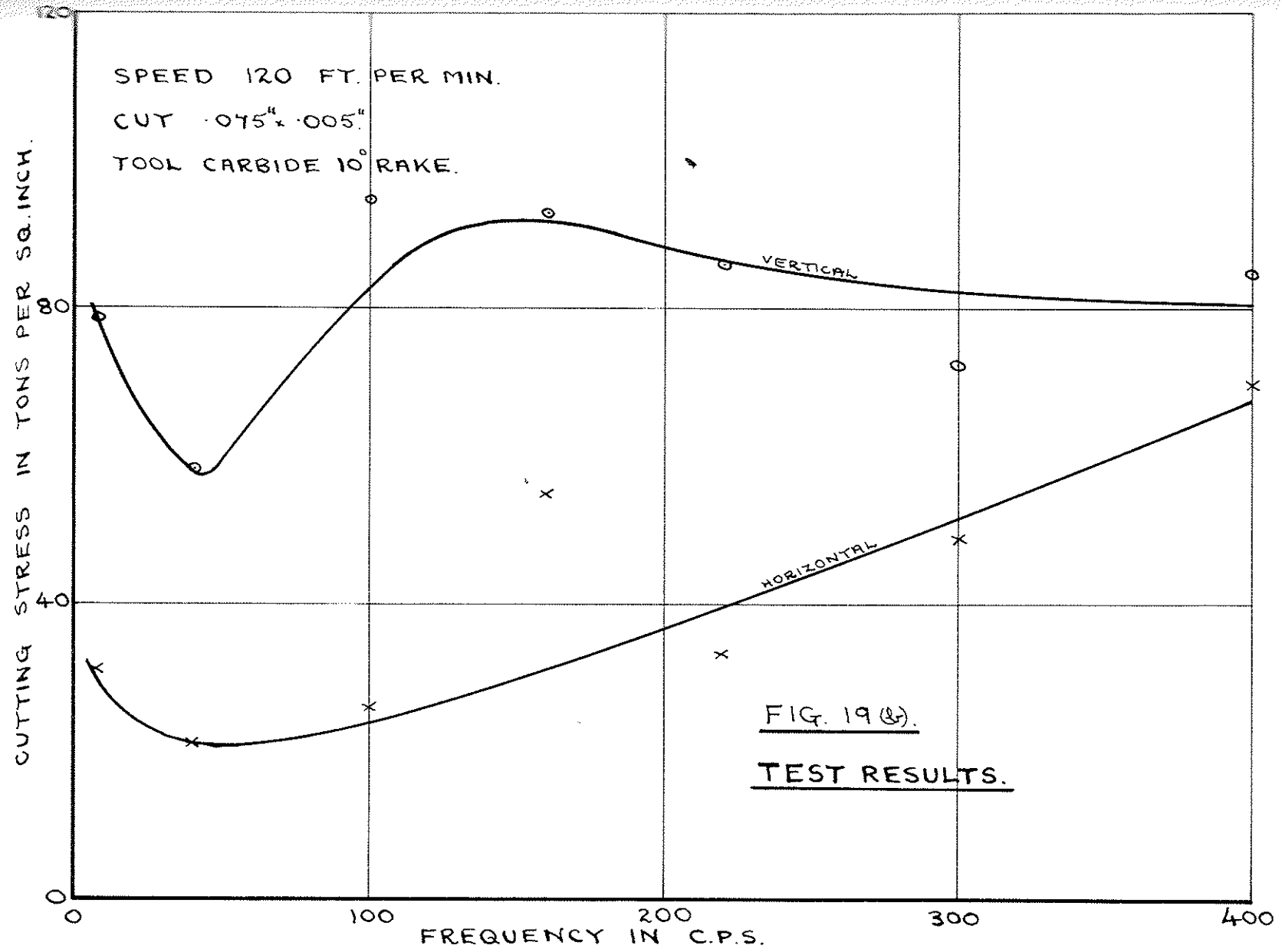

FIG. 19 (a).

TEST RESULTS.

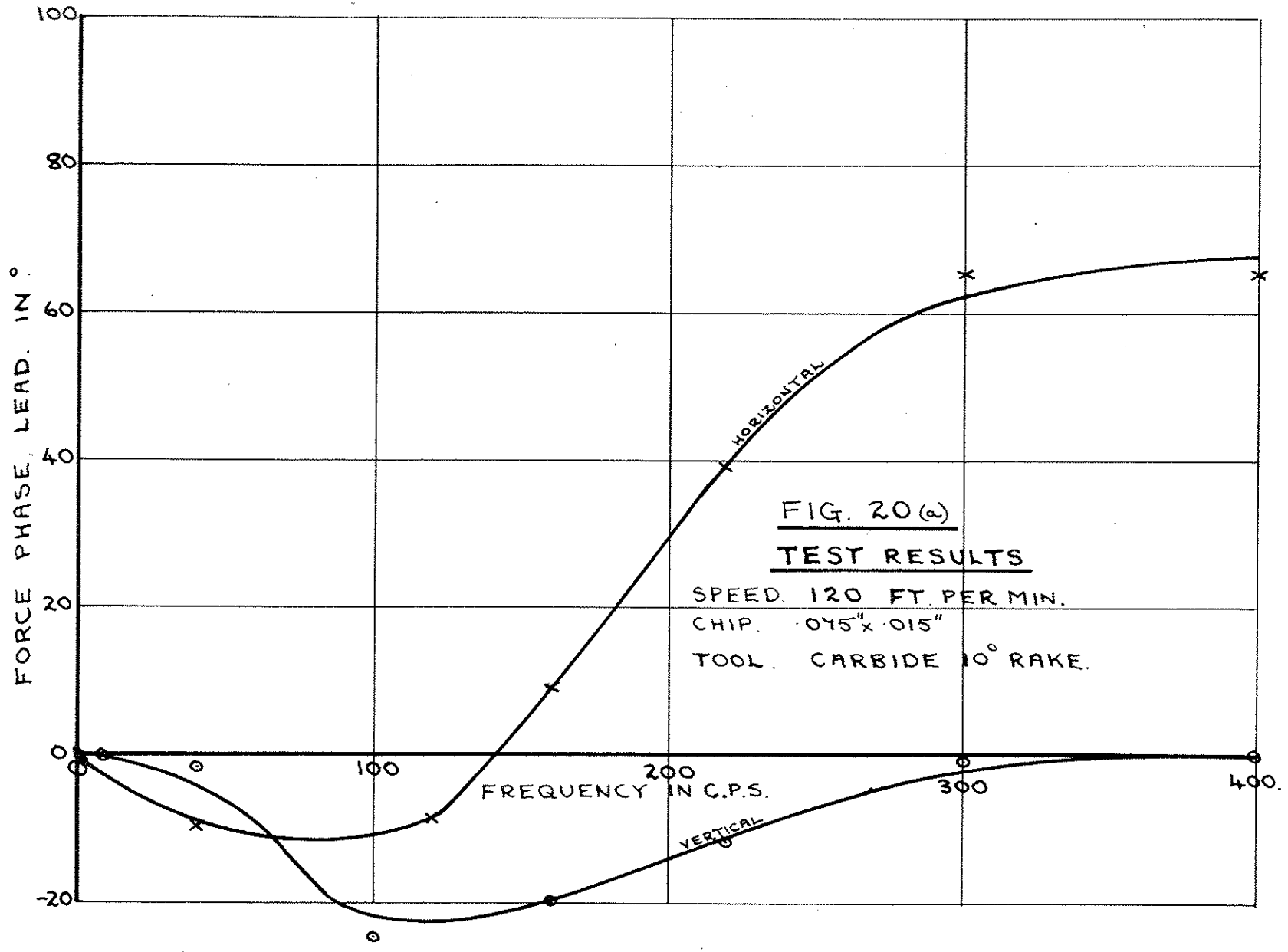
100
80
60
40
20
0
-20
FORCE PHASE, LEAD. IN °.
0
100
200
300
400.
FREQUENCY IN C.P.S.
HORIZONTAL
VERTICAL
FIG. 20(a)
TEST RESULTS
SPEED. 120 FT. PER MIN.
CHIP. ·075"x·015"
TOOL. CARBIDE 10° RAKE.

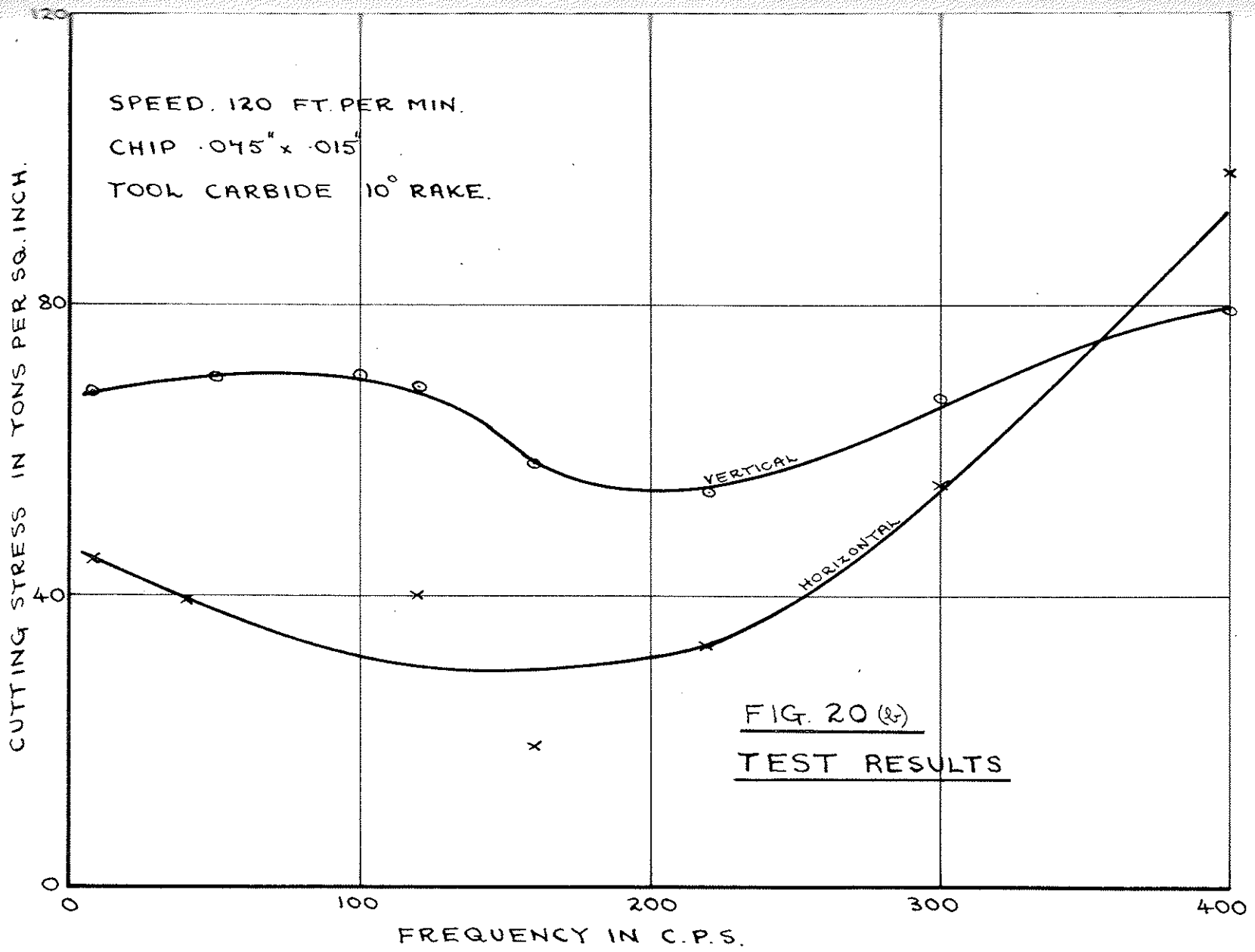

FIG. 20 (b)

TEST RESULTS

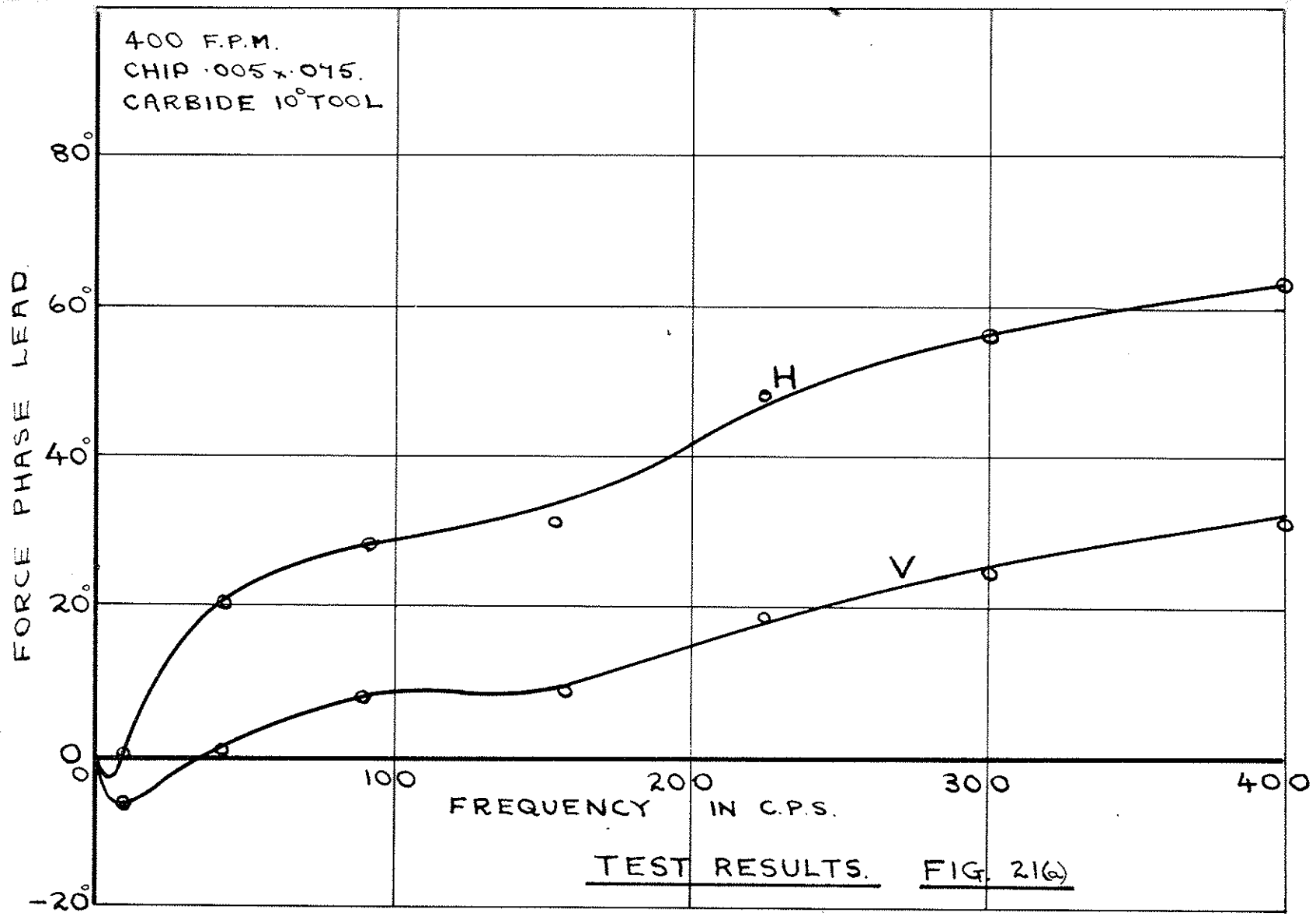

TEST RESULTS. FIG. 21(a)

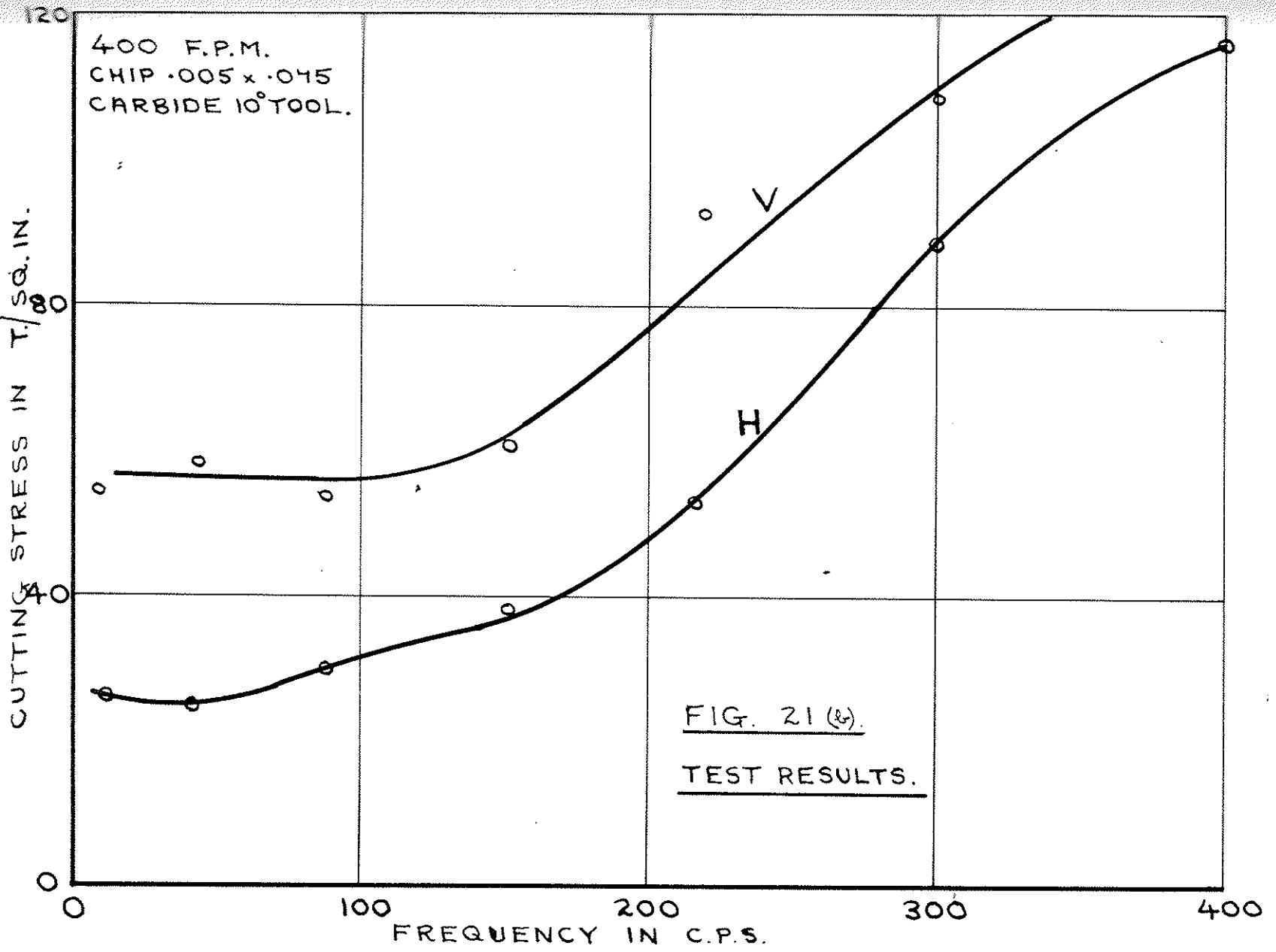

FIG. 21 (b).

TEST RESULTS.

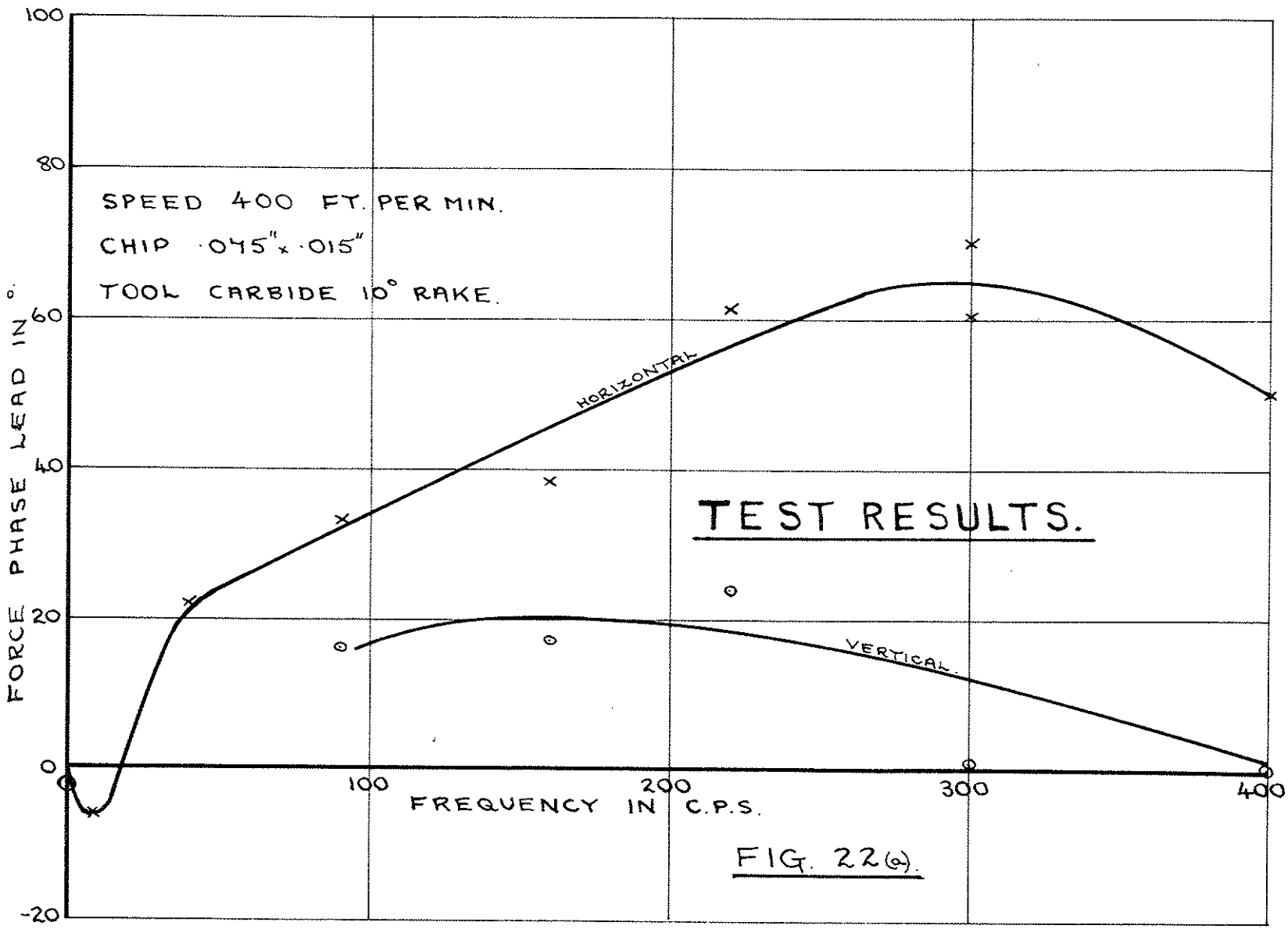
100
80
60
40
20
0
-20
FORCE PHASE LEAD IN °
SPEED 400 FT. PER MIN.
CHIP ·045" x ·015"
TOOL CARBIDE 10° RAKE.
HORIZONTAL
VERTICAL
TEST RESULTS.
100
200
300
400
FREQUENCY IN C.P.S.

FIG. 22(a).

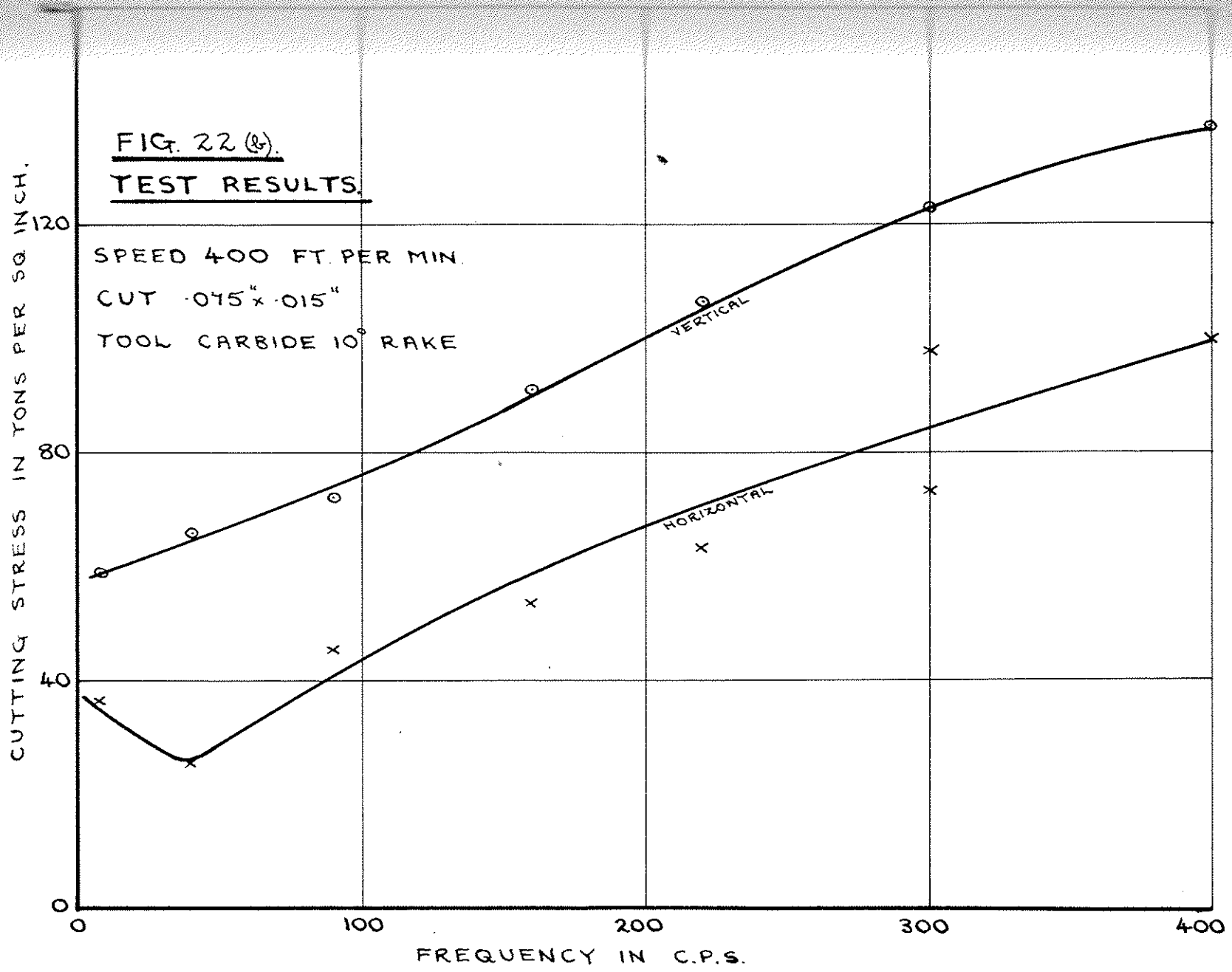
FIG. 22 (g).
TEST RESULTS.
SPEED 400 FT. PER MIN.
CUT ·075" x ·015"
TOOL CARBIDE 10° RAKE
VERTICAL
HORIZONTAL
CUTTING STRESS IN TONS PER SQ. INCH.
120
80
40
0
0
100
200
300
400
FREQUENCY IN C.P.S.

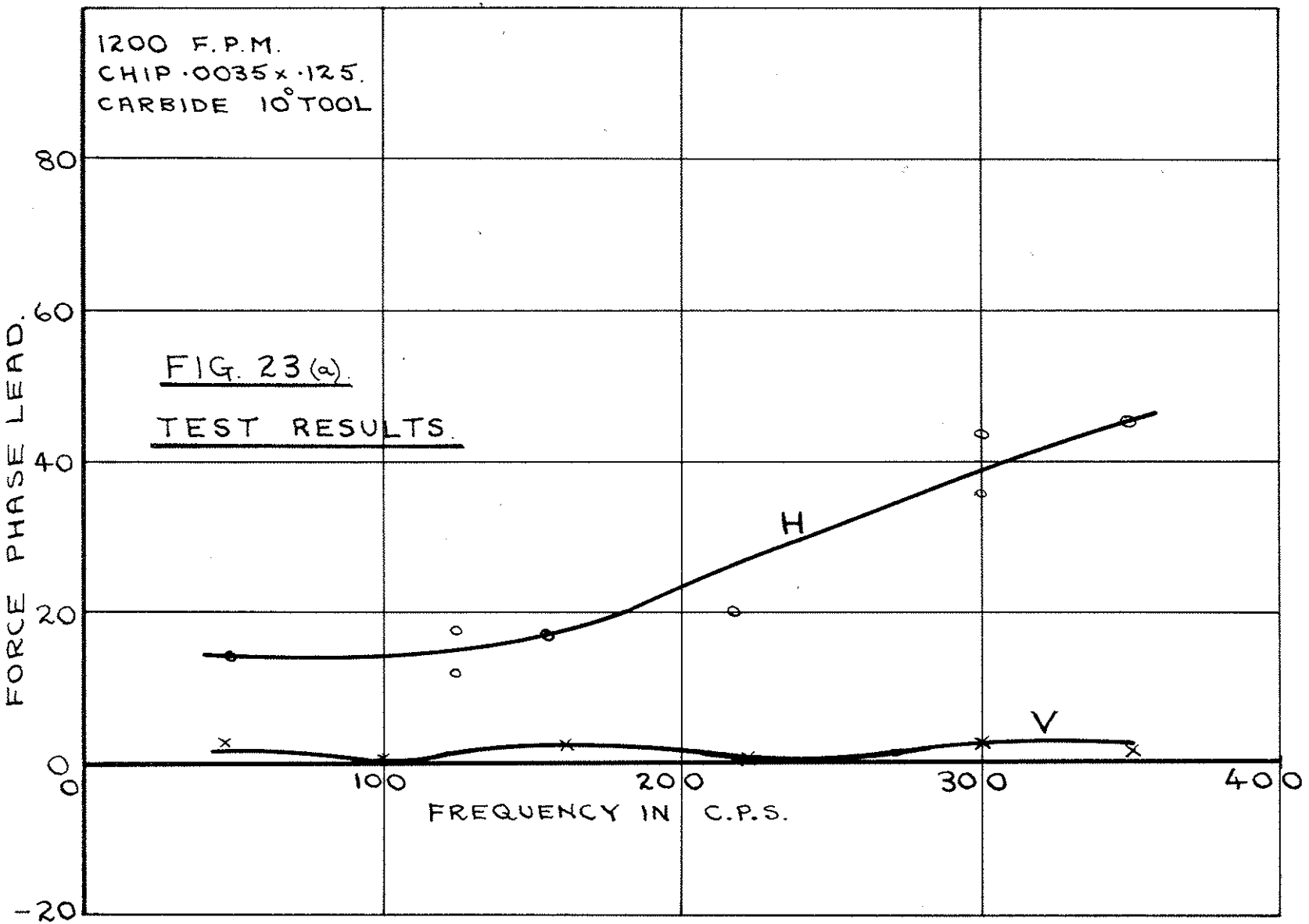
1200 F.P.M.
CHIP ·0035 x ·125.
CARBIDE 10° TOOL
FIG. 23 (a).
TEST RESULTS.
FORCE PHASE LEAD.
80
60
40
20
0
-20
H
V
100
200
300
400
FREQUENCY IN C.P.S.

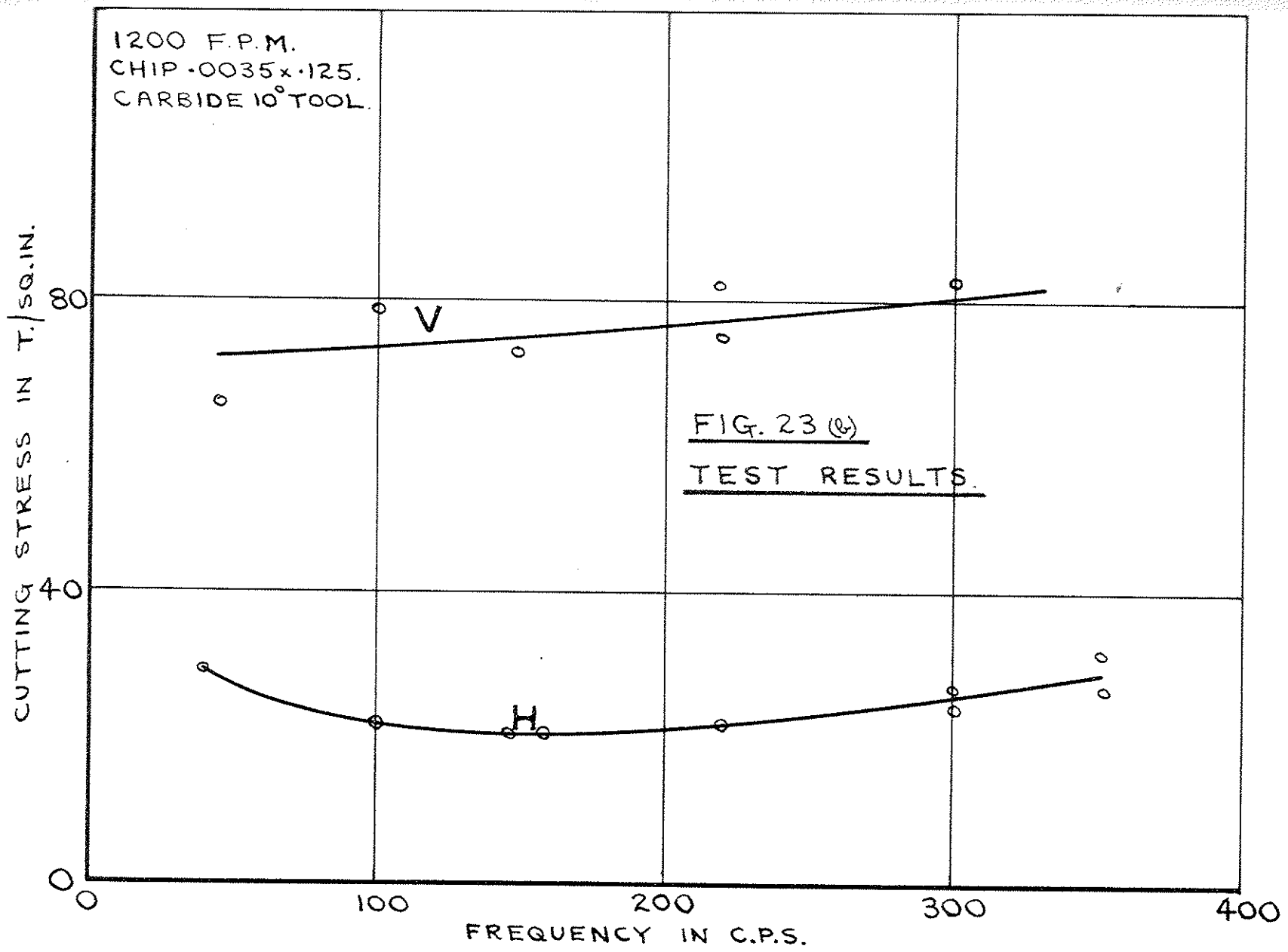

FIG. 23 (b)

TEST RESULTS.

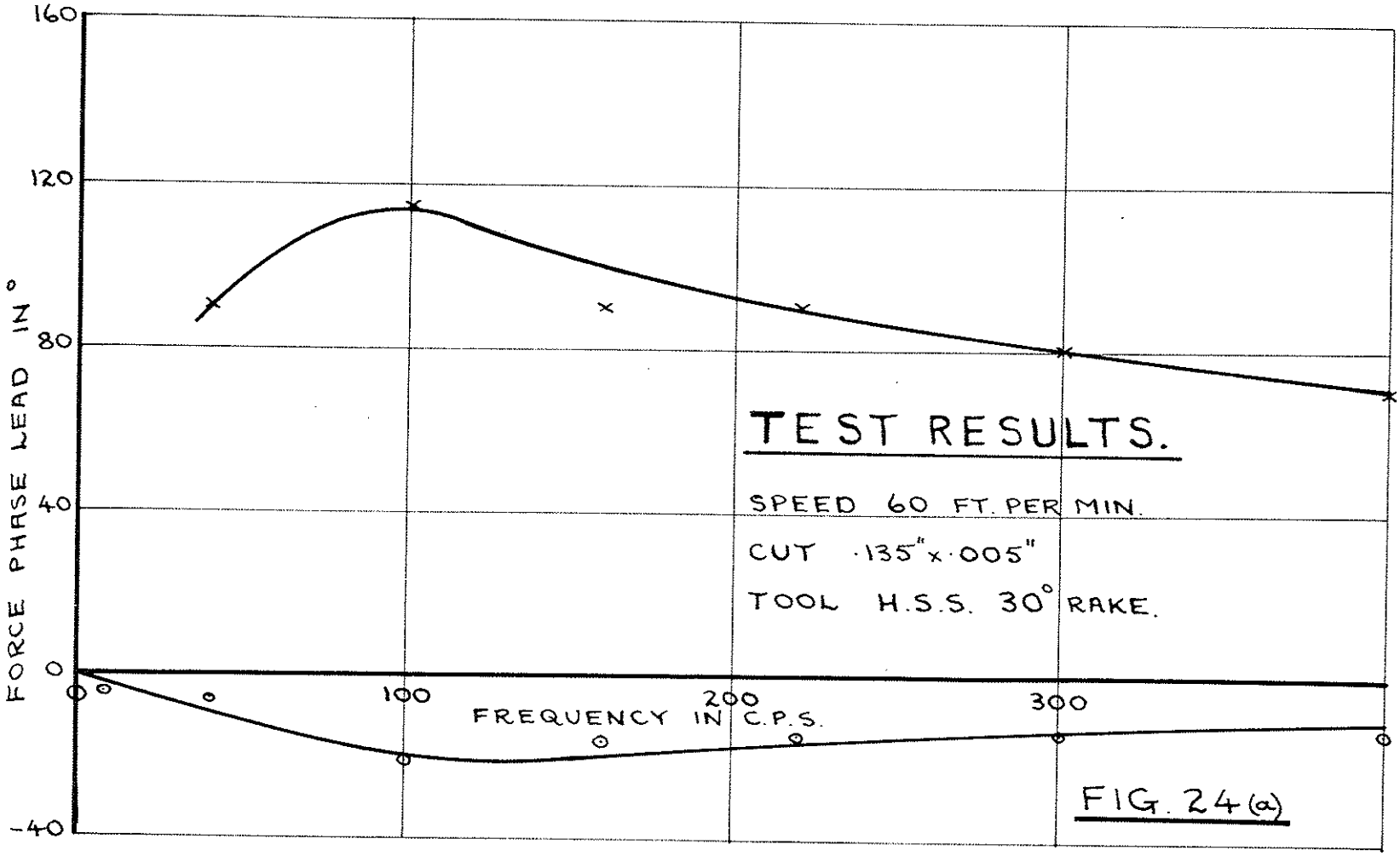
160
120
80
40
0
-40
FORCE PHASE LEAD IN °
100
200
300
FREQUENCY IN C.P.S.
TEST RESULTS.
SPEED 60 FT. PER MIN.
CUT .135" x .005"
TOOL H.S.S. 30° RAKE.

FIG. 24(a)

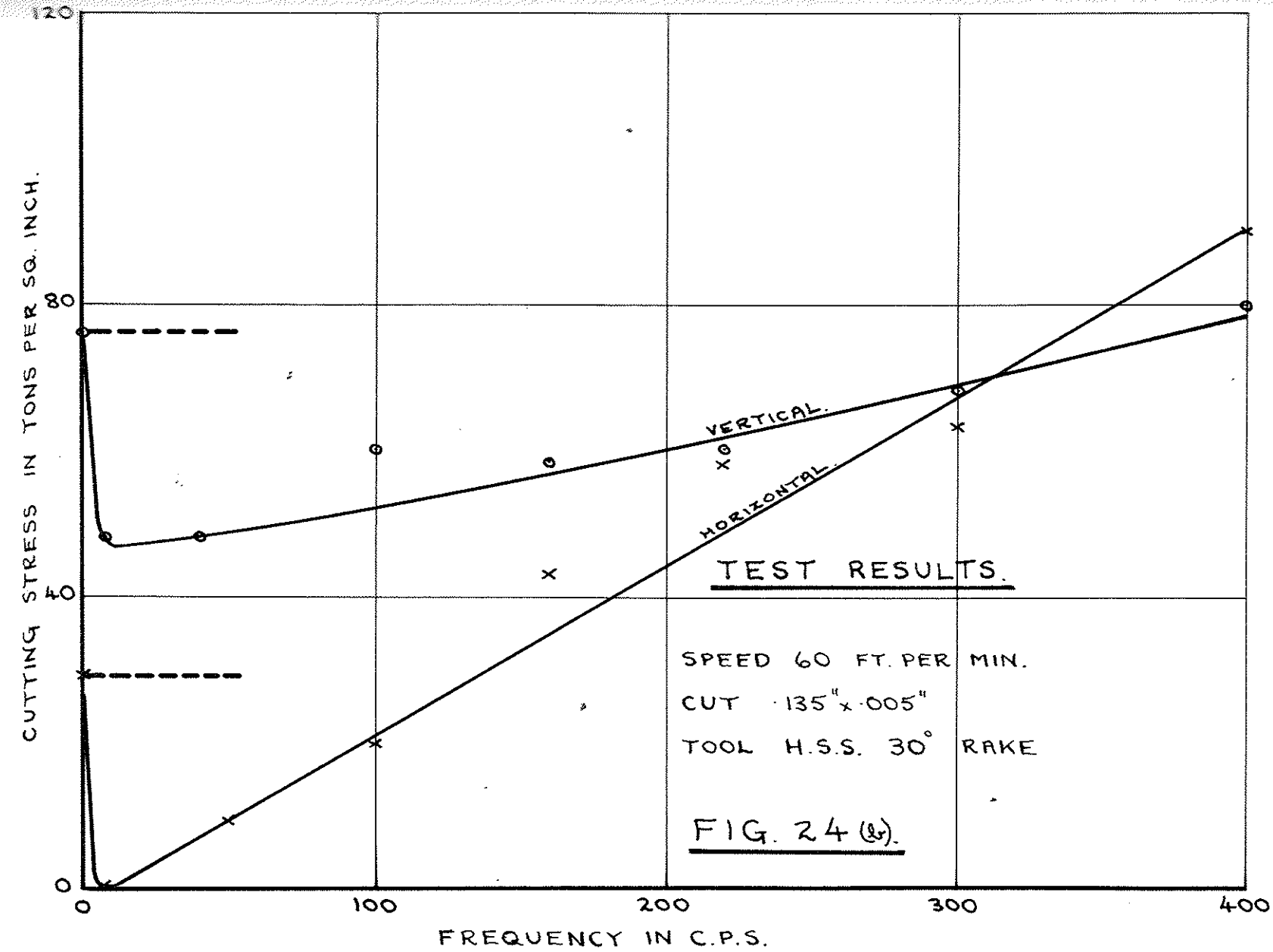
120
80
40
0
CUTTING STRESS IN TONS PER SQ. INCH.
0
100
200
300
400
FREQUENCY IN C.P.S.
VERTICAL.
HORIZONTAL.
TEST RESULTS.
SPEED 60 FT. PER MIN.
CUT .135" x .005"
TOOL H.S.S. 30° RAKE

FIG. 24 (b).

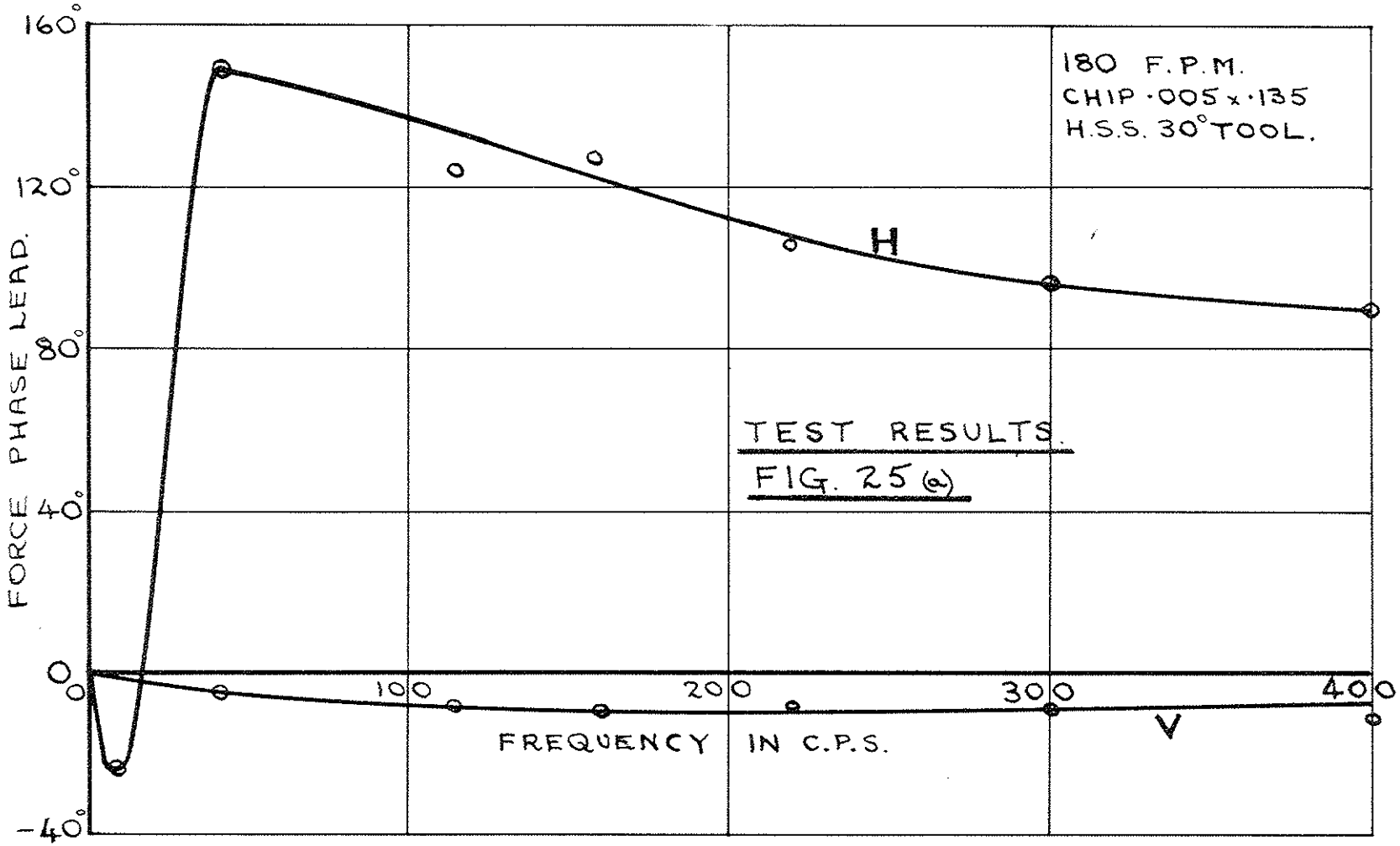
160°
120°
80°
40°
0°
-40°
FORCE PHASE LEAD.
100
200
300
400
FREQUENCY IN C.P.S.
H
V
180 F.P.M.
CHIP ·005 x ·135
H.S.S. 30° TOOL.
TEST RESULTS.
FIG. 25 (a)

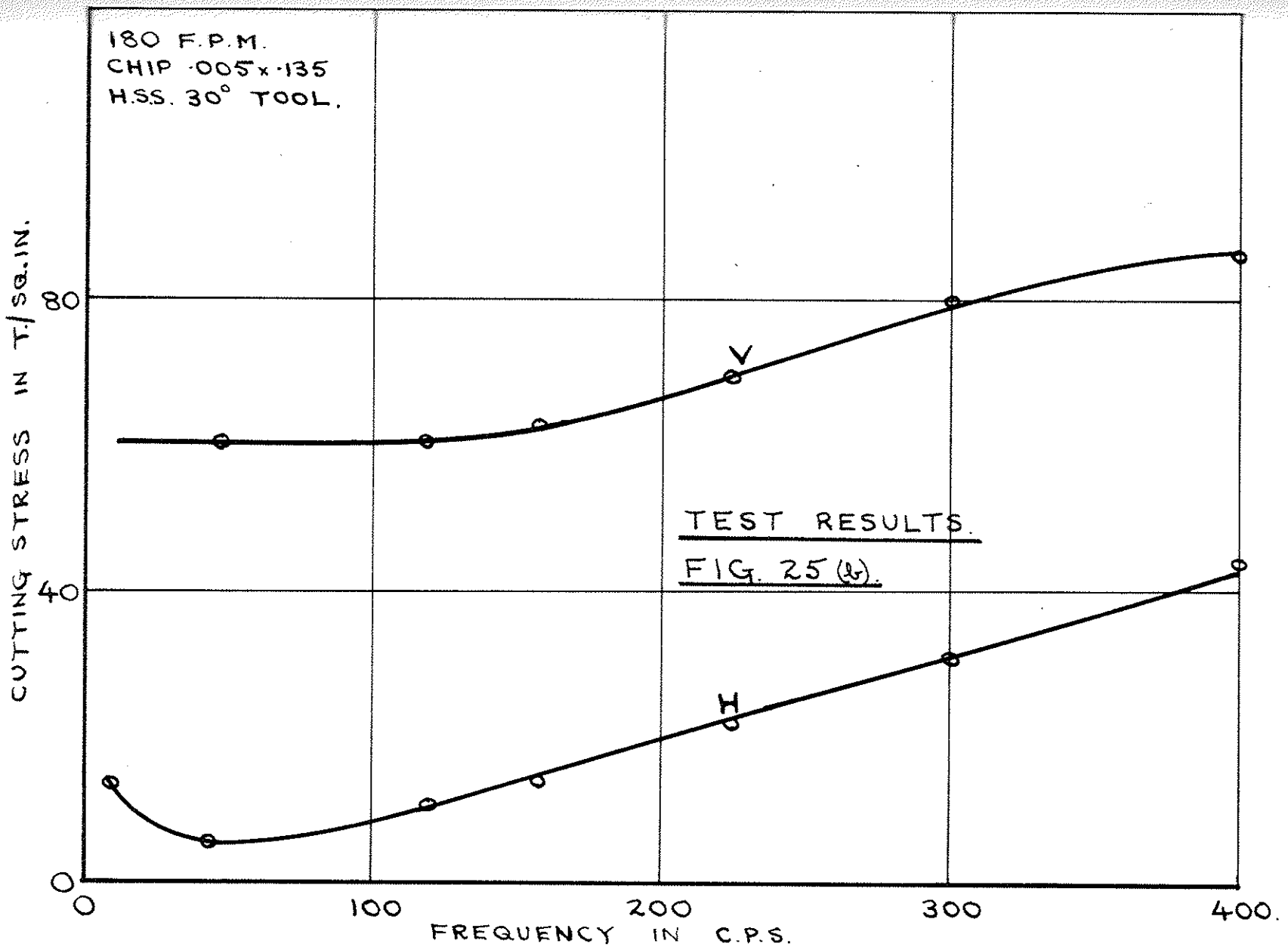
180 F.P.M.
CHIP ·005 x ·135
H.S.S. 30° TOOL.
CUTTING STRESS IN T./SQ.IN.
80
40
0
V
H
TEST RESULTS.
FIG. 25 (b).
0
100
200
300
400.
FREQUENCY IN C.P.S.

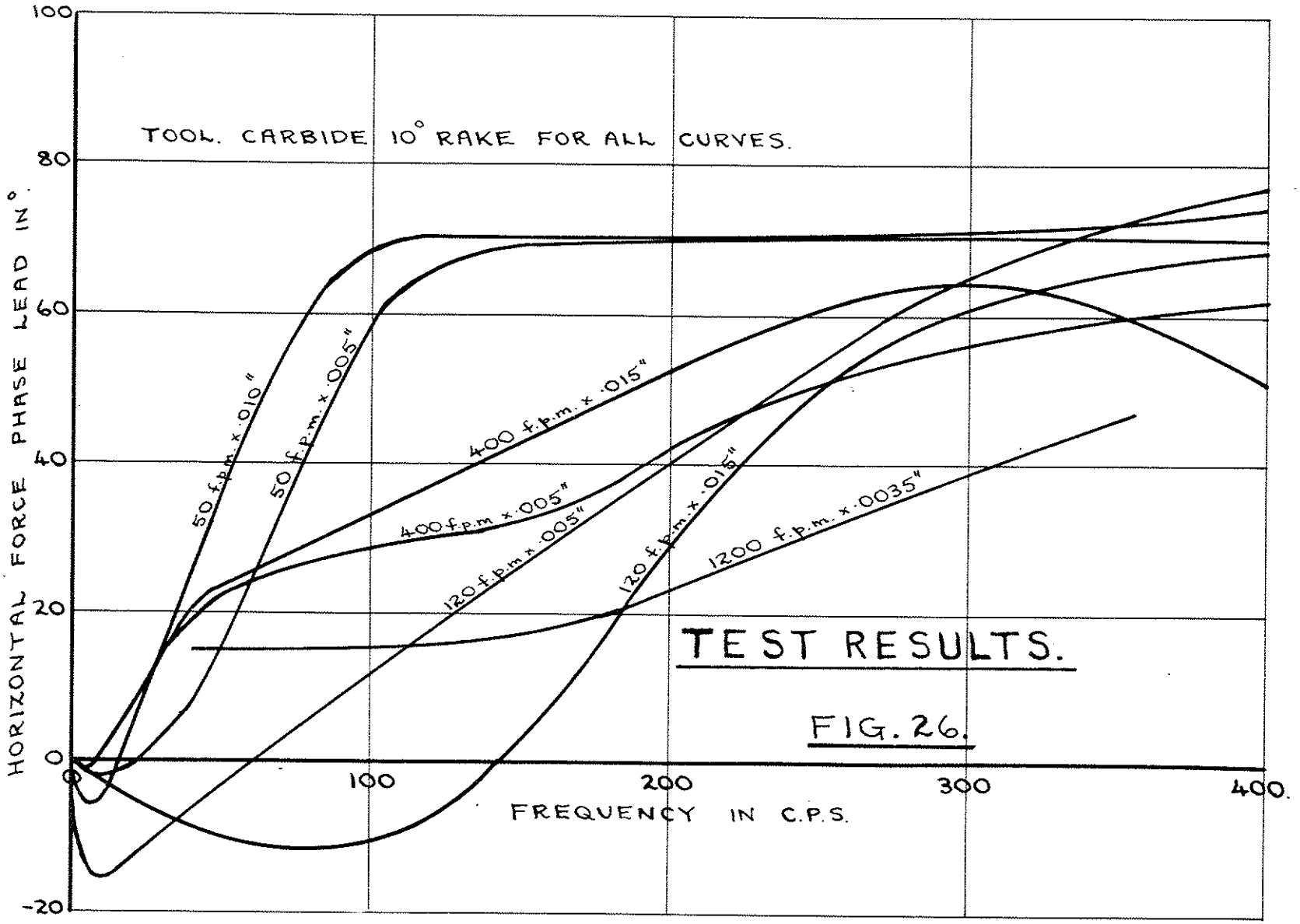

TEST RESULTS.

FIG. 26.

5. Low Frequency Tests.

5.1 Introduction.

In addition to the main set of tests using an electromagnetic control of the tool vibration, a series of tests at low frequency using a mechanical system was attempted.

5.2 Apparatus.

The rig was similar to that used in the main series of tests except that a cam was used to force the oscillation instead of an electromagnetic vibrator. A standard electric motor, coupled to a rolling ball infinitely variable gear, drove a bevel reduction gear on which an eccentric cam was mounted. The cam, rotating at speeds between 3.4 and 25 revolutions per second, drove a roller on the rear of the dynamometer block, forcing the block to oscillate on its supporting leaf springs. Force and displacement were measured, as in the other tests, by strain gauges.

5.3 Results.

The force phase angles derived from these tests are given in Figures 27 and 28 for the vertical (or tangential) and the horizontal (or normal) forces respectively. In these tests, as in paragraph 4.2, high noise levels and small horizontal forces associated with large built up edges made it impossible to derive results in some cases. Rig limitations restricted tests to four

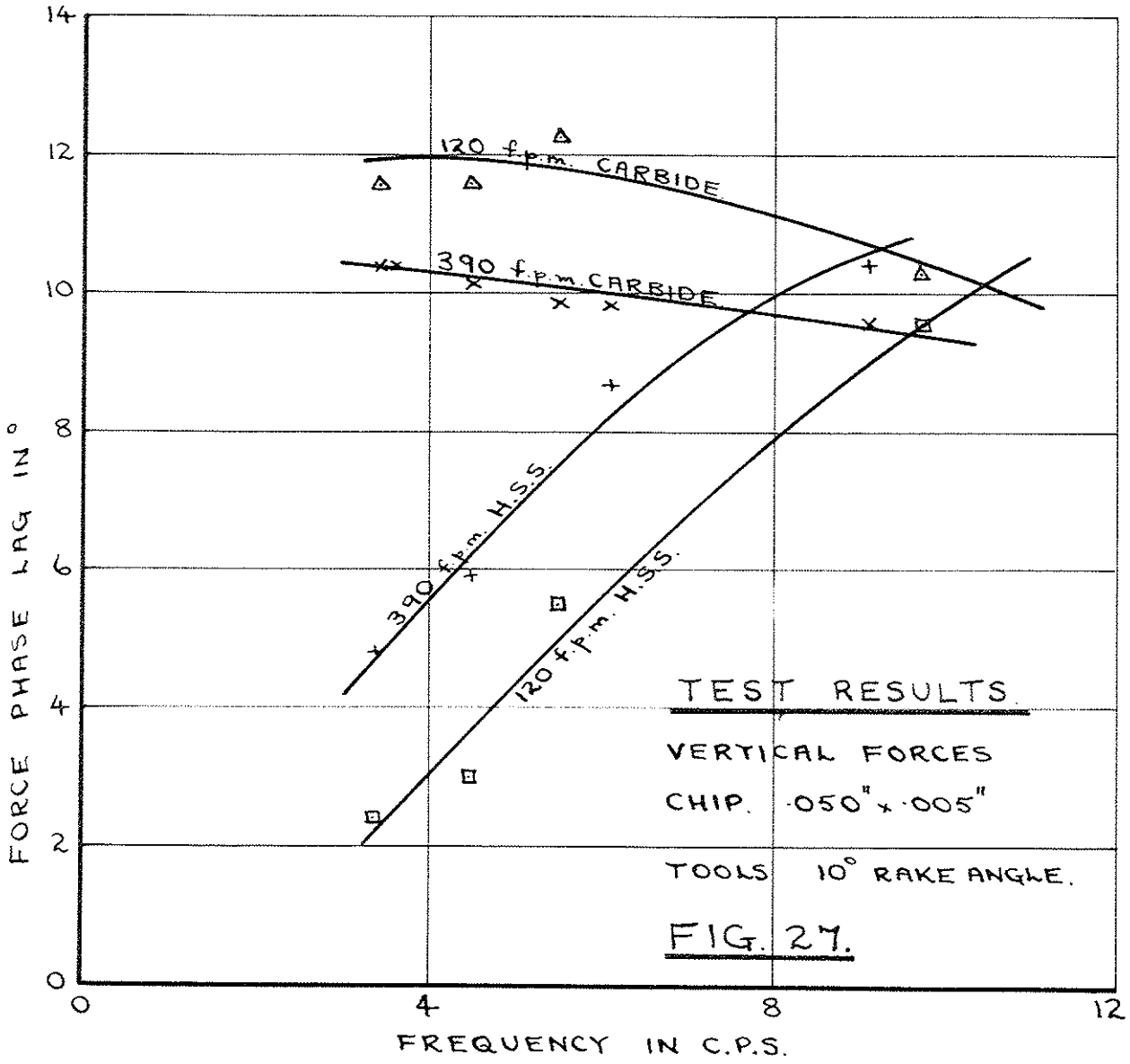
14
12
10
8
6
4
2
0
0
4
8
12
FORCE PHASE LAG IN °
FREQUENCY IN C.P.S.
120 f.p.m. CARBIDE
390 f.p.m. CARBIDE
390 f.p.m. H.S.S.
120 f.p.m. H.S.S.
TEST RESULTS
VERTICAL FORCES
CHIP. ·050" x ·005"
TOOLS 10° RAKE ANGLE.

FIG. 27.

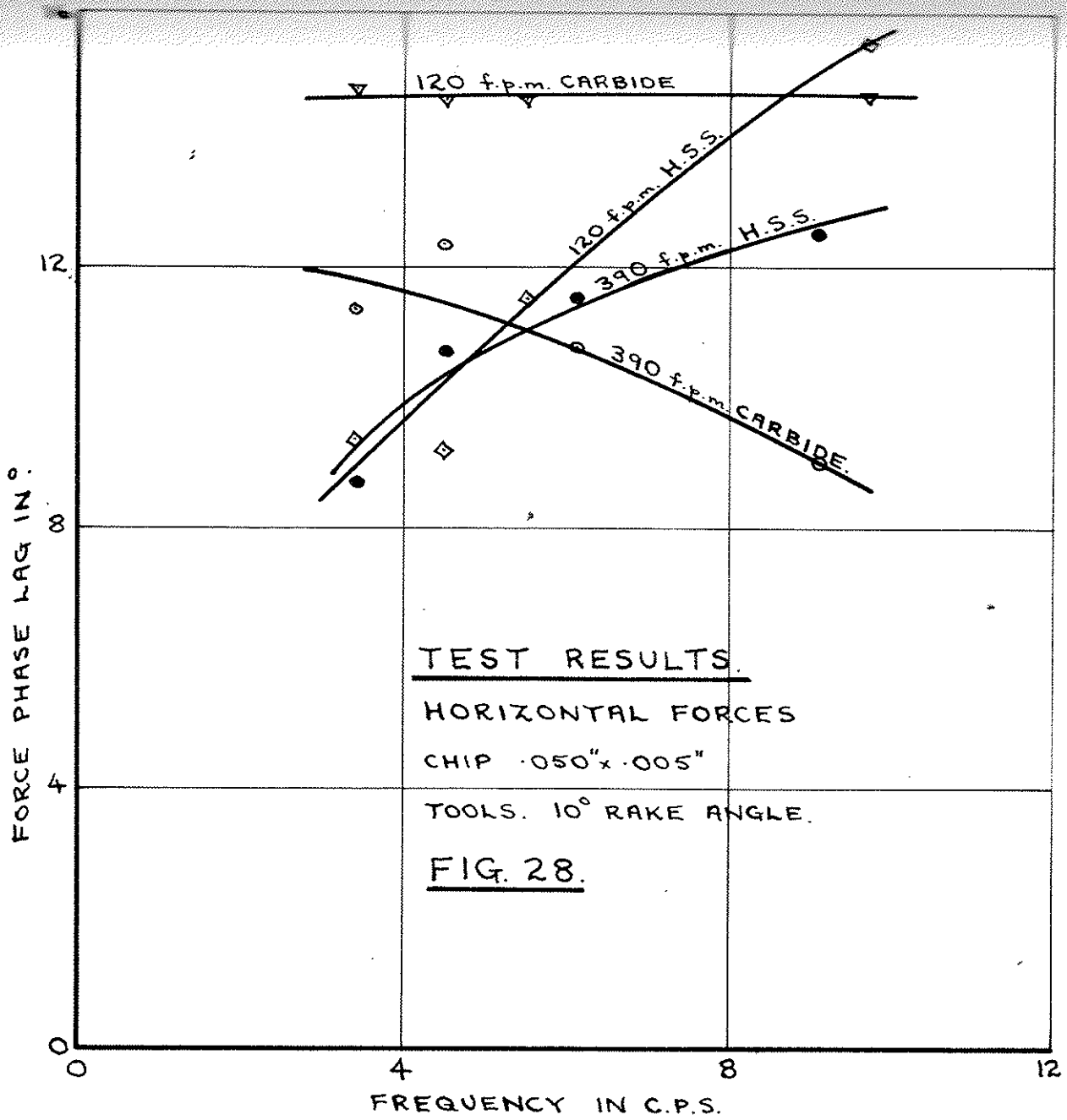
120 f.p.m. CARBIDE
120 f.p.m. H.S.S.
390 f.p.m. H.S.S.
390 f.p.m. CARBIDE.
FORCE PHASE LAG IN °.
0
4
8
12
0
4
8
12
FREQUENCY IN C.P.S.
TEST RESULTS.
HORIZONTAL FORCES
CHIP ·050"x·005"
TOOLS. 10° RAKE ANGLE.
FIG. 28.

or five points for each cutting condition so that, allowing for the large random variation in the results, it was not possible to determine trends from this narrow frequency range.

6. Intermittent Cutting Tests.

6.1 Introduction.

The object of these tests was to examine the cutting forces under conditions similar to those encountered in milling cuts. Typically when face milling, a given tooth cuts a chip of nearly constant thickness for a quarter of a revolution then does not cut for the remainder of the revolution.

Since face milling is probably the most common industrial method of removing large quantities of metal rapidly, it is of considerable economic importance to determine whether chatter stabilisation effects, i.e. leading phase angles, occur at the start of a cut. In all previous tests at least 5 seconds of cutting had been allowed to give temperatures and hence cutting forces time to reach equilibrium before starting to record. In these tests records were made of the forces at the start of a cut of constant chip thickness. Since a cutting tooth may only be in contact with the workpiece for a tenth of a second or less it is the first tenth that is of interest.

6.2 Apparatus.

The rig used for intermittent tests was fundamentally similar to the rig described in section 4.1.

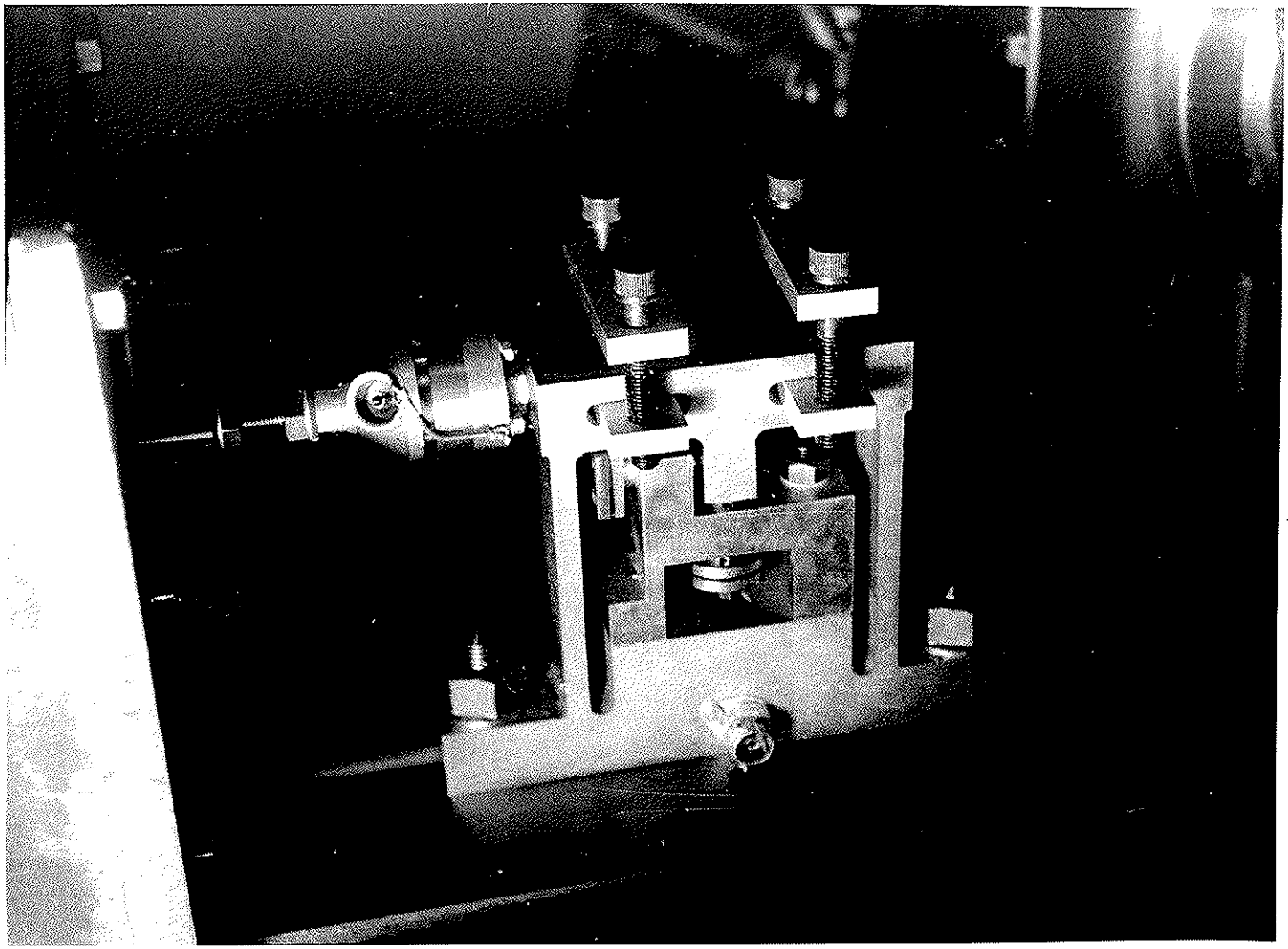

FIG. 29. VIEW OF "INTERMITTENT" RIG.

A standard 20" Archdale mill had a specimen mounted on the arbor while the cutting tool and its control and measurement equipment was mounted on the table of the machine which could then be used as a lathe. The specimen was a segment of a disc so that cutting only occurred for approximately half a revolution. A general view of the rig is shown in Figure 29 while Figure 30 is a sketch of the dynamometer and suspension system.

In this dynamometer the vertical leaf springs or struts were used both as the tool suspension units and as measuring elements, instead of using a set of struts for measurement purposes and a separate set of leaf springs for suspension as in the previous rig. The use of this system together with inductive pick ups instead of strain gauges, was dictated by the availability of equipment.

The vertical force was measured directly by the central vertical inductive pick up which measured the vertical deflection of the head, due to the shortening of the support struts under load. The horizontal force is the vector sum of the support stiffness, damping, and inertia forces required to move the head of the dynamometer and the applied force from the electromagnetic vibrator on the left.

The combined damping and excitation force from the vibrator was measured by the capacity force pick up between the vibrator

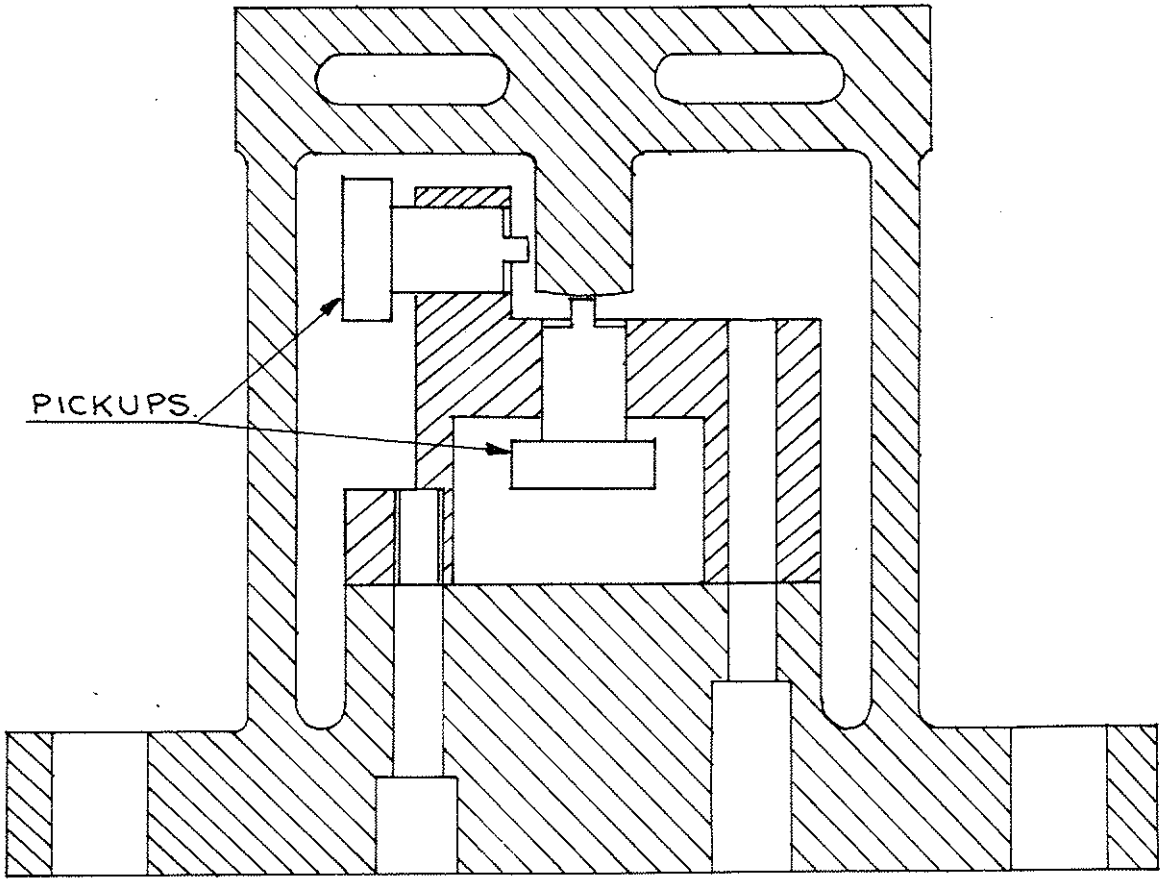

FIG. 30. INTERMITTENT RIG DYNAMOMETER.

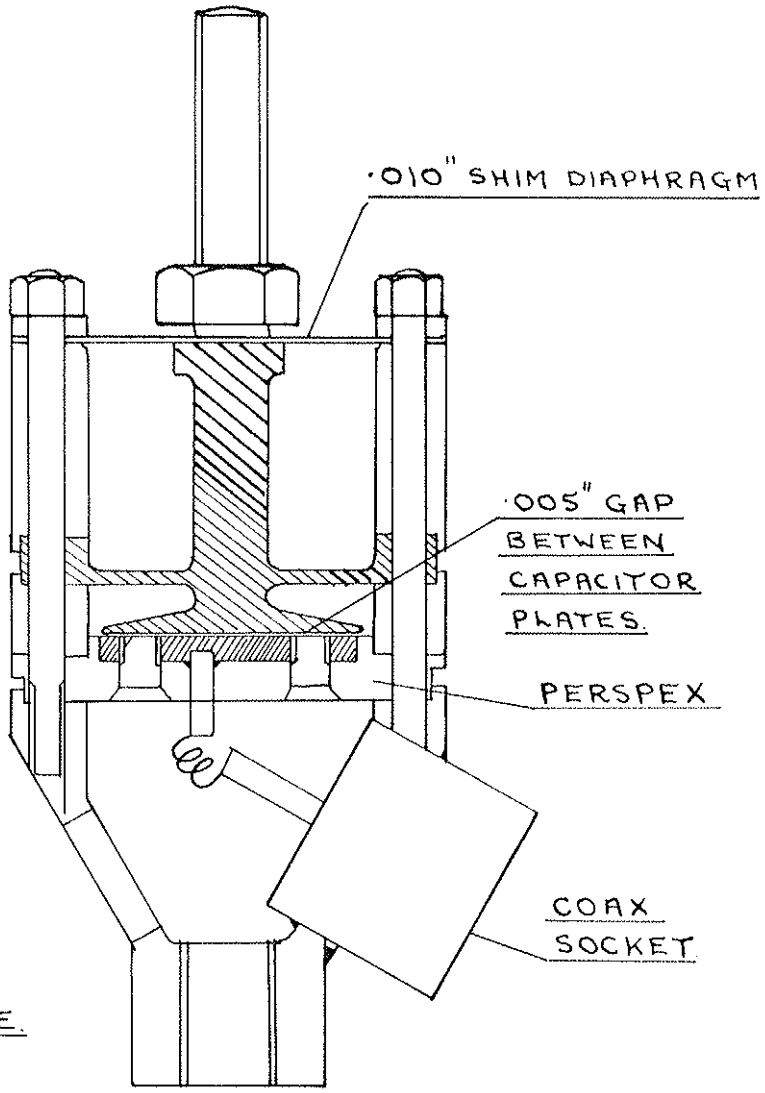

SCALE
2 x FULL SIZE.

DIAPHRAGM
·030" THICK $\frac{3}{4}$" DIA.
LOWER CAPACITOR
PLATE OF BRASS,
BOLTED INTO PERSPEX.

FIG. 31.
FORCE
TRANSDUCER.

spindle and the dynamometer head. Oscillation without cutting then gave the force required to oscillate the dynamometer head; this force varied in amplitude and direction as the frequency changed. Figure 31 gives a cross-section of the force pick up, which was modified from a Cambridge design. The displacement of the head was measured by the horizontal inductive pick up.

Both inductive pick ups and the capacity transducer were used with standard commercial frequency-modulated gauge oscillator systems. The reactive element forms part of a resonant circuit so that a change in reactance gives a change in resonant frequency; this frequency change is detected by frequency discriminator circuit comprising two circuits tuned to frequencies slightly above and below the oscillator frequency. The difference in output between the detector circuits is a measure of the pick up reactance change.

The control and excitation circuit was similar to that described in Section 4.1. In this case however the damping signal was derived from the horizontal inductive pick up. Since this displacement signal must be differentiated to give a damping force proportional to velocity, the signal from the pick up was fed through a condenser to the virtual earth of the adding amplifier. A small series resistor was also required on the input

to prevent instability in the amplifier.

The output of the amplifier, which was the sum of the damping force and forcing signal, fed the power amplifier via an impedance matching network; the amplifier output was connected directly to the electromagnetic vibrator which could give 140 lb. force peak to peak. Figure 32 gives a circuit diagram and Figure 33 gives experimentally determined dynamometer response curves with, and without, the damping circuit in operation. Care must be taken when setting up such a circuit since the load impedance on the output of the frequency modulated amplifier units is dominated by the impedance of the measuring equipment; change of recording amplification and hence impedance also changes the servo loop gain and can give instability or insufficient damping.

6.3 Measurements.

An ultra-violet, direct-writing, twelve channel recorder was available for these tests; four channels were used with nominally identical fluid damped galvonometers of 500 c/s. natural frequency. Since the galvonometers were of low impedance (less than 100 ohms), series resistors were used to raise the impedance and to set the effective recording amplification to a suitable value. The four channels recorded were:-

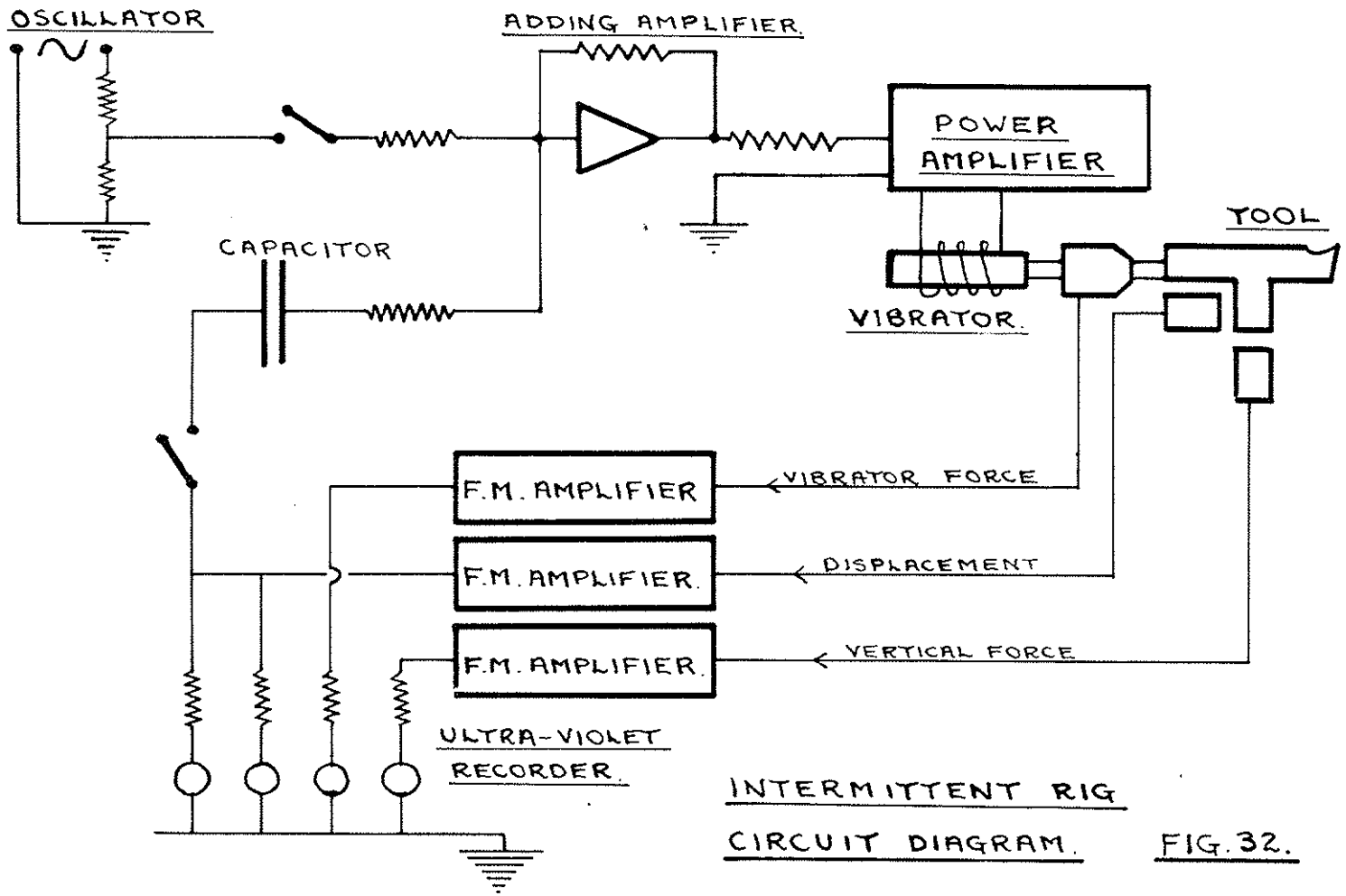

INTERMITTENT RIG CIRCUIT DIAGRAM. FIG. 32.

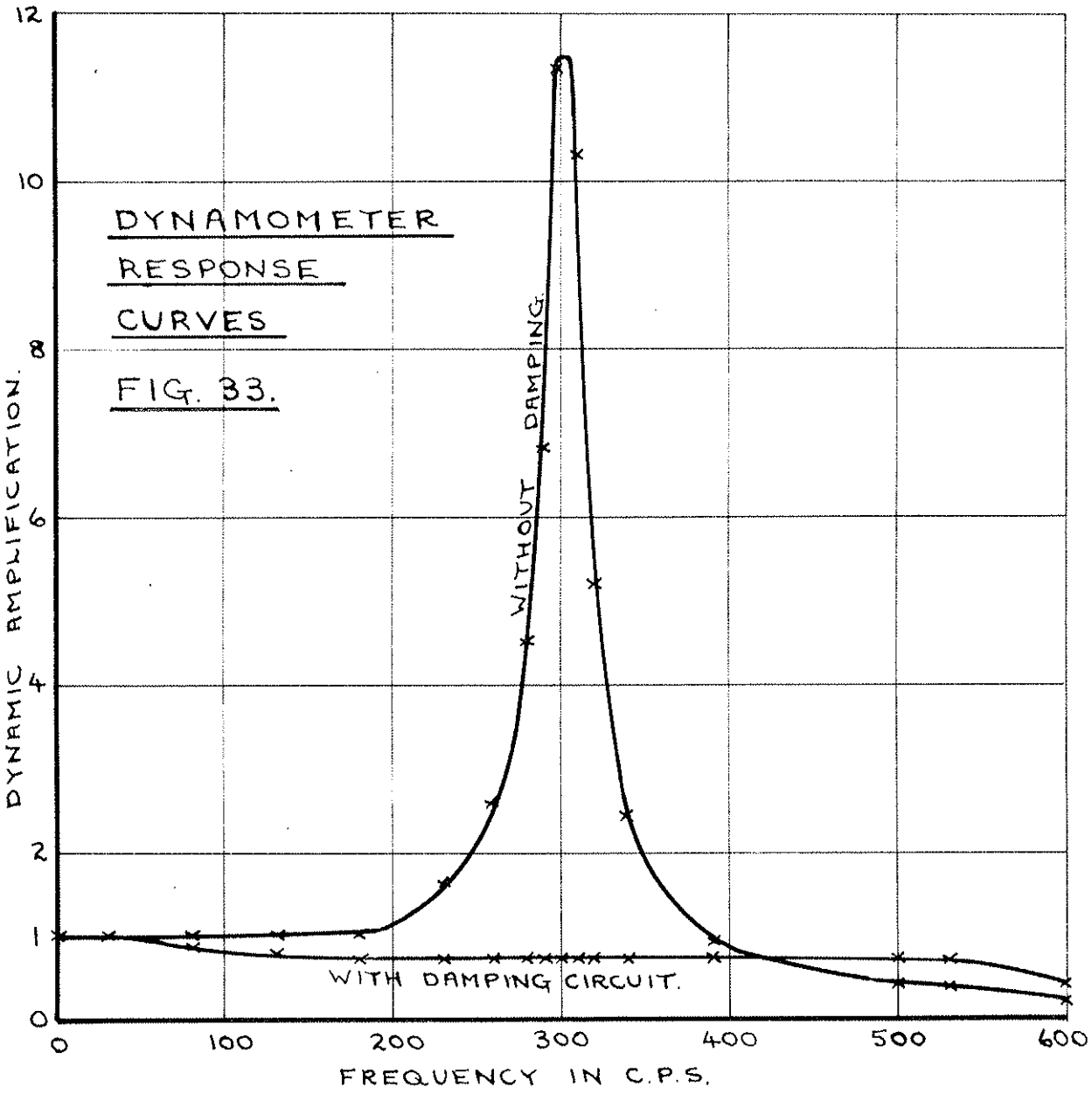
DYNAMOMETER
RESPONSE
CURVES
FIG. 33.
DYNAMIC AMPLIFICATION.
FREQUENCY IN C.P.S.
WITHOUT DAMPING.
WITH DAMPING CIRCUIT.
0
1
2
4
6
8
10
12
0
100
200
300
400
500
600

(i) The displacement from the horizontal pick up

(ii) The vibrator force from the capacity pick up

(iii) The vertical force from the vertical pick up

(iv) The displacement, coupled via a condenser and resistor and amplified to give the reference trace used for phase determination.

The force amplitudes and directions were determined from the traces using the methods described in Appendix 2. A typical vector triangle is shown in Figure 34. The difference between the observed force when cutting and when not cutting gives the net cutting force. The displacement is the difference between the observed displacement and the machine displacement, determined by a resonance test of the machine. All machine resonances were avoided when testing. Figure 35 gives the response curve of the machine. Since machine deflections are small, they can in most cases be neglected; at the start of a cut transients will introduce errors.

Both horizontal and vertical forces were recorded but the results obtained for the vertical forces have not been given because:-

VECTOR DIAGRAMS.

FORCE AND DISPLACEMENT.

FIG. 34.

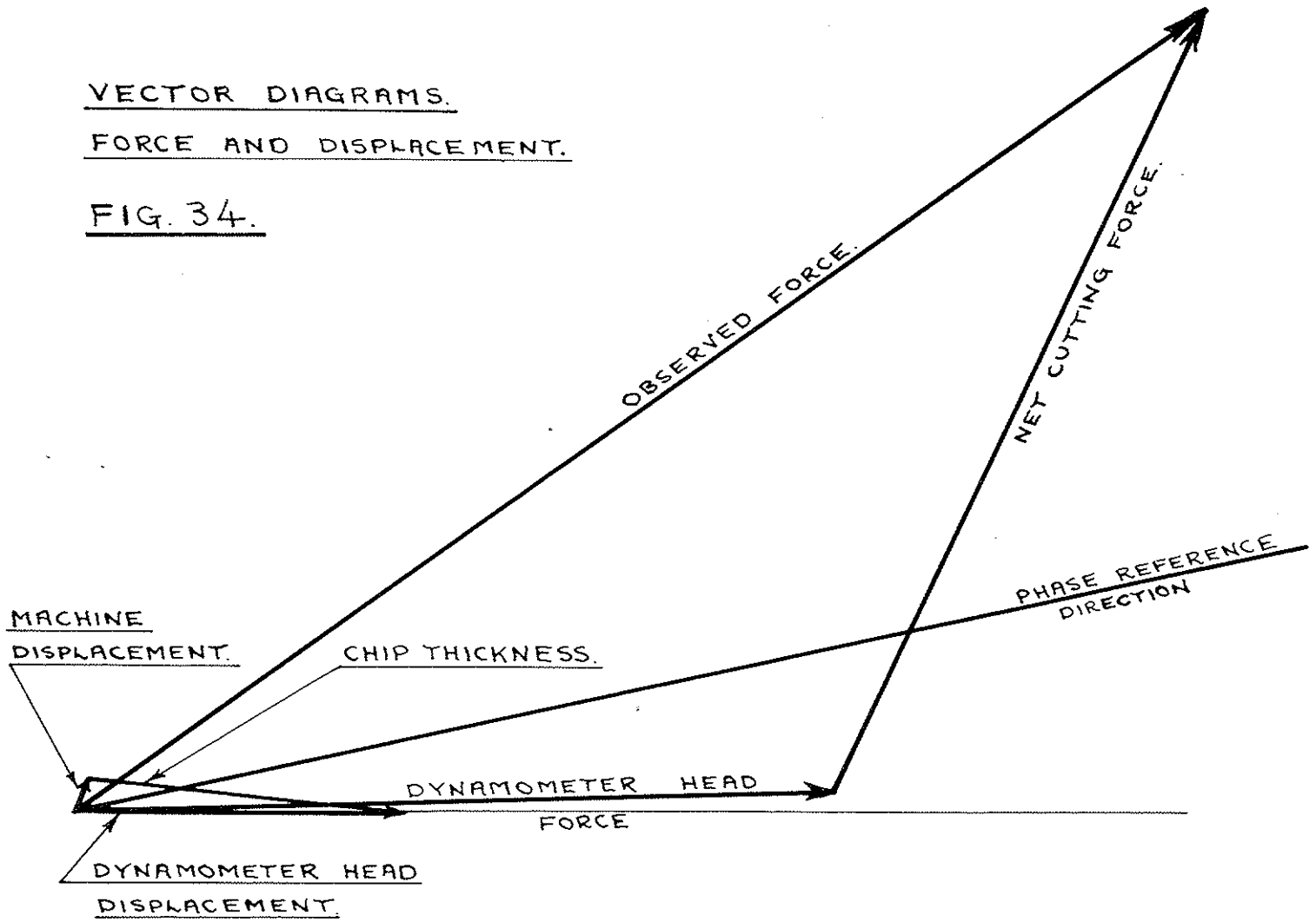

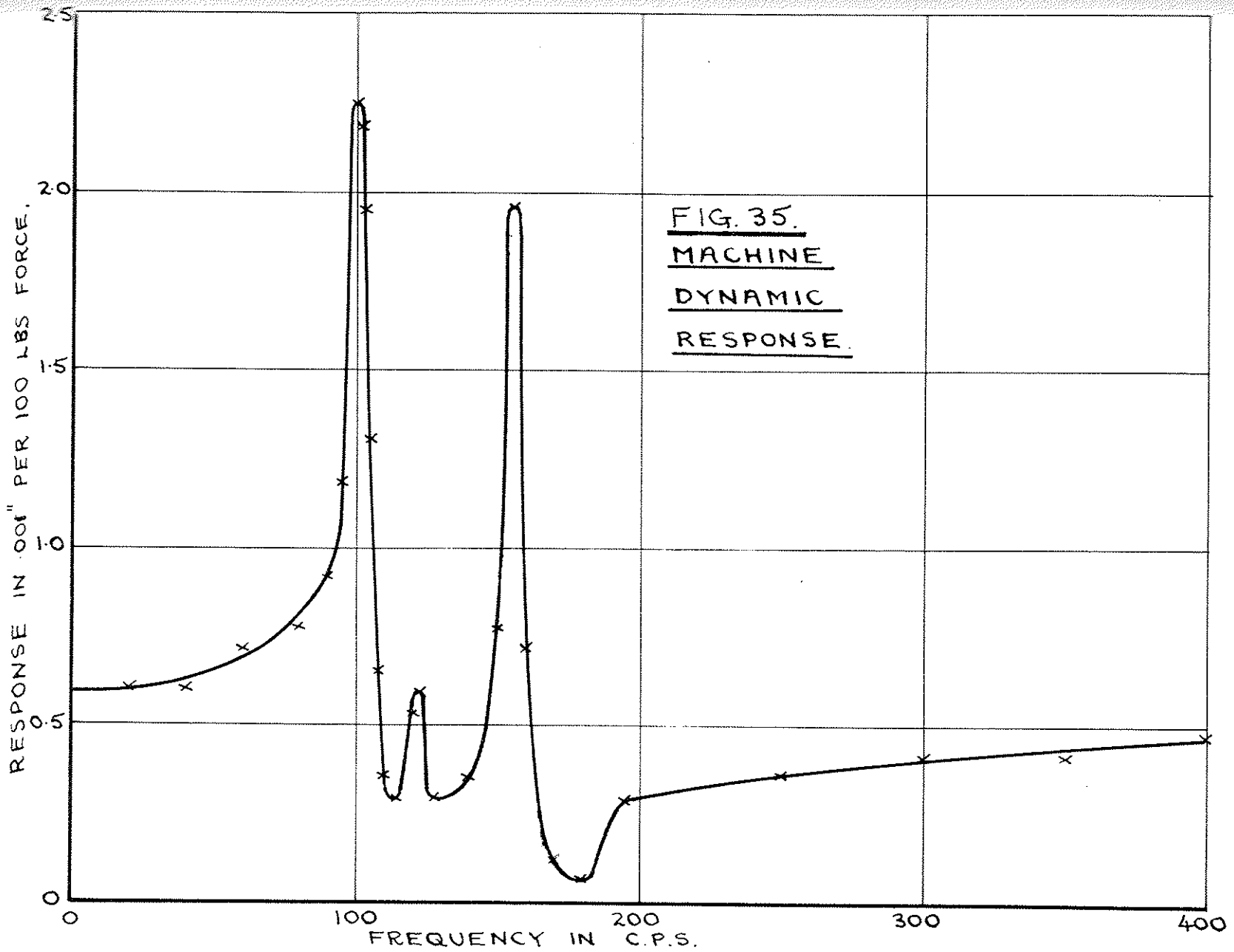

FIG. 35.
MACHINE
DYNAMIC
RESPONSE.

(i) The alternating vertical forces were small relative to the steady state value and hence the noise levels which increase with the steady state force were larger than the signal being measured. When random fluctuations are larger than the fundamental signal it is not possible to measure phase or amplitude accurately.

(ii) The vertical deflection measured by the pick-up is the sum of the vertical deflection of the struts and vertical distortions of the top of the dynamometer. This distortion is due in part to the cutting forces and partly to the stresses induced at the tops of the supporting struts. Unfortunately the head distortions, though not as large as the strut deflections, are indeterminate in amplitude and phase so that the observed vertical forces are not reliable. Modification of this dynamometer to improve the vertical measurement was not considered feasible.

As the previous tests had indicated that changes in the vertical forces were of secondary interest and vertical forces do not influence simple regenerative chatter, lack of vertical phase data was not considered important.

6.4 Results.

A typical test record is shown in Figure 36. The results derived from these tests are given in Figures 37-45.

Figure 37 shows the variation in the horizontal cutting force for a particular cutting condition while Figure 38 shows the corresponding phase angle plotted against vibration frequency; this phase angle is the angle by which the horizontal force leads the chip thickness. The points plotted are the result of taking the average of up to fifty points in the "steady state" i.e. after allowing cutting conditions to stabilise. The cutting forces are expressed as a cutting stiffness given by the increase in force divided by the increase in chip area.

Individual points on Figure 38 were investigated in detail to see how the phase angle varied at the beginning of a cut. The phase angle each cycle was determined and the results are given in Figures 39-42; the derived phase angle is plotted against the particular cycle after the start of the constant chip thickness cut; since the frequency is constant, this scale is also a scale of time after the start of a cut.

As a contrast to the results obtained at low cutting speeds (60 feet per minute surface speed), Figure 43 gives results obtained at 300 feet per minute surface speed with an oscillation

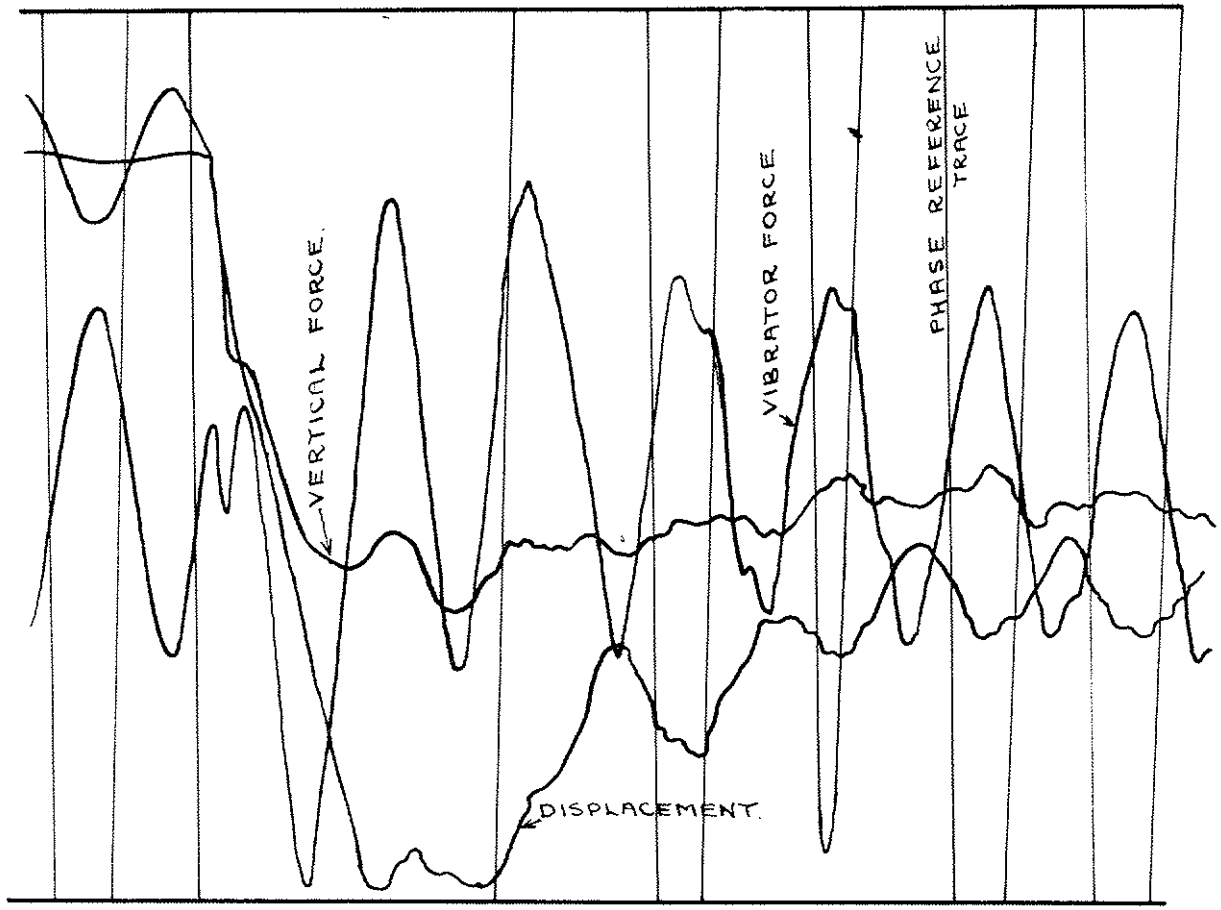

INTERMITTENT RIG.

TEST RECORD. FIG. 36.

80 c.p.s. 60 f.p.m.

CHIP .250" x .0039" TOOL 10° H.S.S.

frequency of 135 c.p.s. and a range of chip thickness.

At the start of a cut, neglecting oscillation effects the force rises to a value above the "steady state" value and then decays approximately exponentially to the "steady state". The ratio between the maximum and the steady value of the horizontal force has been plotted as a function of chip thickness for several cutting velocities in Figure 44. The corresponding decay time constants are given in Figure 45; the figures quoted are not to be taken as accurate since the decay curves are not exponential and the figures have not been corrected for dynamometer response effects.

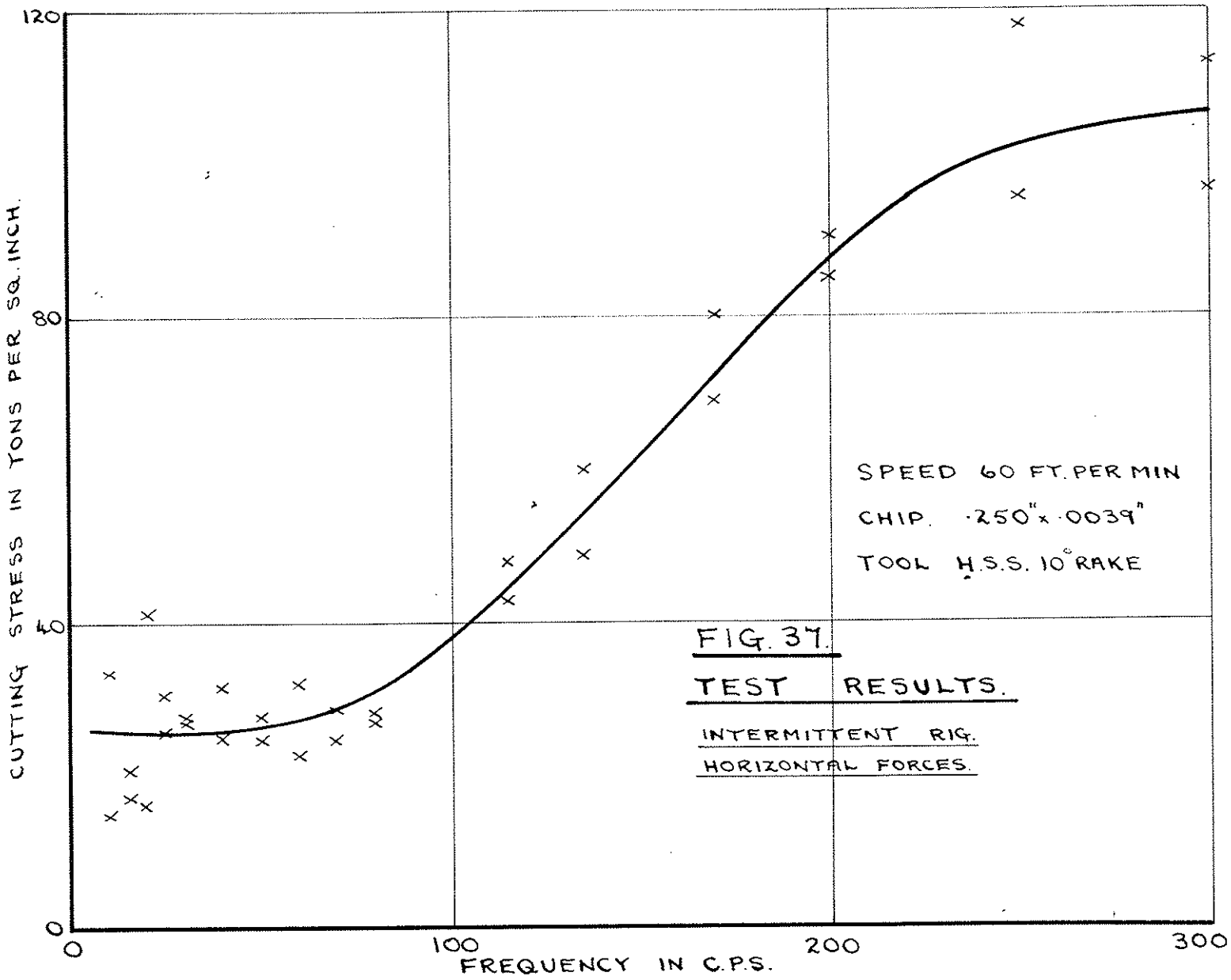

FIG. 37.

TEST RESULTS.

INTERMITTENT RIG.
HORIZONTAL FORCES.

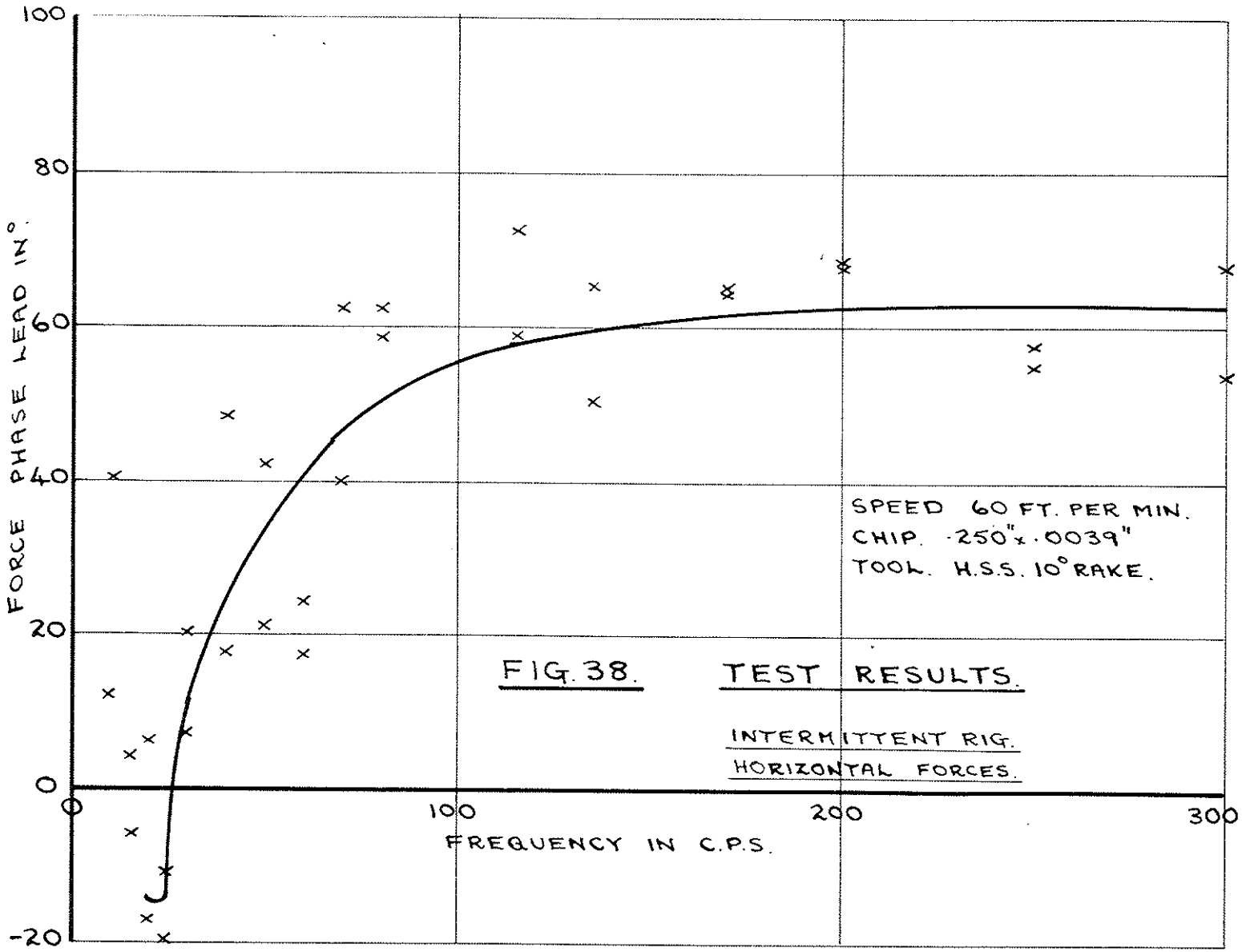

FIG. 38. TEST RESULTS.

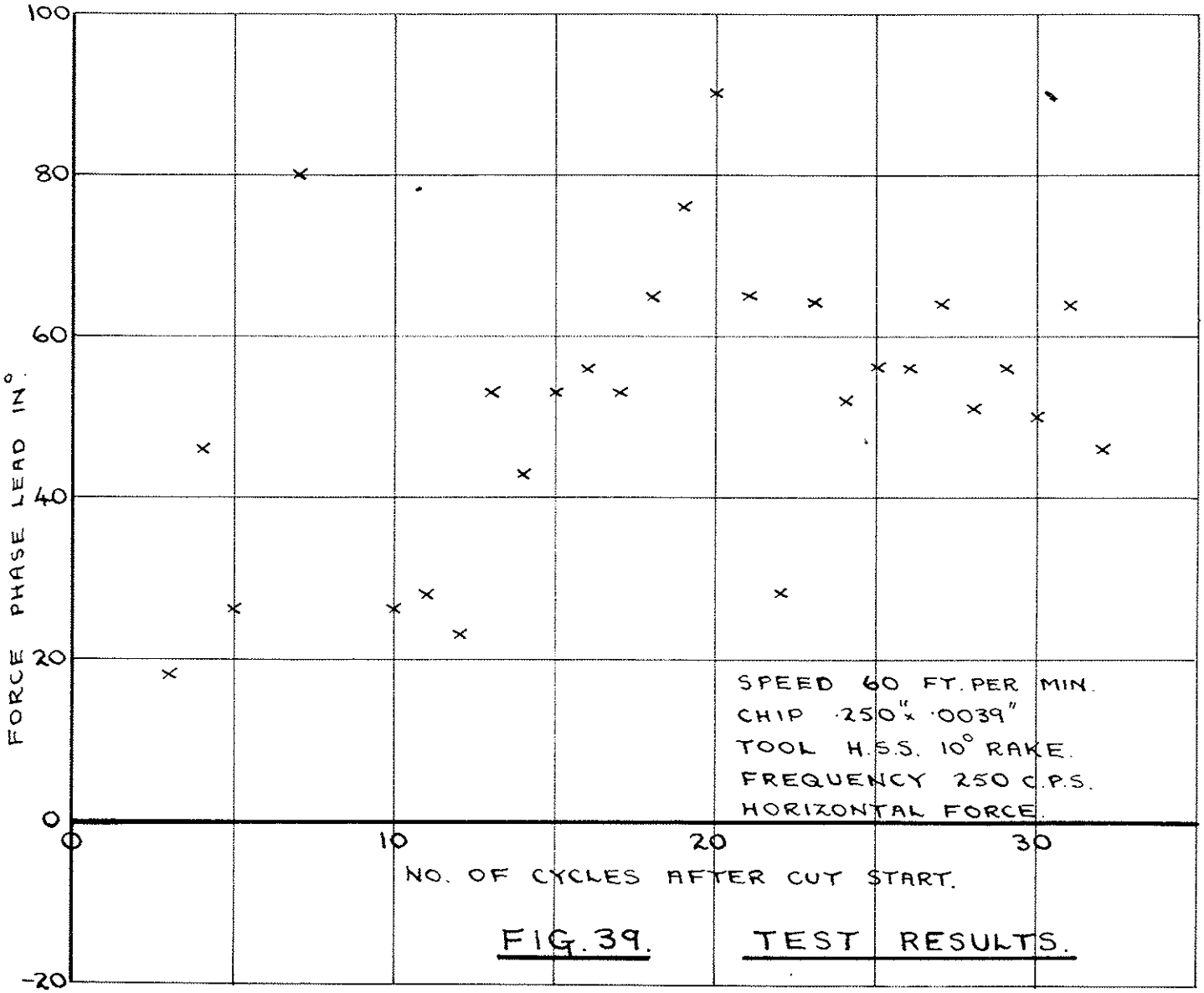

FIG. 39. TEST RESULTS.

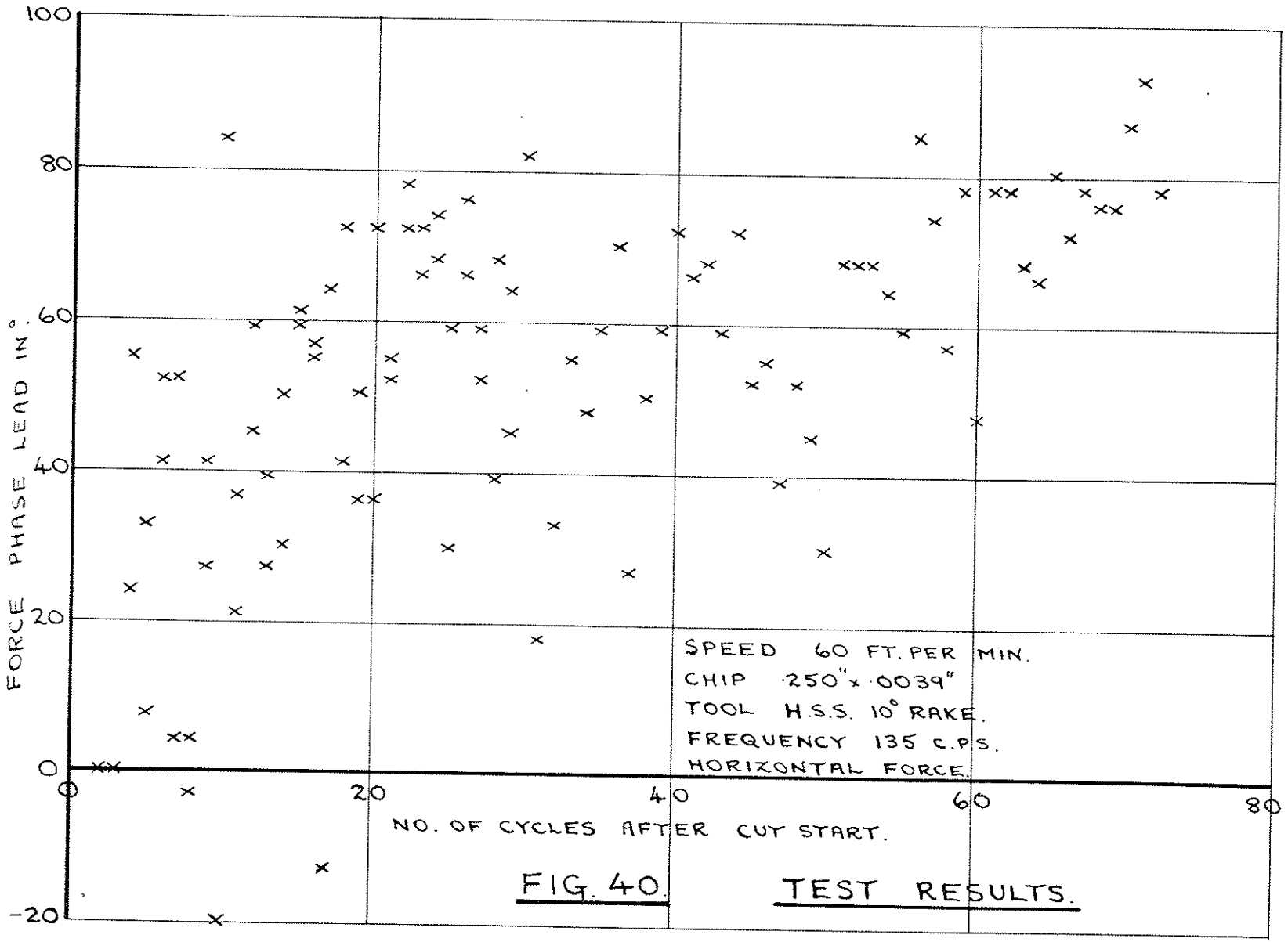

FIG. 40. TEST RESULTS.

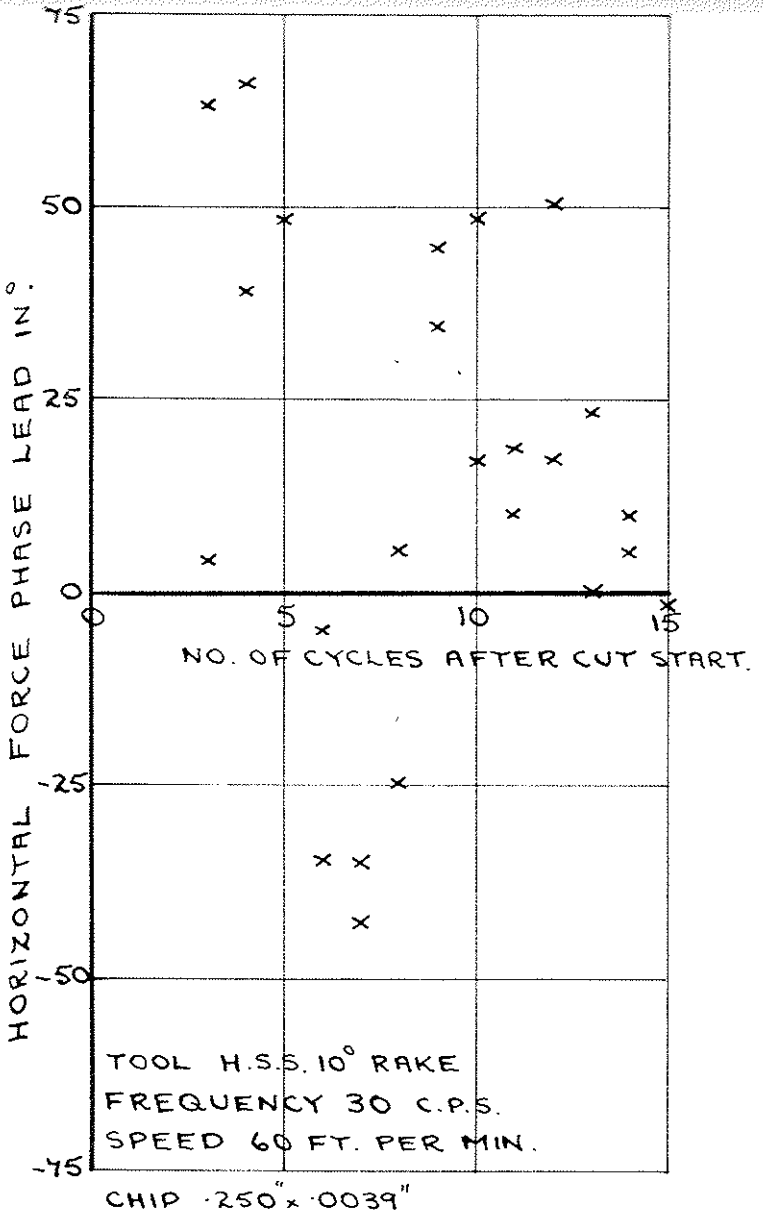

FIG. 41

TEST RESULTS.

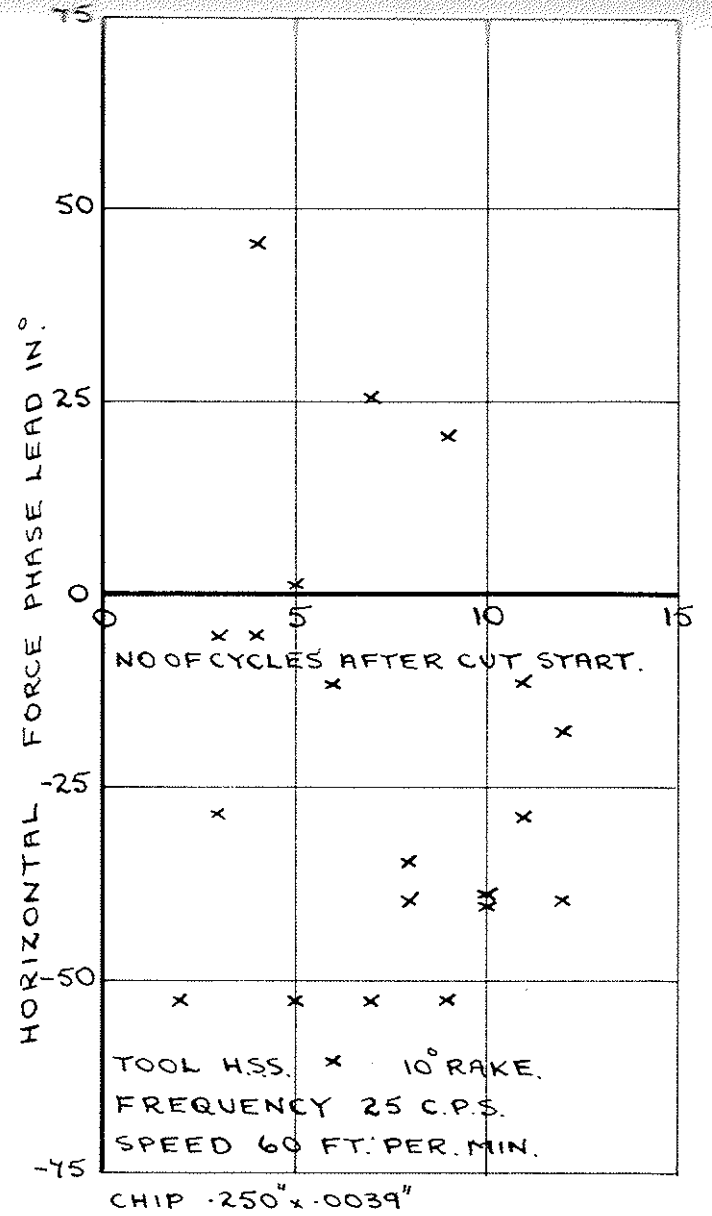

FIG. 42.

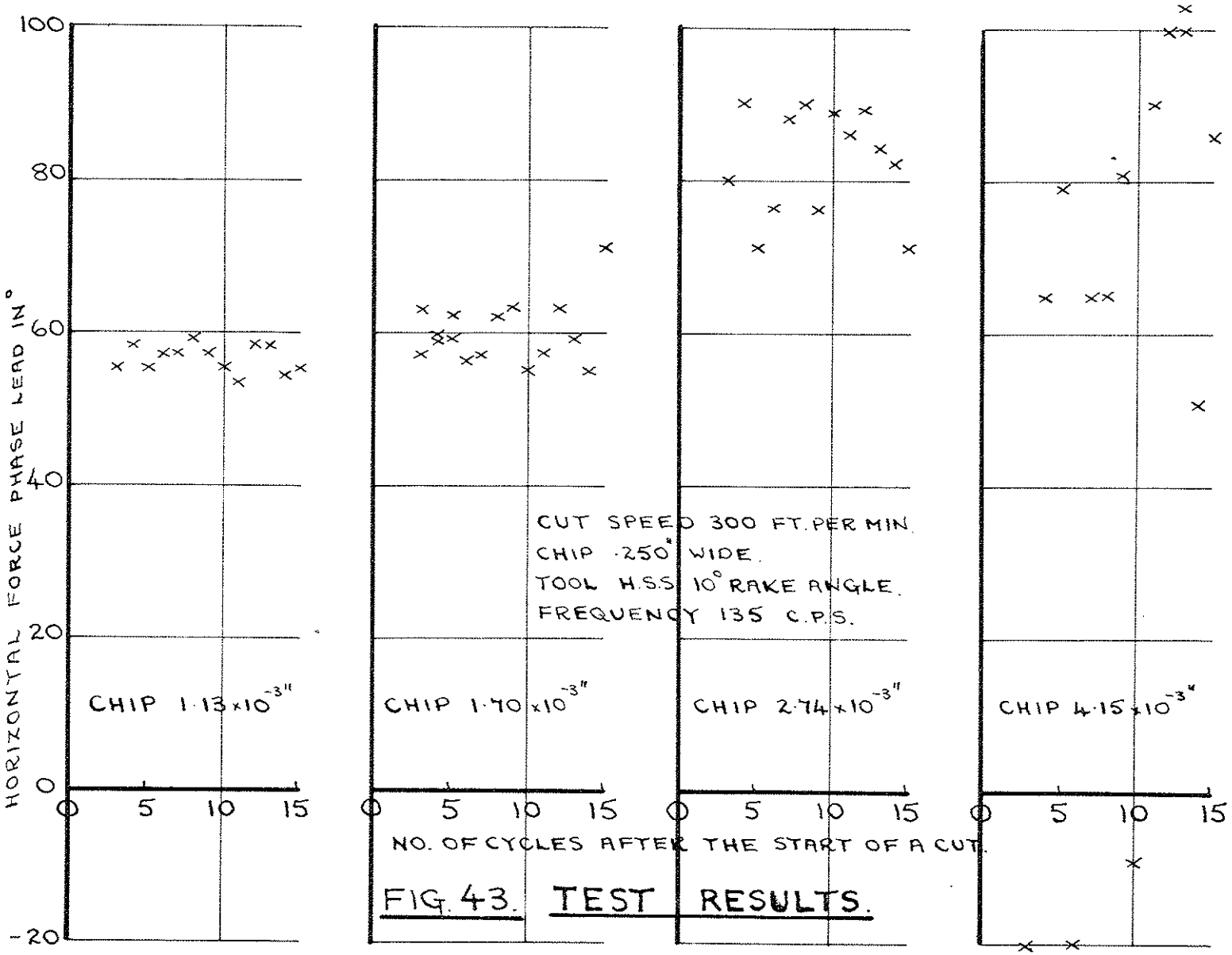

FIG. 43. TEST RESULTS.

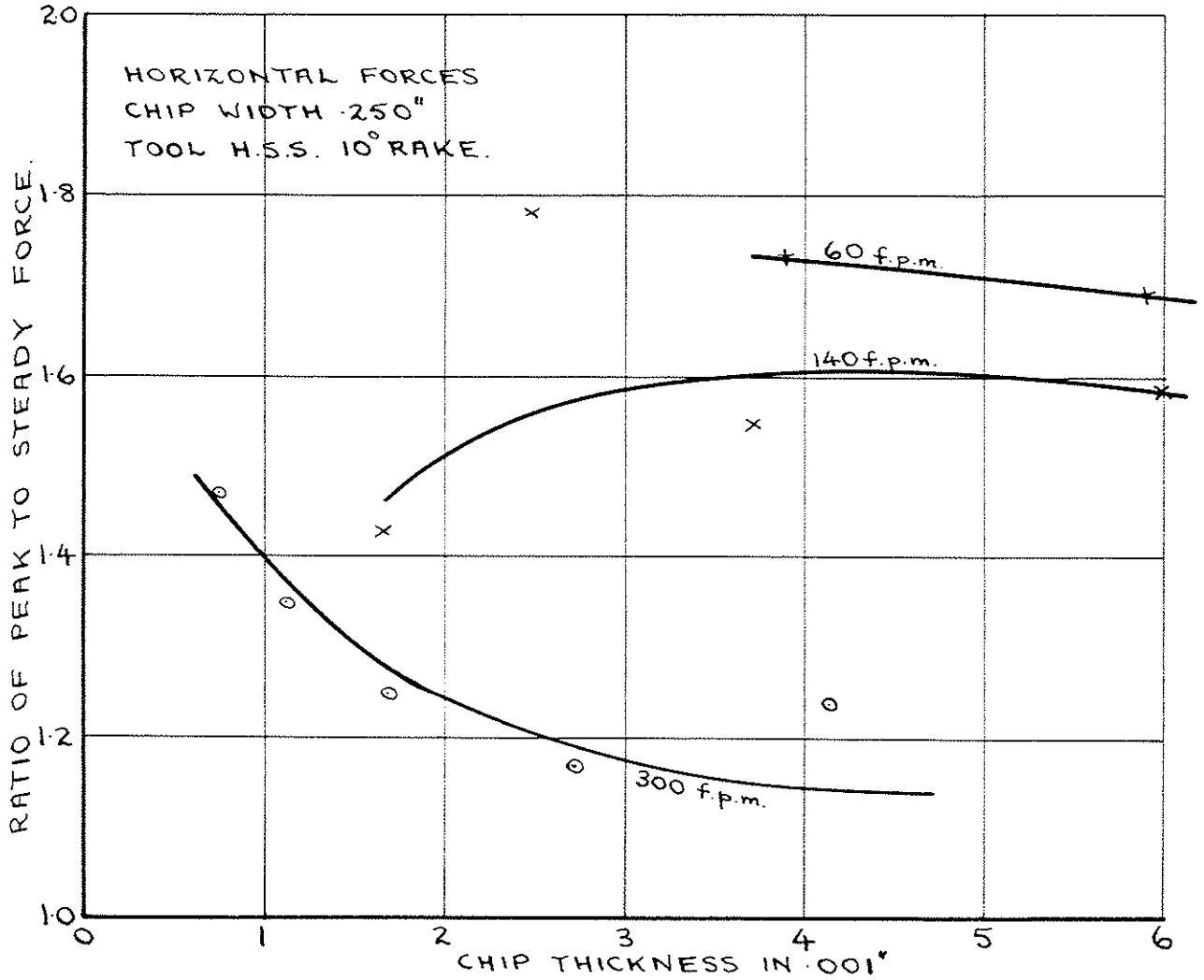

TEST RESULTS. FIG. 44.

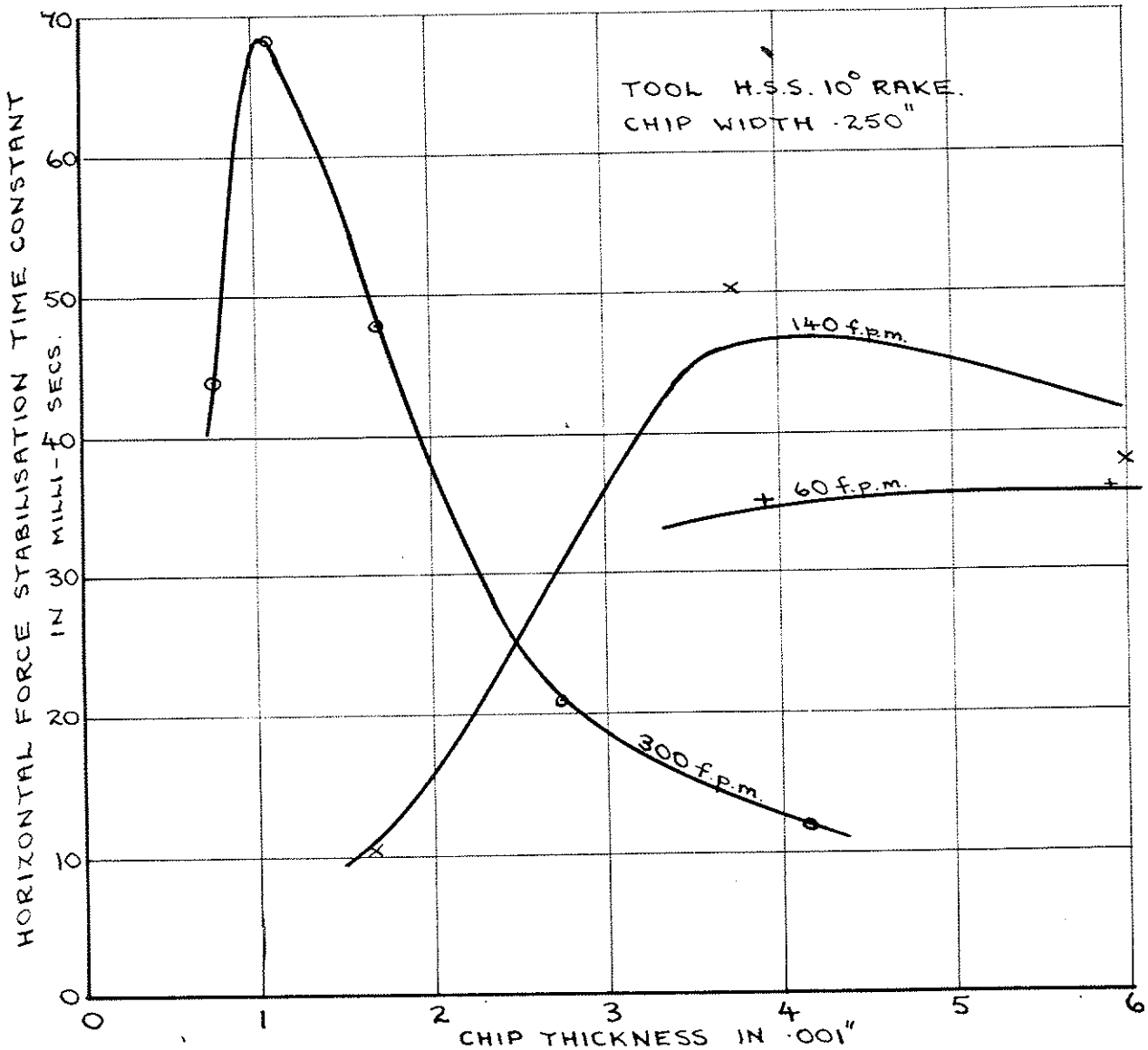

FIG. 45. TEST RESULTS.

7. Main Trends of Results.

As can be seen from the results, as the frequency increases the lag of force behind displacement observed by Doi and Kato decreases to zero, changes sign, and becomes the lead deduced by Tobias.

It is not easy to generalise from such varied results. The main trends, neglecting the results from the high rake tools, which give exaggerated results, can conveniently be divided into high and low frequency effects.

At low frequencies the forces lag behind the displacement for all conditions except high cutting speeds where this effect cannot be seen. Force amplitudes are reduced from the static value and there is no detectable difference between the conditions corresponding to Figures 14(a) and (b).

At high frequencies large angles of lead occur. Low cutting speeds give a large phase angle between horizontal and vertical forces with a corresponding increase in the amplitude of the horizontal force; this effect increases with frequency. High cutting speeds again give high horizontal force phase leads but less force increase and there is not a marked increase in the phase between horizontal and vertical force.

At a given typical chatter frequency such as 100 c/s. the normal force phase lead tends to decrease as the cutting speed increases.

The effect of increase of chip thickness is indeterminate.

The shape of the curves obtained for the "steady state" condition from the "intermittent" rig Figures 37 and 38 agree qualitatively with those obtained in Figure 17; close agreement is not to be expected since tool material and cut width differed.

The detailed "intermittent" tests in Figures 39 and 42 suggest that at low cutting speeds and high frequencies a cool tool gives lower phase leads at the start of a cut but at low frequencies the random variations are so large that no effect can be discerned.

At high cutting speeds, and high frequency (Figure 43) the phase angle does not vary. For small cuts it is remarkably steady; as the depth of cut increases the noise level increases greatly but there is no steady trend at the start of the cut.

8. Suggested Causes of Phase Changes.

8.1 Introduction.

There is apparently little correlation between the results and there is no one simple trend which could be explained by one mechanism. However, logical explanations for the observed results can be proposed, though such explanations are qualitative rather than quantitative. It is simpler to consider the results with reference to the suggested causes of phase change.

The cutting process is so complex that there are invariably several factors affecting any observed results. In the following discussion the nomenclature of Figure 46 (following Merchant (9)) will be used. The shaded sector is the cutting tool while the workpiece, on the left, is moving vertically downwards. The relationships on the left are obtained by differentiation of the expressions for the forces and give the force change due to any change in tool take angle γ, shear plane angle ϕ, friction angle ρ or cutting direction α.

Although work by Palmer and Oxley (10) consider a cutting process in terms of a field of work-hardening plastic flow, their work was carried out at such a low speed of half an inch per minute that their results are not applicable. Inspection of microsections obtained by Heginbotham and Gogia (11), shows that

CUTTING FORCES

$$P_4 = h\,b\,\tau\ \mathrm{COSEC}\,\phi\ \mathrm{SEC}(\phi+\rho-\gamma)\ \mathrm{SIN}(\rho-\gamma)$$

$$\frac{\delta P_4}{P_4} = \left[\mathrm{TAN}(\phi+\rho-\gamma) - \mathrm{COT}\,\phi\right]\delta\phi + \left[\mathrm{TAN}(\phi+\rho-\gamma) + \mathrm{COT}(\rho-\gamma)\right](\delta\rho-\delta\gamma) + \frac{\delta h}{h} + \frac{\delta\tau}{\tau}$$

$$P_1 = h\,b\,\tau\ \mathrm{COSEC}\,\phi\ \mathrm{SEC}(\phi+\rho-\gamma)\ \cos(\rho-\gamma)$$

$$\frac{\delta P_1}{P_1} = \left[\mathrm{TAN}(\phi+\rho-\gamma) - \mathrm{COT}\,\phi\right]\delta\phi + \left[\mathrm{TAN}(\phi+\rho-\gamma) - \mathrm{TAN}(\rho-\gamma)\right](\delta\rho-\delta\gamma) + \frac{\delta h}{h} + \frac{\delta\tau}{\tau}$$

WHERE

τ IS THE SHEAR STRESS
b IS THE CHIP WIDTH.

DUE TO A CHANGE IN DIRECTION OF $\delta\alpha$

$\delta P_4 = P_1\,\delta\alpha$ $\qquad$ $\delta P_1 = -P_4\,\delta\alpha$.

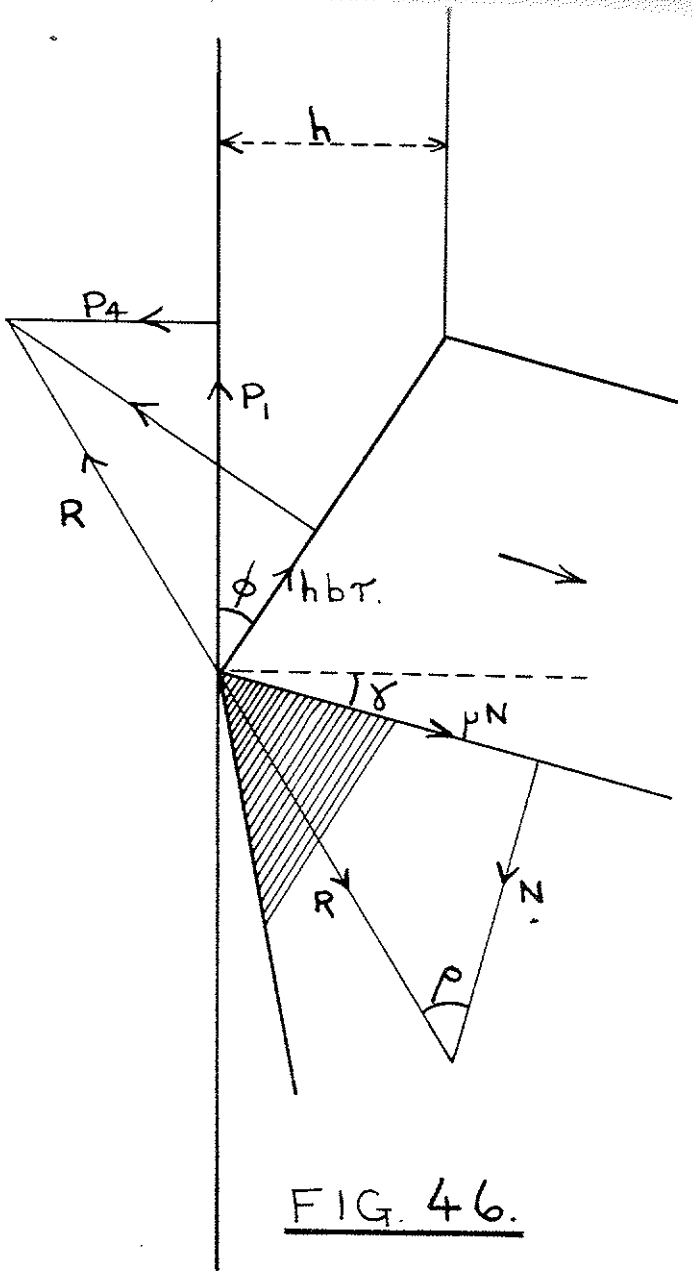

FIG. 46.

at the higher cutting speeds, chip shear is occurring substantially in a single plane so that it is legitimate to use Merchant's approach. At low speeds, associated with large built up edges, use of Merchant's approach is only justified by its convenience for analysis. It is of course important that when there is a built up edge the effective rake angle is not equal to the nominal tool rake angle but is an "effective" value dependant on the shape and size of the built up edge.

The basic assumptions that have been made and the consequent deductions are listed below.

8.2 Viscosity Effect.

The basic assumption is that the "friction" between the chip and the tool rake face is proportional to velocity so that it behaves as a viscous damping force rather than as a "dry" friction. Since the material of the chip, at high temperature and yield pressure, is in a semi-plastic state this is a reasonable assumption.

Appendix 4 gives the derivation of the expression for the horizontal dynamic cutting force; the tangent of horizontal force phase angle is proportional to the frequency and inversely proportional to the cutting speed so that this effect will be most noticeable at low speeds and high frequencies as in

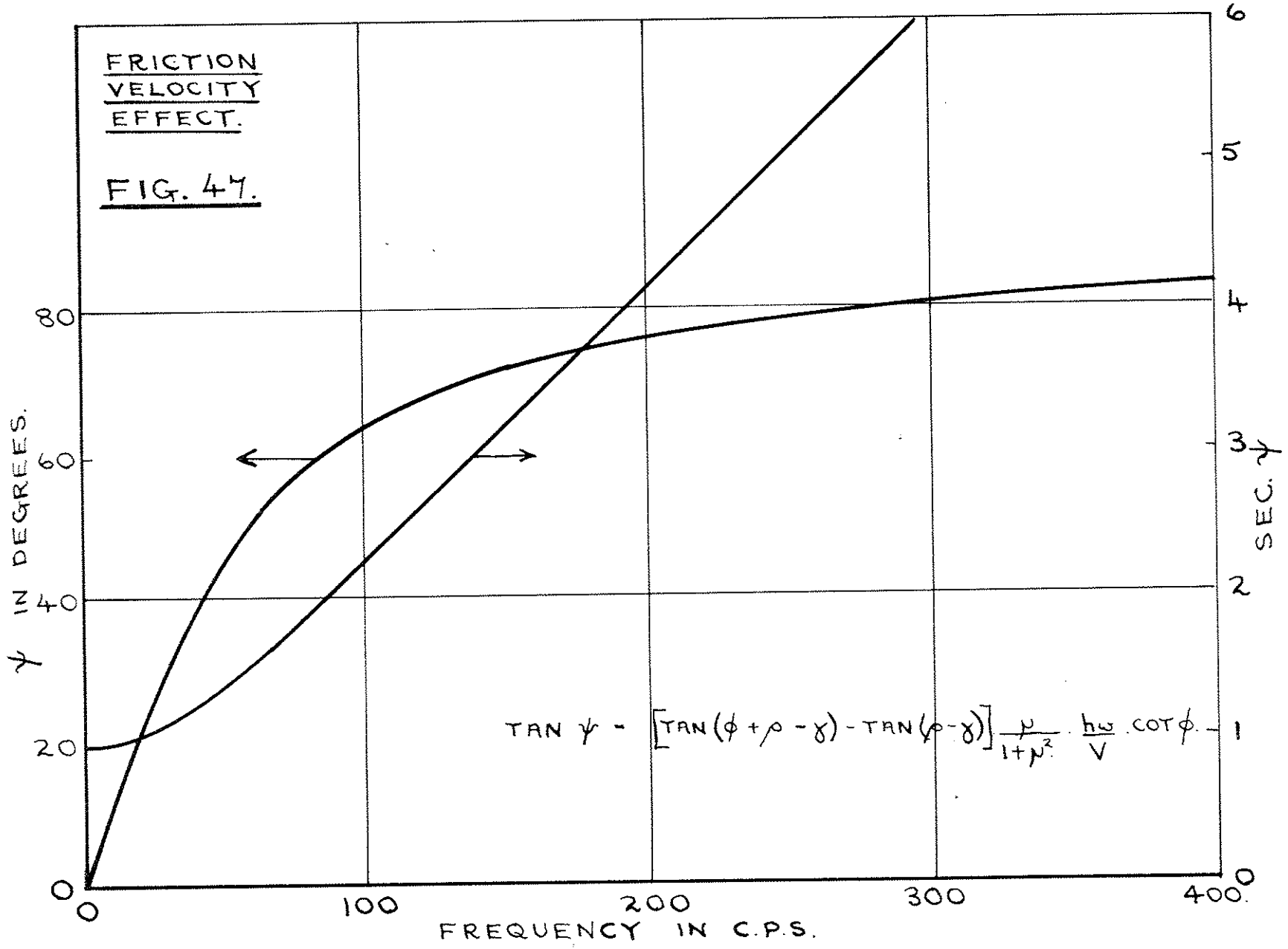
FRICTION
VELOCITY
EFFECT.
FIG. 47.
ψ IN DEGREES.
SEC. γ
FREQUENCY IN C.P.S.
0
20
40
60
80
100
200
300
400
1
2
3
4
5
6
TAN ψ = [TAN(φ + ρ - γ) - TAN(ρ - γ)] μ/(1+μ²) · hω/V · COT φ.

Figures 17 and 18 which should be compared with Figure 47 which corresponds to the expressions derived in Appendix 4. This effect will not occur with the Figure 14(b) type of chip thickness variation.

The effect of these "friction" changes is much smaller on the vertical force than on the horizontal if the effective rake angle is small but is appreciable with large built up edges.

8.3 Friction-Temperature Effect.

For the mechanism the important variable is the temperature of the chip-tool rake interface where semi-plastic sliding is occurring. The "friction" at this interface will be affected by temperature as well as by relative velocity. The chip strength and hence the observed "friction" will decrease as the temperature rises. It is not possible to determine general tool temperature distributions under vibrating conditions analytically but individual conditions can be solved by rather laborious time-relaxation methods as shown in Appendix 7. Qualitatively the effect is to give a horizontal force phase starting at zero, rising to a maximum, then decreasing as the frequency rises, see Figure 48.

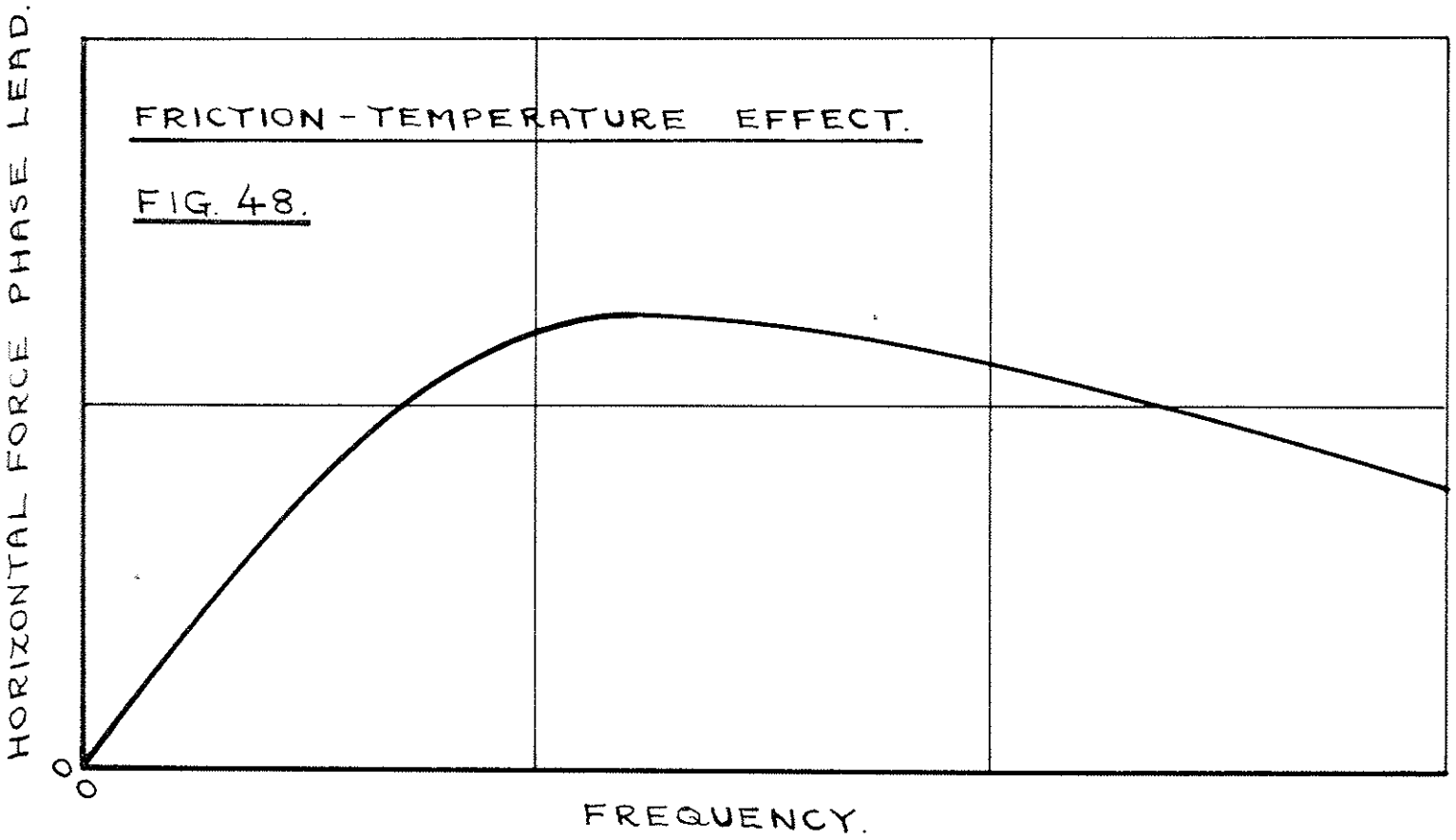
FRICTION - TEMPERATURE EFFECT.
FIG. 48.
HORIZONTAL FORCE PHASE LEAD.
0
0
FREQUENCY.

Unfortunately the "constants" required to give a quantitative check on this mechanism are not available since there is no information concerning the dependence of high strain rate shear strength on temperature at typical cutting temperatures and pressures. Also in practice there is a low speed "boundary layer" of metal moving relatively slowly along the top face of the tool giving shear over a finite thickness of the chip. The problem is analogous to fluid flow in that a knowledge of the velocity profile would be required for drag estimates. Again the vertical force effects are similar but very much smaller.

At low cutting speeds heat conduction to the tool and workpiece is such that the chip-tool interface temperature will be comparatively low. At low temperatures, away from the metal softening temperatures, the shear strength will be less dependant on temperature so that any observed effects would be small. This phase change should occur with both 14(a) and (b) chip thickness variation.

8.4 The "Geometric" Effect.

The preceding effects were concerned with the chip-tool interface and hence principally influenced the horizontal force; the geometric effect concerns the shear plane and so

affects both horizontal and vertical forces.

The basic assumption for this effect is that the power required in cutting is proportional to the volumetric rate of metal removal. This assumption is true to a first order in steady state cutting and is the basis of machine cutting capacity calculations. When applied to vibrating conditions it is important to realise that the instantaneous rate of metal removal is not simply proportional to chip thickness, due to the inclination of the shear plane. Appendix 5 gives the derivation of an expression for the instantaneous rate of metal removal, hence the vertical force and assuming a constant coefficient of friction, the corresponding horizontal force.

The effect is similar to that in section 8.2 but is smaller and affects the horizontal and vertical forces equally. The corresponding expression for 14(b) cutting shows that there will be no increase of cutting stiffness but phase effects will be similar.

8.5 The Built-up Edge Effect.

This effect arises from the inability of the built-up edge on the tool to respond instantaneously to cut variations; the size and angles of the built-up edge vary greatly with change of

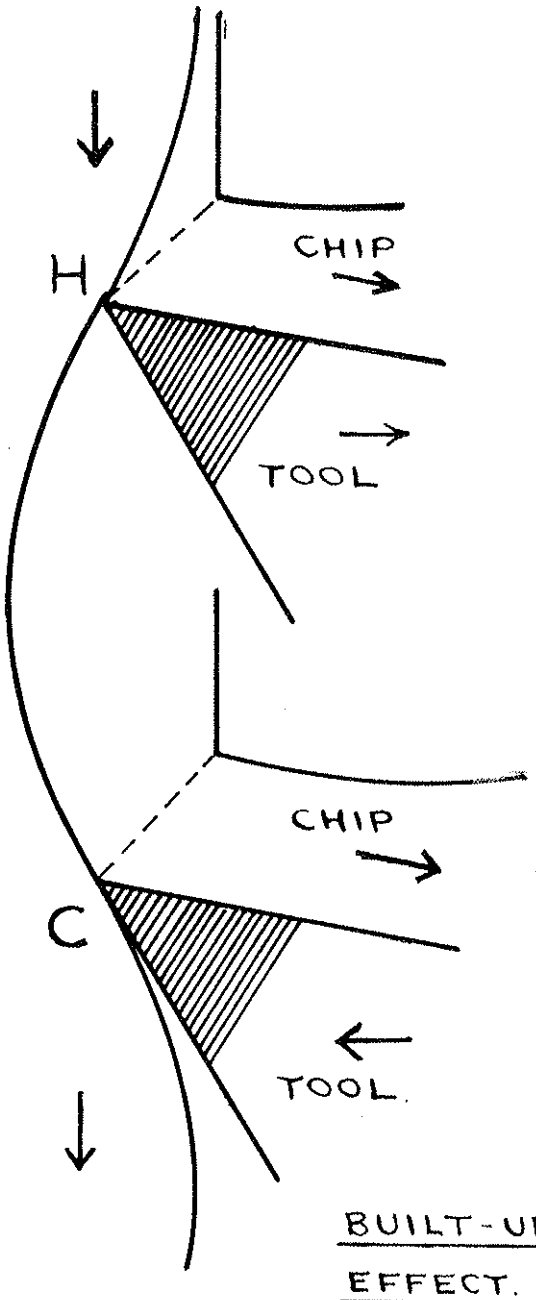

BUILT-UP EDGE EFFECT.

FIG. 49.

chip thickness but it takes an appreciable time (see Section 6.4, Figure 45) for the built-up edge to reach equilibrium.

Consider points H and C in Figure 49. At point H the tool has been cutting a larger than average chip for a considerable time, say of the order of a tenth of a second, and is thus at a comparatively high temperature. This high temperature will tend to give a small built-up edge, hence a low effective rake angle and corresponding high forces. At C, after a light cut, the cool tool will have a high built-up edge, high effective rake angle and hence low forces. Thus though the chip thickness is the same at H and C the forces will be higher at H. Expanding this line of reasoning to the remainder of a cycle gives the result that a lag of force behind displacement i.e. chip thickness, will be observed. The exact lag observed will depend on the thermal properties of the tool, the size of the built-up edge and the rate at which the built-up edge can alter its shape. At high frequencies it will be impossible for the edge to respond quickly enough to cutting changes and so no effect should be observed. At high cutting speeds there is no built up edge and this effect will not occur. Whether the chip thickness variation is caused by 14(a) or (b) cutting, the thermal effects and hence the

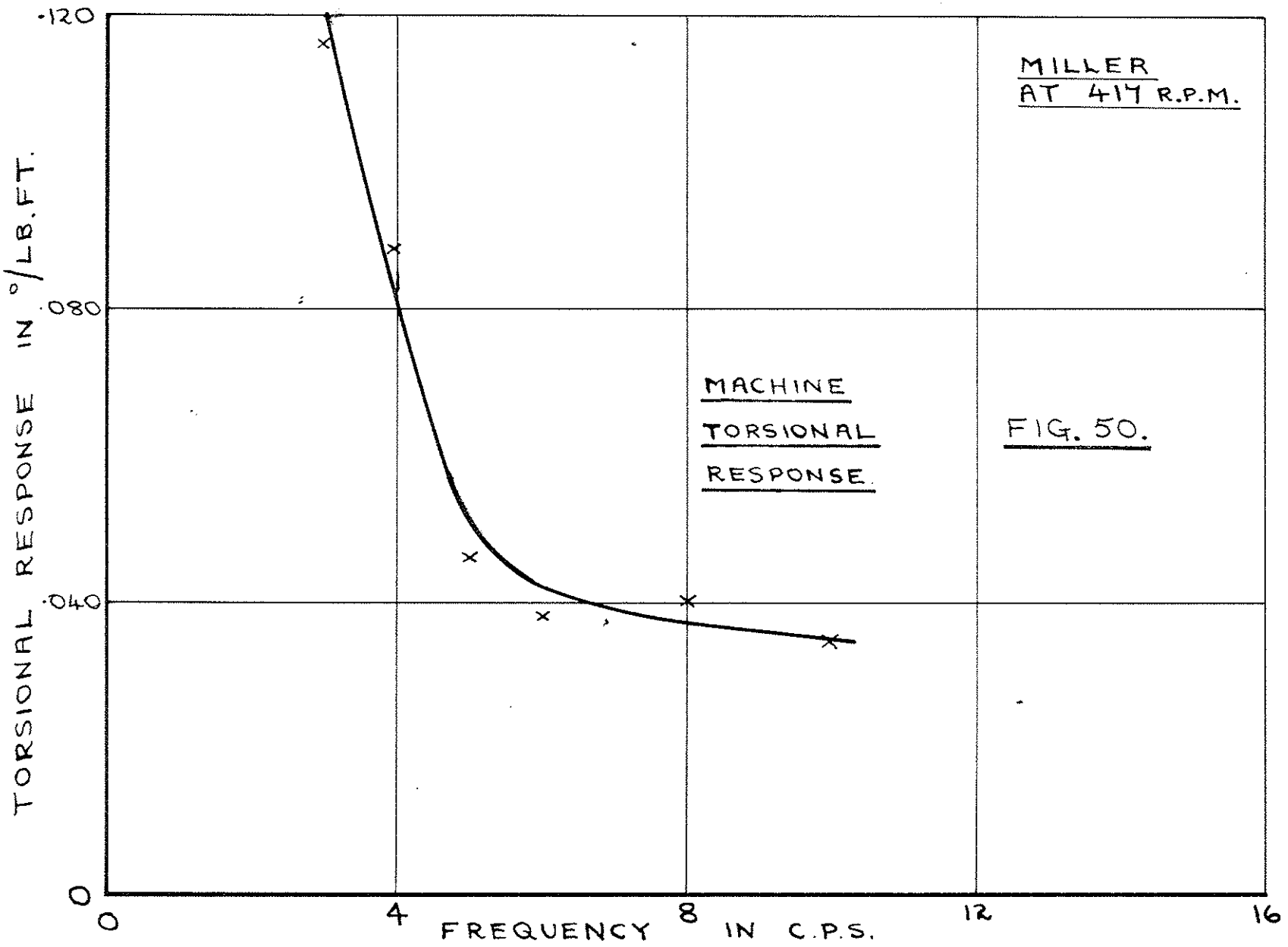
·120
·080
·040
0
TORSIONAL RESPONSE IN °/LB.FT.
0
4
8
12
16
FREQUENCY IN C.P.S.
MILLER
AT 414 R.P.M.
MACHINE
TORSIONAL
RESPONSE.

FIG. 50.

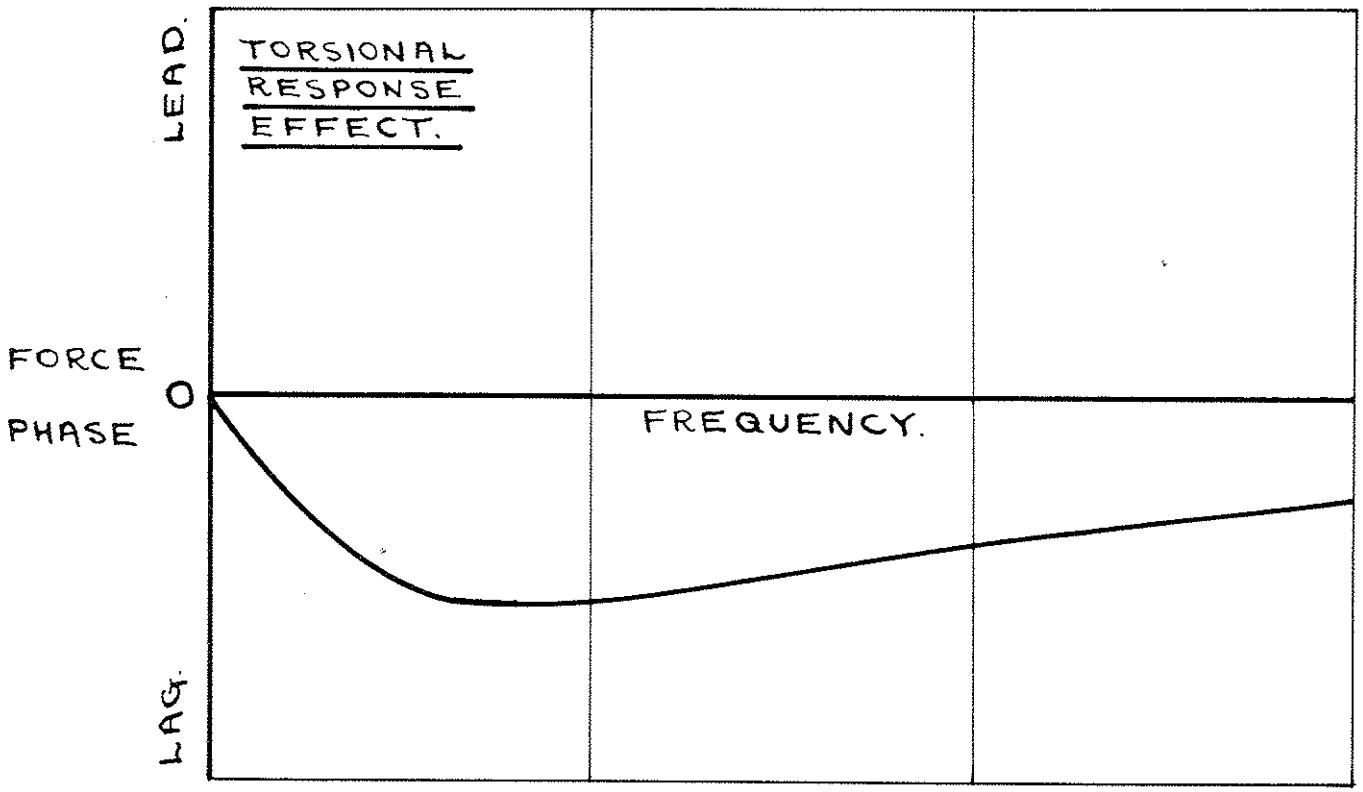
LEAD.
TORSIONAL
RESPONSE
EFFECT.
FORCE
PHASE
O
FREQUENCY.
LAG.

FIG. 51.

are shown qualitatively in Figure 51. The actual values of the observed lag depend on the machine characteristics, the particular cutting conditions and the cutting force characteristics as a function of surface speed. The effects of this mechanism are normally very small and the effect is swamped by the built-up edge effect. At very high rotational speeds the effective moment of inertia of a machine is small and this effect may be comparable in size with the built-up edge effect.

8.7 Tool Bluntness.

The effect of oscillating a blunt tool will be to give increased forces, mainly the horizontal, when the tool is travelling into the workpiece. This effect would be important principally at low surface cutting speeds. The observed effects on phase angle and amplitude would be non-linear but similar to those of the "viscosity" effect; they would probably be much smaller and hence difficult to detect. In all tests the tool was kept sharp and no attempt was made to investigate the effects of bluntness. When there is a built-up edge, this will give a similar effect to that of tool bluntness since both give a flat on the tool clearance face.

8.8 Mechanism Breakdown.

At very high frequencies some of the previously discussed

mechanisms become very small. Effects 8.3 and 8.5 which are dependant on temperature fluctuations tend to zero at high frequency as the temperature changes tend to zero. Torsional effects as in 8.6 are also small at high frequency.

Effects 8.2 and 8.4 theoretically give forces which increase continuously with increase in frequency while the phase will approach 90° at high frequency. When the frequency of vibration approaches that corresponding to the "shear plane" spacing the "geometric" effect must break down; the effect of vibration may then be to control the "shear plane" spacing.

There is no apparent reason why the "viscous" effect should break down at high frequencies. In practice however if the "viscous" damping stiffness becomes very high at high frequencies, any test results will measure the local elastic deflections of the tool and workpiece rather than the very small tool-chip relative deflections.

8.9 Other Effects.

It has been suggested by Doi and Kato (5) that there is an inherent lag effect in the cutting process i.e. the shear plane mechanics. Any such effect, if it existed, would not be easily detectable. At a cutting speed of 400 ft./min. with a 5 thou. depth of cut the total length of the shear plane corresponds to

a time of about one tenth of a millisecond; at 100 c.p.s. this corresponds to only 3° phase change.

Tobias and Fishwick (2) suggested that increased penetration of the tool into the workpiece and change of effective rake angle with penetration would alter cutting forces. Referring to Figure 46 the effect of change in direction i.e. change of α, and change of rake angle γ can be calculated from the expressions given. Unfortunately if account is also taken of the corresponding shear angle change the net change in force is zero. This, though at first surprising, can be seen from the original force diagram; the direction of the force is unaltered since this is controlled by the friction angle and the amplitude is controlled by the shear plane which does not move.

9. Correlation of Results and Theories.

9.1 Relevant Cutting Conditions.

In general, in a cutting process there will be several mechanisms operating simultaneously to affect the observed phase angles. Since torsional mechanisms can be neglected for this set of experiments and the tool was sharp, the relevant theories are the viscous, friction-temperature, geometric, and built-up edge effects with the possible addition of mechanism breakdown at high frequencies.

Separating out these effects, the viscous and geometric effects are high-frequency, low speed effects, the friction-temperature effect is a moderate and high frequency effect which should exist at the higher speeds, and the built-up edge effect should occur at low and moderate speeds and low frequency. Only at high cutting speeds will there be just one of these effects since only the friction-temperature effect can be appreciable at high speeds.

9.2 Vertical Forces.

The geometric effect and the built-up edge effect are of primary importance for vertical force phase effects. At high speeds as in Figure 23 the vertical phase angle is small as the built up edge does not exist and the velocity is high so that

the geometric effect is negligible.

Low speed results as in Figures 17 and 18 show a vertical phase angle which remains negative and small over the experimental range though moderate speed results as in Figures 21 and 22 show a lead at high frequency. The estimated phase angles due to the "geometric" effect are, typically for the cutting conditions of Figure 17, a force lead of the order of 50° at 200 c.p.s. which bears no relation to the observed angles. So at low speeds it appears that the Merchant approach of assuming a plane shear, leading to the "geometric" effect, does not apply and plastic flow theories must be used. Under these conditions the built-up edge effect appears to persist, although small, to a high frequency. The wide divergence between the vertical phase angles in Figures 19 and 20 is difficult to explain; the increase in depth of cut should increase any "geometric" effects but appears to accentuate built up edge effects. The low frequency results in Figures 27 and 28 show no distinct trends.

Thus for the vertical forces though phase angles are in qualitative agreement with "geometric" theory at high speeds there is no satisfactory correlation at low speeds and there is little consistency in the effects which are presumed to be

due to the built-up edge.

9.3 Horizontal Forces.

At high speeds the temperature-friction effect is the only mechanism that can effect the results appreciably so that the results in Figure 23 should be principally due to this effect since even the viscosity effect should give only 6^{o} phase change at 300 c.p.s. Since there is no built-up edge at this speed there should be no low frequency force lag; rig limitations precluded tests below 40 c.p.s. but there is no indication in the results that the phase lead will go negative below 40 c.p.s. There is no indication of a maximum in the curve but the position of the maximum cannot be estimated reliably so a maximum may occur above 350 c.p.s. At this frequency the temperature oscillations will only penetrate about 10 thou. but the amplitude of the temperature variations will still be of the order of 100^{o}F.

Low speeds allow all effects to exist and the separation of effects is difficult; however any geometric effect does not give a phase change between horizontal and vertical force and since the chip is cool the friction-temperature effect should be small. This leaves the viscous and the built-up edge effect as the dominating factors at low speed. Comparison of Figures 17 and 18

with Figure 47 shows good qualitative agreement for viscous effects except at low frequency where built up edge effects distort the results. Of course, accurate quantitative agreement is not possible since the main "constants" in the expression, i.e. the shear plane angle, effective rake angle and angle of friction, are not known; the agreement between theory and experimental results is within the range of experimental error. The difference in force level between the oscillating and cleaning cuts, i.e. Figure 14(a) and (b) cuts, supports the view that this is a viscous or tool bluntness effect rather than a temperature variation effect.

The low frequency effects, presumed due to the built-up edge show no consistent trends; Figure 42 gives an idea of the random nature of the results. Increase of speed or feed will change temperature distributions and hence reduce the size of the built-up edge and hence the effective rake angle and increase the interface temperatures and hence decrease the effective friction. These two results will have opposing effects on the steady horizontal force and may increase or decrease the observed phase angles since the built up edge will be smaller, giving lower phase effects, but at a higher temperature, and hence likely to respond more quickly, giving larger phase effects.

9.4 Intermittent Forces.

At low frequencies and low speed there is such a large random variation in the observed phase angles that any trends are completely masked, while at high cutting speed it was not possible to record sufficient cycles. At high frequency and high speeds as in Figure 43 there is remarkably little change in phase angle, indicating that temperature stabilisation must occur within 3 cycles, i.e. within 20 milliseconds. At low speeds, Figure 40, there is a reduction in phase angle at the start of the cut; the mean phase initially is only about half the phase after stabilisation. The viscous effect is the dominating effect at this frequency; as the tool temperature rises the built-up edge will decrease, lowering the effective rake angle and hence decreasing the shear plane angle which in turn will increase the viscous effect. Also as temperatures rise, the greater plasticity of the metal gives a "friction" which is more velocity sensitive.

9.5 High Rake Angles.

The results in Figures 24 and 25, using a 30° rake tool show quadrature force effects in an exaggerated form. The significance of the high rake angle lies in the fact that the horizontal force is very small when $(\rho - \gamma)$ becomes small: see Figure 46.

Thus in Figures 24 and 25 the horizontal in-phase force is very small at all frequencies other than zero and the observed force is almost a pure damping force whose amplitude increases with frequency. This corresponds to the effect to be expected from a viscous friction mechanism.

The large difference between the steady state stiffness and that at low frequency gives an idea of the dominating effect the response of the built-up edge has at low frequencies.

10. Effect of Phase Changes on Chatter.

10.1 Chatter Criteria.

Basically, any lead of horizontal force relative to tool displacement gives a damping force and will give increased stability in the machining process while any lag will correspondingly tend to instability.

In the expression derived in Appendix I the phase changes simply alter c' and hence v'. Increase of cut damping or machine damping have the same effect of increasing the permissible cutting stiffness k and hence increasing machining capacity.

For the full analysis of chatter, the methods of Tobias and Fishwick (2), Tlusty and Polacek (3) or Gurney and Tobias (4) should be used. These methods must be used when there is more than one degree of freedom and when there is a small number of oscillation cycles between successive cuts.

The method given in Appendix I gives the worst possible case for a single degree of freedom system and is convenient for consideration of phase change effects. The result may be simply expressed as

$$k_r < (c + c') \omega$$

This can be derived easily from a vector force triangle since spring and inertia forces cancel at resonance leaving the exciting

force equal and opposite to the total damping force from machine and cutting process.

10.2 Unconditional Stability.

There is a special case which is of particular interest. This is the condition where the cut damping $\omega c'$ is equal to or larger than the forcing stiffness k_r; when this occurs the system will be stable even when there is no machine damping i.e. $c = 0$.

This condition occurs in practice in the test results when the quadrature damping force from Figure 14(a) cutting exceeds the forcing force from Figure 14(b) cutting. This occurs in Figure 17 above 110 c.p.s., in Figure 18 above 75 c.p.s., in Figure 24 above 40 c.p.s. and in Figure 25 above 30 c.p.s. The theory thus predicts that for these ranges chatter will be impossible.

Such a prediction is surprising and so was tested experimentally. The cutting conditions were those of Figure 17 with a machine natural frequency of 150 c.p.s. The machine damping was set to zero by reversing the polarity of the damping circuit and adjusting the gain till any disturbance oscillated indefinitely instead of dying away. When cutting no chatter occurred and external disturbances were rapidly damped out by the heavy damping in the cutting process. This verified the prediction which cannot be deduced by any theory which assumes that force is in

phase with chip thickness.

10.3 Effect on Stability Chart.

Even though this "unconditional stability" criterion cannot usually be obtained, a phase lead of 27° i.e. $\tan^{-1}\frac{1}{2}$ will make $c'\omega$ half k_r and hence double the chatter-free capacity of a machine tool.

Conversely when the damping is negative, if $c + c'$ tends to zero then the cutting capacity will be very small. Phase changes will thus raise or lower the stability envelope (Figure 6).

The shape of the stability envelope depends on the variation of damping i.e. phase change, with cutting velocity and depth of cut. The effects which are important at low surface speeds and normal milling chatter frequencies are the "viscosity" and the "geometric" effects in which the damping force is proportional to depth of cut and inversely proportional to cutting speed. These were the fundamental assumptions made in the previous work (8) on chatter band theory; this explains the good agreement between theory and experiment in this work.

For high speed machining the principal effect is the friction-temperature effect which is less sensitive to speed and cut depth changes. Thus the damping is constant and the stability bands will be bounded by a straight line similar to line B in Figure 6.

11. Effect of Dynamic Cutting on Tool Life.

11.1 Temperature Variations.

Under heavy chatter conditions the life of a carbide tool is very short as cracks appear on the rake face and tip fracture occurs. It is difficult to explain this rapid breakdown purely on a basis of stress variations since the peak loads involved are not sufficiently high to cause fracture and the number of stress cycles involved is too low for fatigue effects to be appreciable.

In Appendix 7 rough estimates are made of the temperature fluctuations at a particular point on the rake face of a tool for typical chatter conditions at high cutting speed; the friction-temperature phase effect depends on these temperature fluctuations. The figures obtained for the temperature variations are rather startling. The bulk temperature i.e. the mean temperature of the first 8 thou. below point P fluctuates by approximately 160°F for a typical chip temperature 1000°F above ambient. The temperature swing of the surface layer is probably much higher than this; when the chip is not in contact, the surface temperature will be of the order of 500°F above ambient but when the surface is being scrubbed by a high velocity hot chip the temperature may approach the chip temperature. The surface temperature swing may thus be of the order of 400°F.

11.2 Thermal Stresses.

Such a temperature variation will have disastrous effects on the tool, since the thin surface layer will be physically restrained by the remainder of the tool. There is no information available on the thermal expansion and modulus of carbide mixtures at this temperature but substitution of the corresponding figures at room temperature gives an idea of the thermal stresses involved. A modulus of 77×10^6 lb. per square inch, an expansion coefficient of 3.5×10^{-6} per ^{o}F with a temperature swing of $400^{o}F$ correspond to a thermal stress variation of 48 Tons per square inch. Stresses of this order, particularly if tensile, oscillating at 100 c/s. are very likely to give surface cracking since at this frequency it is not possible for creep in the material to relieve the stresses.

If, during part of the cycle the tool surface is exposed to a high velocity coolant stream at below boiling point only $150^{o}F$ above ambient temperature the surface layers will be cooled even more and greater temperature fluctuations will occur. Coolant could thus be expected to further shorten tool life under these conditions.

11.3 Milling.

When lathe turning normally, chatter is not usually allowed

to develop so that the effects estimated above will not occur. However the milling process, whether face, side or roll milling, involves intermittent contact between tool and workpiece with tool surface cooling between contacts.

It would appear that this effect will contribute to tool rake wear in milling even when chatter is not present although the thermal shock only occurs once per revolution instead of a hundred times per second. This is probably the main cause of the comparatively low tool life obtained when milling steel compared with the corresponding life when turning steel.

12. Discussion of Results.

The experimental results which have been obtained give a good idea of the dominating effect of cutting force phase changes on machine chatter. In most cases it is possible to stop regenerative chatter by the use of a suitable tool giving low horizontal forces or by machining at low speed so that high viscous forces oppose vibration.

The suggested explanations for the observed phase changes are based on well-known physical effects and are plausible theories. The agreement between theory and experiment for the vertical forces is not good. It seems likely that no theory will adequately fit the vertical force results due to their random variations; reliable experimental determinations are difficult in the presence of high "noise" levels. The behaviour of the built-up edge appears to be the dominating factor in all vertical force phase changes for mild steel.

For the horizontal force phase changes the correlation between theory and experiment is good at speeds where the viscous effect dominates. Here again, the built-up edge plays a large part at low frequency but its effect is swamped by the viscous effect at high frequency. It is not possible to estimate, even roughly, the effects of the temperature-friction effect at high cutting

speeds so there is no quantitative check on this effect.

There is at present no method of telling how much of the observed "viscosity" effect is due to friction on the rake face and how much is due to the built-up edge behaving as a blunt tool. It seems likely that it is the rake face which provides most of the effect but confirmation of this would require further work.

From the point of view of chatter, all cutting tools should have high rake angles. This is unfortunately the opposite to the requirement for long tool life so in practice a rather difficult compromise must be reached between tool life and chatter stability. Each case will warrant a different solution, depending on the size of the work batch and the rigidity of the machine.

Intermittent cutting forces appear to stabilise very quickly, particularly at the higher cutting speeds. The effect of the low tool temperature at the start of a cut is to reduce any stabilising phase effects slightly at low cutting speeds but for most purposes it should be sufficient to use steady cut results when milling. The effect of coolant should be similar to that of having a cool tool.

The dynamic force results obtained give a clearer picture of the variables affecting the cutting process and so throw some light

on the steady state force values. Probably the best method of investigating steady state conditions is to cut dynamically, if a only to determine the variation in shear angle as in section 4.3. The fact that the force against chip thickness curve is not straight line may be explained by the variation in temperature and hence "friction" coefficient and built-up edge. The variation of chip curvature at the start of a cut and the effect of cutting speed on curvature may be explained also.

13. Further Work.

In the light of the results obtained and the corresponding suggested theories, there is a great amount of further experimental work necessary.

13.1 Rig Development.

The experimental range of conditions, though very wide in relation to previous work, needs to be widened even further. For further work it would be advisable to have a rig capable of determining dynamic forces at least up to 1000 c/s. and possibly higher; this would give an idea of the position of the maximum in the phase curve, if one exists, at high cutting speeds if temperature effects are responsible. At low speeds, high frequency results should allow determination of "geometric" phase changes more clearly and also allow vibration at frequencies approaching that corresponding to the "shear plane" spacing.

If a rig can be devised to measure low frequency phase changes at high cutting speeds, the results will determine whether lagging angles at low frequency are associated with built-up edges and hence disappear when there is no built-up edge; such a rig is not easily designed.

13.2 Workpiece Material.

All the tests described used mild steel workpieces. Other

materials such as cast iron, free-machining steel, brass and duralumin will have different characteristics for built-up edge effects. Tests on a wide range of materials may then allow separation of built-up edge effects from "viscosity" and "geometric" effects. Unfortunately, cast iron does not give continuous chips so there will be a very high noise level in the cutting forces, making experimental work difficult. With mild steel it is not possible to test at high cutting speeds with high speed steel tools or using high rake angles since failure occurs; with workpieces of duralumin, comparative high speed tests can be attempted to determine the effects of tool conductivity on phase change, and the effect of high rake angles.

13.3 Tool.

The effect of tool bluntness, or a high built-up edge cannot easily be distinguished from a "viscosity" effect experimentally; cutting with a tool with an artificial built-up edge, with clearance on the relief face of the built-up edge would finally determine which effect was giving the phase change. Such a tool would be extremely weak so that a soft workpiece would probably be required. High productivity cutting usually requires the use of chipbreakers on a tool to allow easy swarf removal; the presence of a constraint on the cut chip will alter

the horizontal cutting forces and hence machine stability. It will probably be impossible to estimate the effect of a chip-breaker but experimental determination of the effects should allow design of a chip-breaker to give the maximum stability; again, noise levels will be high with a discontinuous chip.

Since temperature is presumed to have such a large effect on high speed phase changes, elimination of heat conduction should reduce, if not eliminate, phase changes. This can be done by raising the temperature of the tool to approach that of the chip so that all temperatures are then constant and large temperature fluctuations can then not occur; tool life tests under vibrating conditions should then be of interest.

13.4 Vertical Vibration.

To extend any chatter prediction to two degrees of freedom or to the case where a single mode is not normal to the cut surface it will be necessary to determine the horizontal and vertical forces for vertical vibration. Since force phase changes for vertical vibration will probably be nearly as complex as those for horizontal vibration, a similar rig will be required.

14. Conclusions.

The experiments described in this thesis and the associated deductions suggest that very much more attention should be paid to the dynamics of the cutting process. In many cases it will be more economic to alter tool geometry, even at the expenses of tool life, rather than tolerate low productivity or provide a more rigid machine.

The observed force phase changes have shown the dominating effect of the damping in the cutting process on the stability of machining. In many cases the cutting process damping will be greater than the machine damping while in some cases the cutting damping is sufficient by itself to prevent chatter regardless of machine damping.

Estimated temperature variations in a tool during fully developed chatter have been shown to be sufficiently high to cause tool failure in brittle materials. It is possible that the life of carbide tools under intermittent cutting conditions may be extended by temperature control.

There is very much more to be learnt about the cutting process but these tests have shown basic general trends of results. The theories suggested to explain the observations show the areas of most interest to further work to gain understanding of the peculiarities of the cutting process.

APPENDIX 1.

Chatter Criteria.

Consider the simplest possible regenerative chatter case i.e. a single degree of freedom where the tool is assumed to have mass M, damping c and restraint stiffness λ. The cutting force is proportional the the instantaneous chip thickness and the tool velocity.

The equation of motion is

$$M\ddot{x} + c\dot{x} + \lambda x = -k_1(x) + k_r x_r - c'\dot{x}.$$

Where $k_1 x$ is the inphase cutting force.

$k_r x_r$ is the force due to the previous cut surface

$c'\dot{x}$ is the quadrature cutting force.

Then:

$$\ddot{x} + \left(\frac{c}{M} + \frac{c'}{M}\right)\dot{x} + \frac{(\lambda + k)}{M} x = k_r x_r$$

This may be written as:

$$x + 2(v + v')\omega_o x + \omega_o^2 x = \frac{k_r}{M} \cdot x_r$$

Where $2v\omega_o = \frac{c}{M}$ and $\omega_o^2 = \frac{\lambda+k}{M}$

If the diameter is large so that the oscillation has disappeared by the end of a revolution then at the start of a revolution $x = \dot{x} = 0$.

If a single impulse is given at the start of the first rev-

olution then by Laplace or similar methods the solutions become:-

1st revolution

$$x = X\, e^{-(v + v')} \sin \omega t.$$

2nd revolution

$$x = X \left(\frac{k_r}{M.2\omega^2} \right) e^{-(v + v')\, \omega_o t} (\sin \omega t - \omega t \cos \omega t)$$

3rd revolution

$$x = X \left(\frac{k_r}{M.2\omega^2} \right)^2 e^{-(v + v')\, \omega_o t} \left[\sin \omega t \left(\frac{3 - \omega^2 t^2}{2} \right) - \frac{3}{2} \omega t \cos \omega t \right]$$

4th revolution

$$x = X \left(\frac{k_r}{M.2\omega^2} \right)^3 e^{-(v + v')\, \omega_o t} \left[\sin \omega t \left(\frac{5}{2} - \omega^2 t^2 \right) + \cos \omega t \left(- \frac{5}{2} \omega t + \frac{\omega^3 t^3}{6} \right) \right]$$

5th revolution

$$x = X \left(\frac{k_r}{M.2\omega^2} \right)^4 e^{-(v + v')\, \omega_o t} \left[\sin \omega t \left(\frac{35}{8} - \frac{15}{8} \omega^2 t^2 + \frac{\omega^4 t^4}{24} \right) + \cos \omega t \left(- \frac{35}{8} \omega t + \frac{5}{12} \omega^3 t^3 \right) \right]$$

6th revolution

$$x = X \left(\frac{k_r}{M.2\omega^2} \right)^5 e^{-(v + v')\, \omega_o t} \left[\sin \omega t \left(\frac{63}{8} - \frac{7}{2} \omega^2 t^2 + \omega^4 t^4 + \frac{\omega^4 t^4}{8} \right) + \cos \omega t \left(- \frac{63}{8} t + \frac{7 \omega^3 t^3}{8} - \frac{\omega^5 t^5}{120} \right) \right]$$

etc.

For the normal case of a long cut as in planing or large diameter turning the chatter criterion is simply that the maximum amplitude should increase. Providing $v + v'$ is small the condition is for the n^{th} revolution.

$$\frac{1}{e}\ \frac{k_r}{M.2\omega^2}\ \frac{\omega}{\omega_o}\left(\frac{n}{n-1}\right)^{n-1}\ \frac{1}{(v+v')} < 1$$

This as n increases, reduced to:

$$2\ (v + v') > \frac{k_r}{k_1 + \lambda} \quad \text{for stability.}$$

Rewriting this

$$\left(\frac{c}{\omega_o M} + \frac{c'}{\omega_o M}\right) > \frac{k_r}{\omega_o^2 M}$$

i.e.

$$(c\omega_o + c'\omega_o) > k_r.$$

APPENDIX 2.

Phase Measurement.

Measurement of phase by conventional methods is extremely difficult when total experimental times are short, amplitudes vary, and there is a very high noise level. Neither the vector addition type of phasemeter or the triggered square wave type is suitable under these conditions. Two graphical methods were used for these tests.

For low frequencies and small phase angles the force and displacement values were recorded against time as sketched in Figure 52. Then consider two waveforms $A_1 \sin \omega t$ and $A_2 \sin (\omega t + \phi) + B_2$ i.e. of differing amplitudes, relative phase ϕ and D.C. difference B_2, then solving for the points of intersection of these two waveforms.

$$A_1 \sin \omega t = A_2 \sin (\omega t + \phi) + B_2$$

This gives two solutions

$$\sin \omega t = \frac{B_2 (A_1 - A_2 \cos \phi) \pm \sqrt{B_2^2 (A_1 - A_2 \cos \phi)^2 - \left[(A_1 - A_2 \cos \phi)^2 + A_2^2 \sin^2 \phi\right]\left[B_2^2 - A_2^2 \sin^2 \phi\right]}}{(A_1 - A_2 \cos \phi)^2 + A_2 \sin \phi^2.}$$

$$\sin\phi = \frac{b}{2A_1}\left[1 + \frac{A_1}{A_2}\right]$$

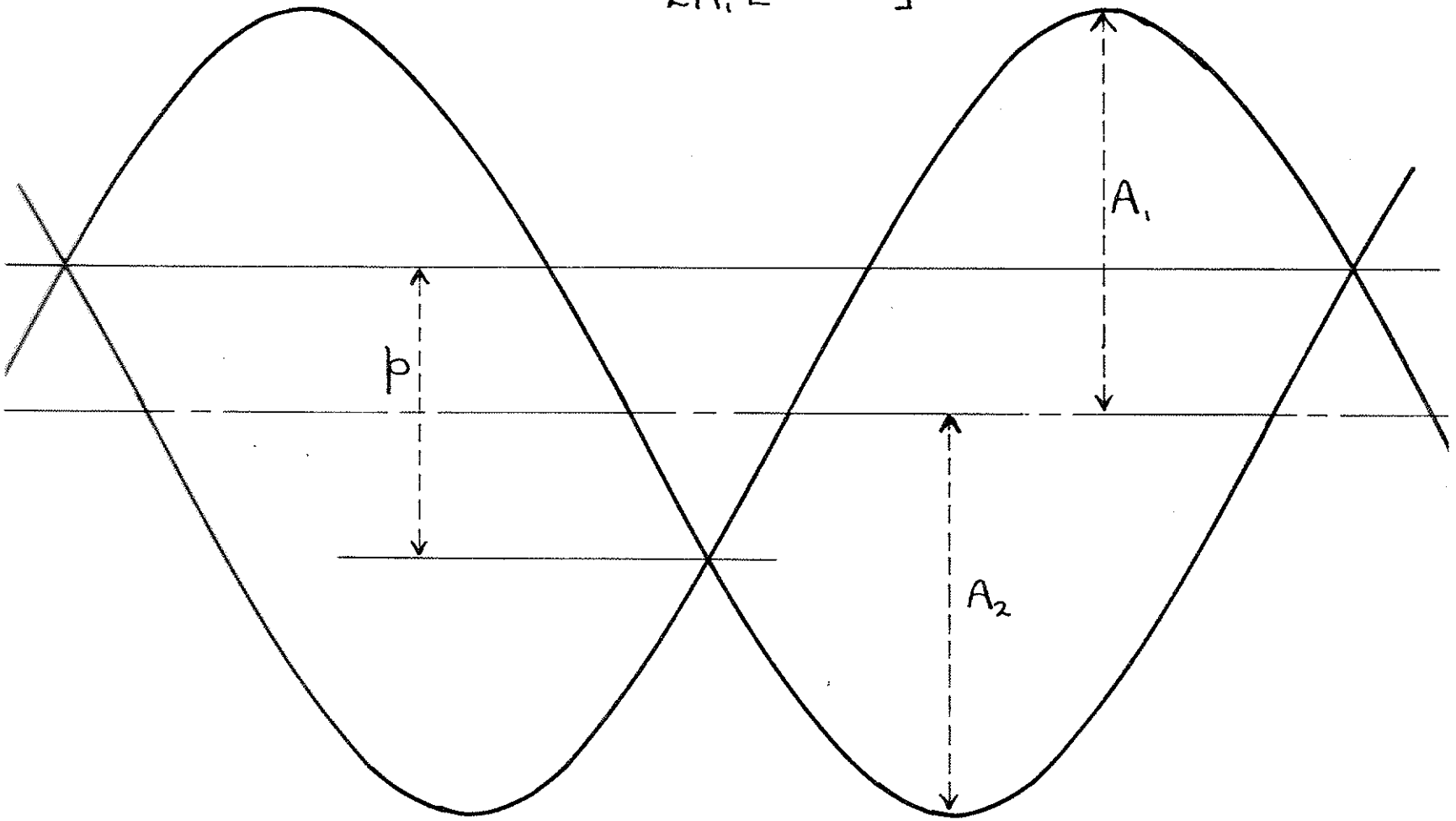

PHASE MEASUREMENT. FIG. 52.

So the difference in height between the two intersection points is $h = A_1 \sin \omega t_1 - A_1 \sin \omega t_2$ where ωt_1 and ωt_2 are the roots obtained above.

Substituting gives

$$h = \frac{2 A_1 A_2 \sin \phi \sqrt{A_1^2 - 2A_1 A_2 \cos \phi + A_2^2 - B_2^2}}{A_1^2 - 2A_1 A_2 \cos \phi + A_2^2}$$

This cannot be expressed easily to give a value for ϕ. However if ϕ is near 180° then $\cos \phi$ may be taken as 1 with sufficient accuracy, and

$$h = \frac{2 A_1 A_2 \sin \phi \sqrt{(A_1 + A_2)^2 - B_2^2}}{(A_1 + A_2)^2}$$

Further if B_2 is reasonably small compared with $A_1 + A_2$ which is easily arranged experimentally then

$$h = \frac{2 A_1 A_2}{A_1 + A_2} \sin \phi$$

or $$\sin \phi = \frac{h}{2A_1} \left(1 + \frac{A_1}{A_2}\right)$$ as indicated in Figure 52.

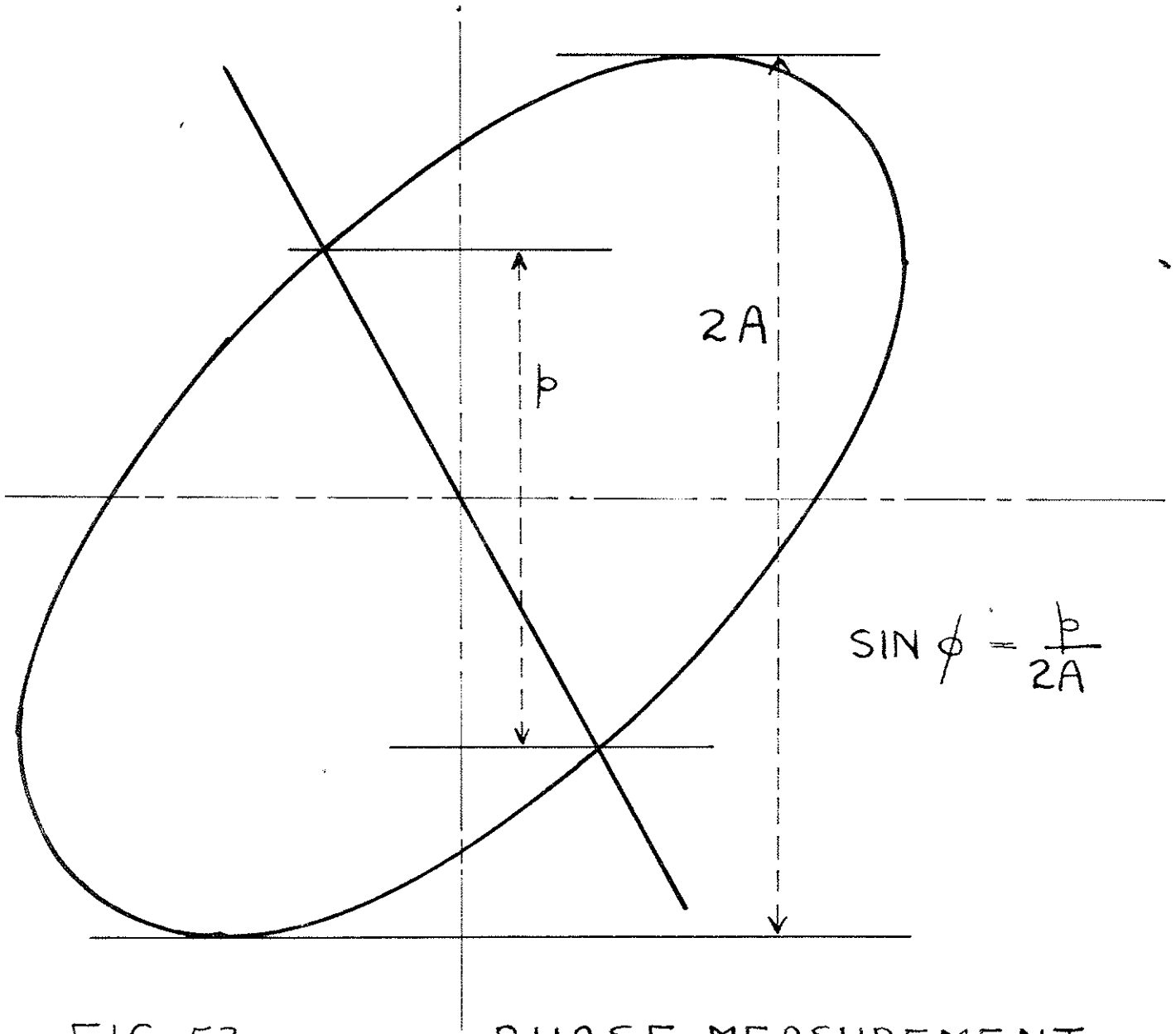

FIG. 53. PHASE MEASUREMENT.

For large phase angles e.g. 30^{o} and upwards the method described above becomes inaccurate. Phase angles can then be measured conveniently by the use of a Lissajous ellipse. Referring to Figure 53, the displacement signal is applied to the Y-plates of an oscilloscope and the force signal to the X-plates.

At any time t the displacement will be $\delta = a \sin \omega t$ and the force observed by the strain gauges will be $F = F_o \sin (\omega t + \phi) + M \ddot{\delta}$ where the actual cutting force F_o leads the displacement by the angle ϕ and $M \ddot{\delta}$ represents the force required to accelerate the tool and head of the dynamometer. When the tool is not cutting the force will be solely the inertia force $M \ddot{\delta}$ giving a straight line trace.

Consider the points at which the straight line obtained when not cutting intersects the ellipse when cutting. Then:-

$F = M \ddot{\delta}$ and hence the cutting force $F_o \sin (\omega t + \phi) = 0$ so $\omega t = -\phi$ or $\pi - \phi$.

As the displacement $\delta = a \sin \omega t$, at these points $\delta = \pm a \sin \phi$. So again taking the vertical distance p between the intersection points,

$$p = 2 a \sin \phi$$

$$\text{so } \sin \phi = \frac{p}{2a}$$

APPENDIX 3.

Accuracy and Repeatability.

Analysis of the experimental results involves the determination of the amplitudes of force and displacement and their relative phase. For the main body of tests the results were filmed on 35 mm. paper direct from an oscilloscope; typically, traces were of the order of 10 mm. amplitude. Measurement from these traces was accurate to 0.2 mm. with care so that the basic order of measurement accuracy was 1% giving some 2% accuracy on stress values and, when phase angles were measured by the method of Figure 52, an accuracy of $\pm 1^{\circ}$. When phase was measured as in Figure 53 the order of accuracy in sin $\emptyset$ was again 2%; for angles of the order of 45° this corresponds to about 1° but as angles approach 90° the variation possible is of the order of 10°.

Calibration accuracy was again basically 2% except for the displacement calibration which used 1/10th. thou. dial gauges to measure quantities of the order of 4 thou. The accuracy of displacement calibration would thus be only 5% and that of force 2%. The accuracy of the measuring and recording equipment was sufficiently high that any errors from this source could be neglected. Levels of accuracy when using the ultra-violet recorder were

similar.

The comments above are relevant for steady forces and phase angles; this applies at high cutting speeds and frequencies particularly with small cuts as in Figure 43. For lower cutting speeds and frequencies the dominating effect controlling accuracy is noise. The variations in phase and amplitude from one cycle to the next are large; Figures 37 and 38 give some idea of the variation in values even though the points plotted were averaged over up to 50 complete cycles. Figures 39 - 42 give the spread of phase angle in a typical cutting condition. This high noise level means that it is difficult to get repeatability even when quite large samples are taken. A typical root mean square error in Figure 40 is of the order of 15°.

High noise levels greatly reduce attainable accuracies; measurement of amplitude in the presence of the high distortion encountered in some cuts is only accurate to about 5% and amplitudes may vary from cycle to cycle so that the net accuracy of stiffness determination is of the order of 15% in bad cases and the corresponding accuracy of phase determination about 10°. In cases where amplitudes are small, as with high rake tools, it is often not possible to obtain a result.

Thus, though the measurement systems and experimental tech-

niques give reasonable accuracy, usually within 5%, the inherent behaviour of the metal cutting process means that accuracies and repeatability are low.

APPENDIX 4.

Viscosity Effect.

See Figure 54. While the tool moves from A to B the metal originally at A has moved to C i.e. has moved the distance BC along the tool.

Then:

$$\frac{AB}{\text{Sin } BCA} = \frac{BC}{\text{Sin } BAC}$$

i.e. $\dfrac{V\, S_t \sec \alpha}{\sin (90-\phi+\gamma)} = \dfrac{v_r\, S_t}{\sin (\alpha+\phi)}$ where v_r is the relative tool chip velocity.

$$\text{i.e.} \quad v_r = \frac{V \sec \alpha \sin (\alpha+\phi)}{\cos (\phi-\gamma)}$$

Now providing α is small which is always so in practice, this reduces to $v_r = \dfrac{V}{\cos (\phi-\gamma)} \sin \phi\, (1 + \cot \phi\, \alpha). = V_m\, (1 + \cot \phi . \alpha).$

So if the assumption is made that $\mu \propto V_r$ i.e. a viscous type of resistance.

Then: $$\frac{\delta\mu}{\mu m} = \frac{\delta v_r}{v_m} = \alpha \cot \phi$$

Then by differentiating as in Figure 46

$$\frac{\delta P_4}{P_4} = \left[\tan (\phi + \rho - \gamma) + \cot (\rho - \gamma)\right] \delta\rho$$

and since $\mu = \tan \rho$, $\delta \mu = \delta \rho\, (1 + \mu^2)$

so $$\frac{\delta P_4}{P_4} = \left[\tan (\phi + \rho - \gamma) + \cot (\rho - \gamma)\right] \frac{\mu \alpha}{(1 + \mu 2)} \cot \phi$$

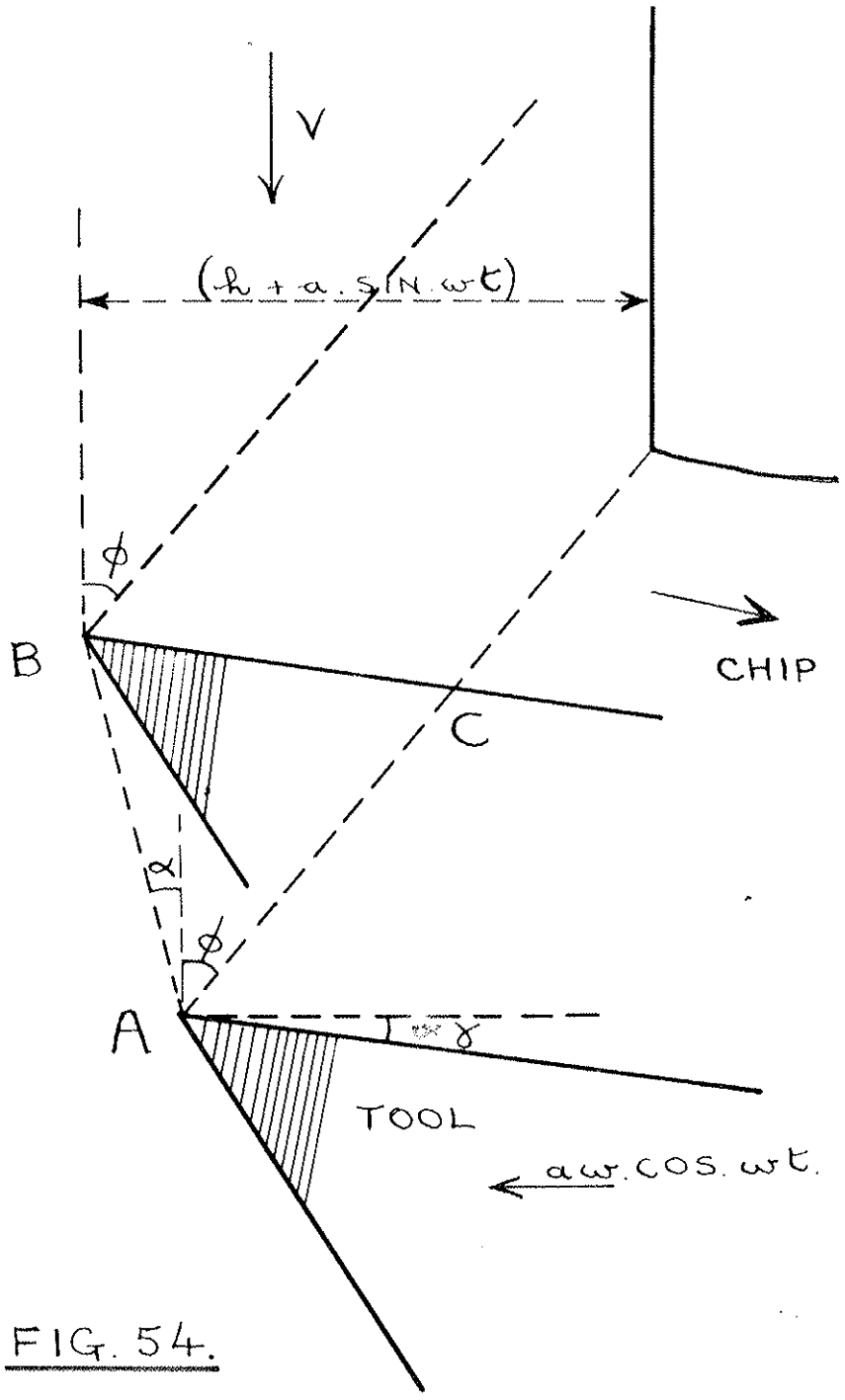

FIG. 54.

CUTTING FORCE GEOMETRY.

Then α is given by $\frac{a\omega \cos \omega t}{V}$ where the amplitude of vibration is $a \sin \omega t$. So due to the change in velocity there is a quadrature force

$$\frac{\delta P_4}{P_4} = \left[\tan (\phi + \rho - \gamma) + \cot (\rho - \gamma)\right] \frac{\mu}{1 + \mu^2} \frac{a\omega}{V} \cot \phi \cos \omega t$$

There is also the inphase force due to the displacement $a \sin \omega t$.

$$\frac{\delta P_4}{P_4} = \frac{a \sin \omega t}{h}$$

where h is the mean chip thickness.

Combining these forces gives

$$\frac{\delta P_4}{P_4} = \frac{a}{h} \sec \psi \sin (\omega t + \psi)$$

where $\tan \psi = \left[\tan (\phi + \rho - \gamma) + \cot (\rho - \gamma)\right] \frac{\mu}{1 + \mu^2} \cdot \frac{h\omega}{V} \cot \phi$

Similarly for the vertical force

$$\frac{\delta P_1}{P_1} = \tan (\phi + \rho - \gamma) - \tan (\rho - \gamma) \quad \delta \rho$$

and similarly

$$\frac{\delta P_1}{P_1} = \frac{a}{h} \sec \psi \cdot \sin (\omega t + \psi).$$

where $\tan \psi = \left[\tan (\phi + \rho - \gamma) - \tan (\rho - \gamma)\right] \frac{\mu}{(1 + \mu^2)} \cdot \frac{h\omega}{V} \cdot \cot \phi.$

APPENDIX 5.

The Geometric Effect.

From Figure 54.

At any time t the length of the shear plane will be $(h + a \sin \omega t) \times \operatorname{cosec} \phi$. The upward displacement of the shear plane will be $(a \sin \omega t) \cot \phi$. So the upward velocity of the shear plane will be $a\omega \cos \omega t \cot \phi$. The rate of volume removal will then be the product of the resolved length of the shear plane and the relative velocity between workpiece and shear plane i.e.

$$\text{Volume rate} = (h + a \sin \omega t) \operatorname{cosec} \phi \sin \phi \; (V + a\omega \cos \omega t \cot \phi)$$

$$\text{i.e. } Vh \left[1 + \frac{a}{h} \sin \omega t + \frac{a\omega}{V} \cot \phi \cos \omega t + \text{2nd harmonic terms}\right]$$

Neglecting the last term which is a small harmonic distortion, the resultant force is proportional to

$$V \left[h + a \sec \psi \sin (\omega t + \psi)\right]$$

$$\text{where } \tan \psi = \frac{h\omega}{V} \cot \phi$$

It may be seen qualitatively that the geometric effect must exist by considering an extreme case in which the tool travels along the line of the shear plane during an oscillation. The depth of cut will be finite but the forces will be zero as no metal is being cut.

For Figure 14(b) type cutting then, very approximately when a is small compared with h, the shear plane will intersect the surface a distance h cot ϕ ahead of the tool. This corresponds to a phase advance of $\frac{h\omega}{V}$. cot ϕ. but there will be no force amplification as with type 14(a) cutting.

APPENDIX 6.

Torsional Effects.

Consider a torsional system with inertia I and viscous damping torque $\beta\dot{\theta}$ acted on by a cutting force at radius R. To simplify this approach assume that the cutting force is not dependant on feed velocity but solely on the chip thickness S, and cutting velocity which in turn is proportional to angular velocity $= \Omega_o + \dot{\theta}$

The equation of motion is then

$$I\ddot{\theta} + \beta\dot{\theta} = -R\,(k_1 S + k_2 \Omega)$$

Neglecting the steady state components this becomes

$$I\ddot{\theta} + (\beta + R\,k_2)\,\dot{\theta} = -R\,k_1\,a \sin \omega t.$$

This gives the torsional vibration,

$$\dot{\theta} = \frac{R\,k_1\,a \cos(\omega t + \gamma)}{\sqrt{I^2\omega^2 + (\beta + R\,k_2)^2}} \quad \text{where } \tan\gamma = \frac{\beta + R\,k}{I\,\omega}$$

$$= \frac{R\,k_1\,a}{I\,\omega} \cos\gamma \cos(\omega t + \gamma)$$

Substitute this into the expression for force i.e. $k_1\,a \sin \omega t + k\,\dot{\theta}$ and the observed force is

$$k_1 \, a \, (1 - k_\beta R \sin\eta \cos\eta) \sec\psi \sin(\omega t + \psi)$$

$$\text{where } \tan\psi = \frac{k_\beta R \cos^2\eta}{1 - k_\beta R \sin\eta \cos\eta}.$$

The observed force will have an amplitude of approximately $k_1 a$ but will lead by the angle ψ as given above. In practice k_β is negative so the observed force will lag behind the displacement. Figure 50 shows the shape of the phase lag to be expected.

APPENDIX 7.

Temperature Estimates.

For the friction-temperature effect the controlling factor is the temperature of the interface between cut chip and tool rake surface.

At moderate and low cutting speeds the built-up edge accentuates the effect of temperature variations. Figure 55 is a sketch of a tool with a built-up edge. The forces transmitted through the built-up edge from T to C are roughly vertical due to the high effective rake angle. Thus nearly all the observed horizontal force is being developed by friction over the small section from C to L. Temperature changes and the consequent friction changes over this section will have a disproportionately large effect on the observed horizontal force.

High speed cutting is a simpler problem since there is no built-up edge and the chip temperature does not vary greatly.

The general problem of determining tool temperatures during vibration is not soluble analytically. The majority of the heat generation occurs in the shear plane but some also occurs on the chip-tool interface and this generation is dependant on the existing friction and hence the existing temperature. Conduction to the tool is through the chip-tool interface which is

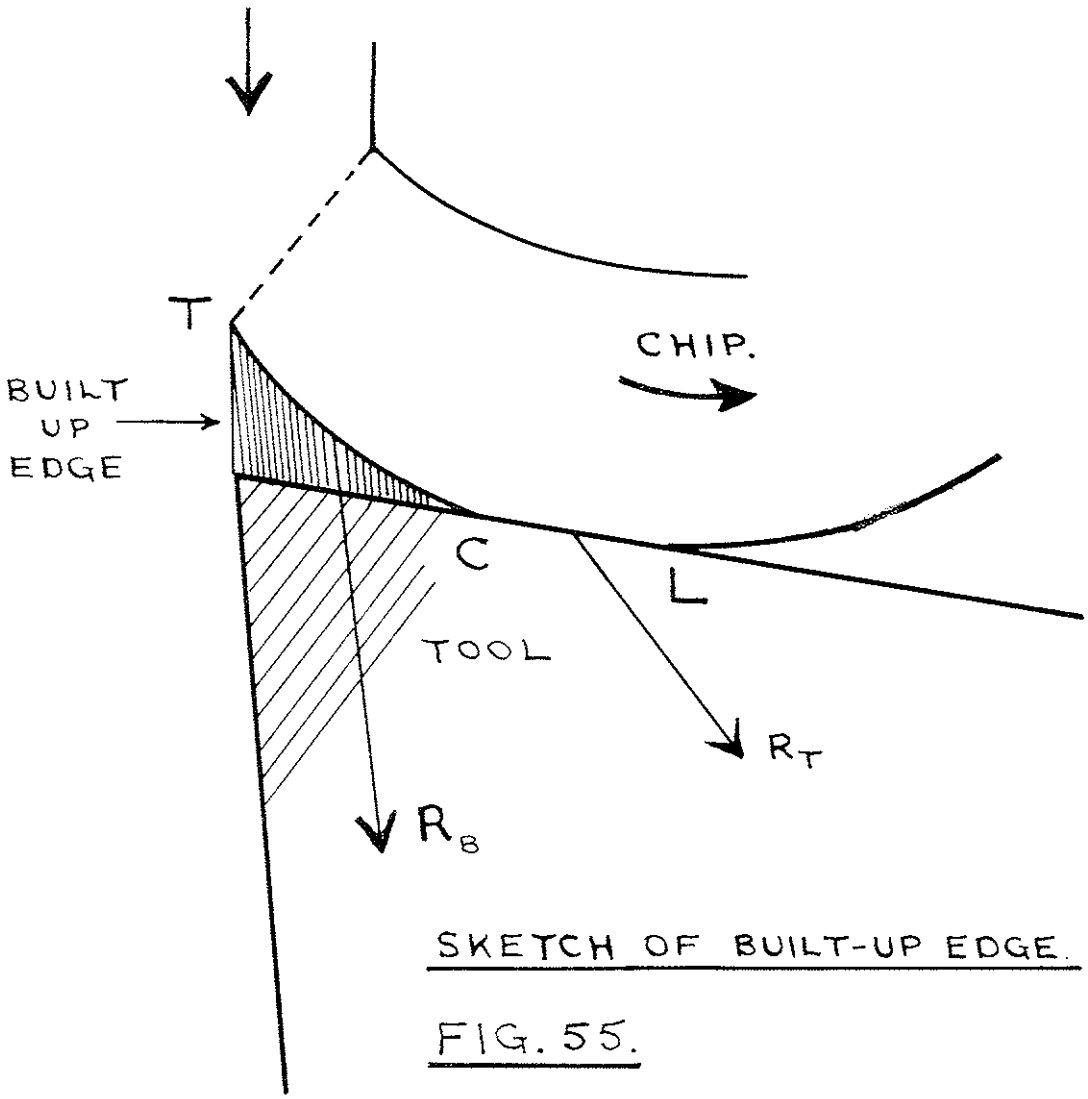

SKETCH OF BUILT-UP EDGE.

FIG. 55.

varying in size throughout the oscillation; this gives temperature variations which are not sinusoidal.

If the simplifying assumption is made that all the heat generation occurs in the shear plane a particular problem may then be solved by step-by-step methods. The dynamic case may be solved by a finite difference equation; see Eckert (12). The conditions selected for this example were typical conditions for a developed chatter. The heat flow was taken to be two-dimensional for simplicity and a grid size of 8 thou. was suitable.

Vibration Conditions.

Frequency 100 c.p.s. Amplitude of oscillation equal to mean chip thickness. Grid size δ x is .008".

Chip speed 43.2 ins. per sec. corresponding to a cutting speed about 500 ft. per minute.

Thermal diffusivity D = 0.8×10^{-4} ft.^{2} per second.

Then if a time interval δt corresponding to 20° angular motion is selected i.e. $\frac{20}{360} \times 10^{-2}$ secs.

$$(\delta\theta)_T = \frac{D.\delta t}{(\delta x)^2} \left\{ (\delta\theta)_x \right\} = 0.1 \left\{ (\delta\theta)_x \right\}$$

i.e. the rise in temperature in a time interval is one tenth of the sum of the surrounding temperature differences. Allowance must be made for the varying contact area between chip and tool when summing

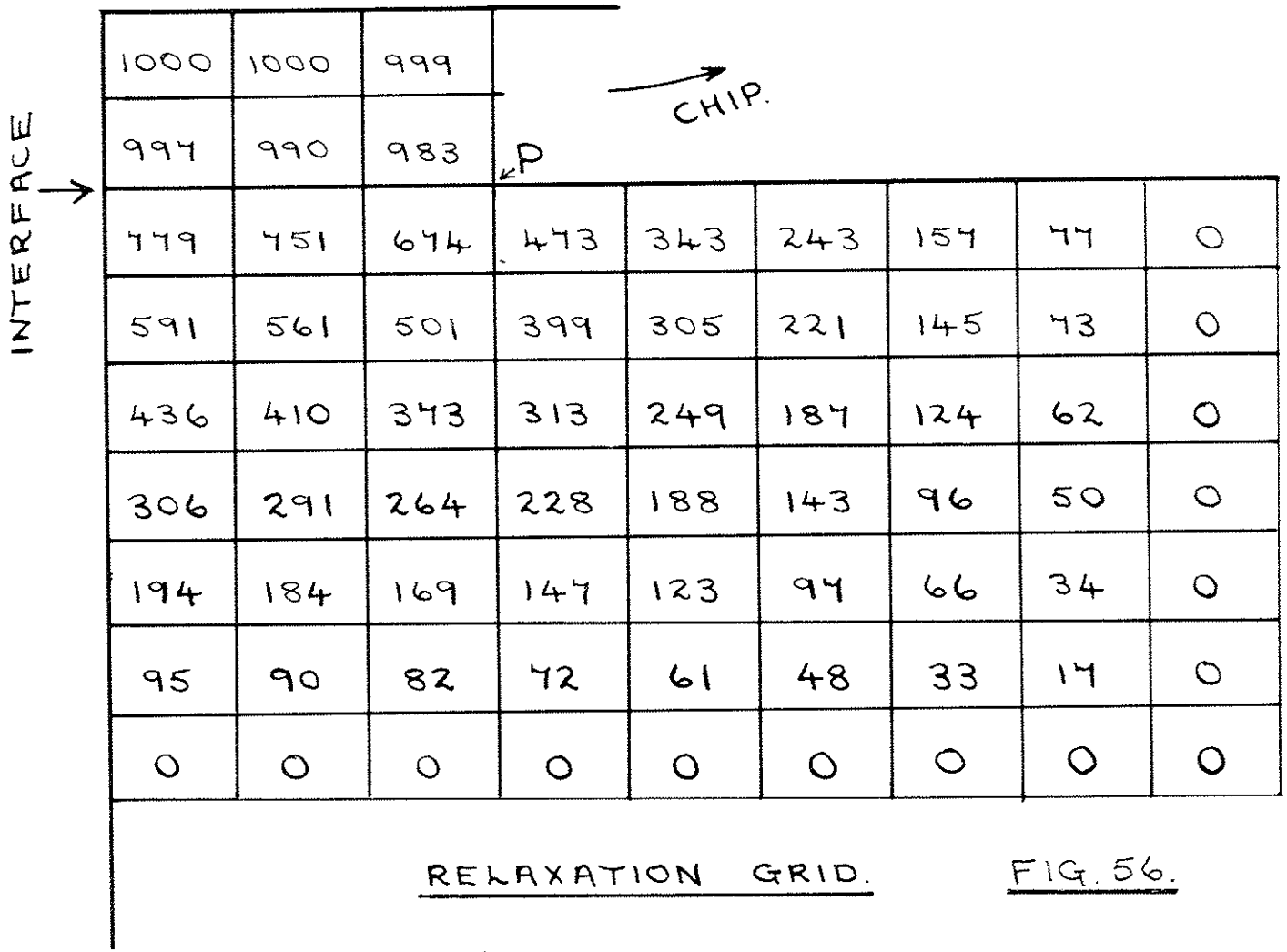

RELAXATION GRID. FIG. 56.

temperature differences.

Application of this difference relation for each point in the grid gives the temperature distributions through the tool throughout a cycle. Figure 56 shows a grid with the initial steady state temperatures inserted; arbitrary curtailment of the grid, though affecting the steady state distribution, does not greatly alter the oscillating temperatures since the penetration of temperature changes into the tool is small at this frequency. The characteristic distance for this frequency, Eckert (13), $2\sqrt{\frac{\pi a}{r}}$ is .038" so that appreciable temperature oscillations will only penetrate about 1/32nd. of an inch.

Figure 57 gives the resultant tool bulk temperature for the first 8 thou. below point P which corresponds to the limit of chip contact at the mean chip depth. The amplitude is large, of the order of 160° F, but the temperature variation on the surface will be even larger.

The interface temperature, which will control the friction and hence the force phase lead, will be intermediate between the chip and tool bulk temperatures. The chip bulk temperature is nearly constant at high cutting speeds but the tool temperature lags nearly 90° behind the chip thickness variation. This temperature variation gives a coefficient of friction which will

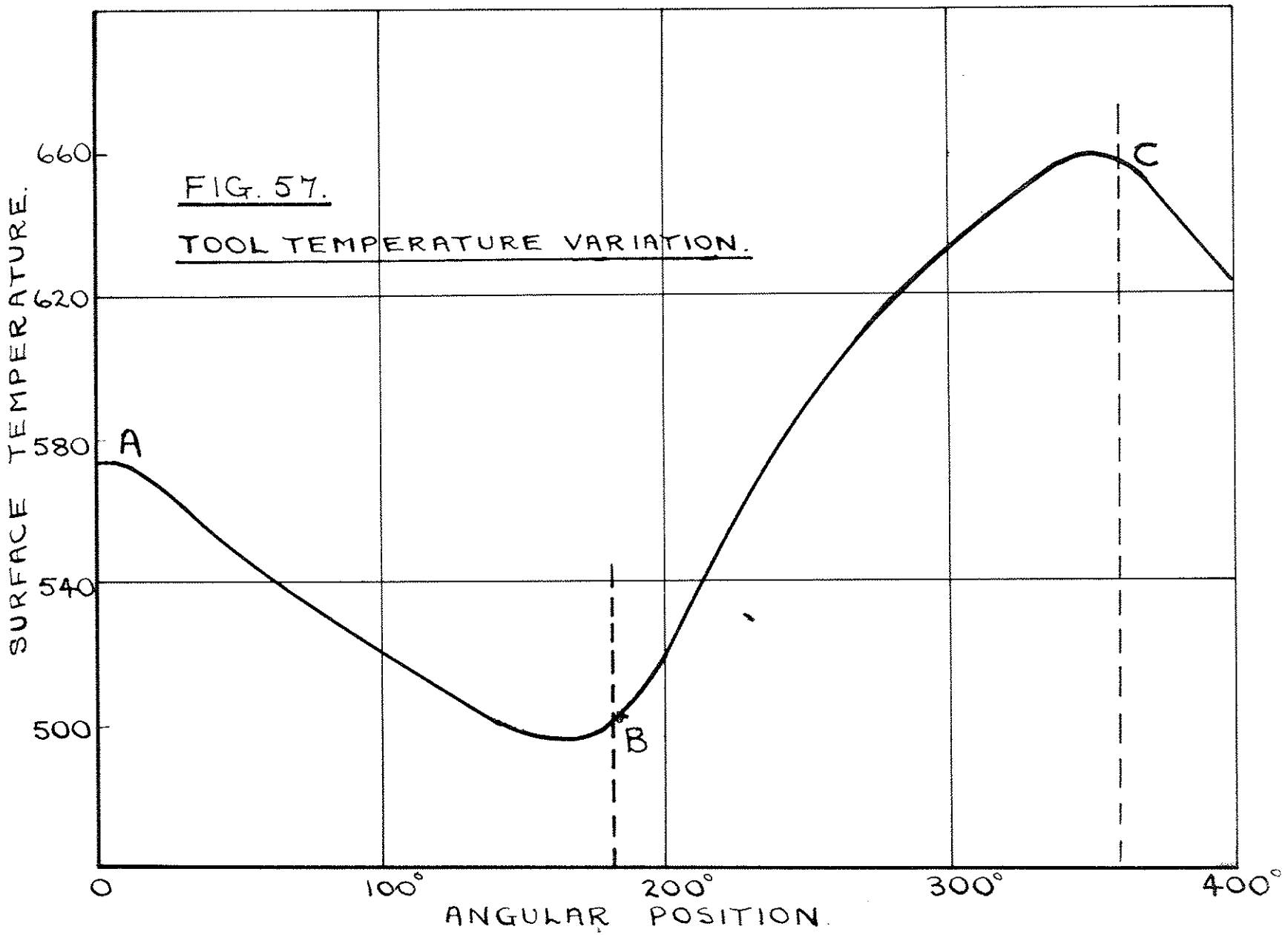
FIG. 57.
TOOL TEMPERATURE VARIATION.
SURFACE TEMPERATURE.
660
620
580
540
500
A
B
C
0
100°
200°
300°
400°
ANGULAR POSITION.

lead by over 90° so that the observed horizontal force will lead the chip thickness.

References.

1. R.N. Arnold. The Mechanisms of Tool Vibration in the Cutting of Steel. Proceedings of the Institution of Mechanical Engineers. Vol.154, 1946. pp.261-276.

2. S.A. Tobias and W. Fishwick. The Chatter of Lathe Tools under Orthogonal Cutting Conditions. Trans. A.S.M.E. Paper 57-SA19 June, 1957.

3. J. Tlusty and M. Polacek. 1957 - Beispiele der Behandlung der selbsterregten Schwingung der Werkzeugmaschinen. 3 FoKoMa Vogel-Verlag, Wuerzburg. p. 131.

4. J. Gurney and S.A. Tobias. A Graphical Method for the Determination of the Dynamic Stability of Machine Tools. 1st M.T.D.E. September, 1960. International Journal for Machine Tool Design and Research, Jan., 1961.

5. S. Doi and S. Kato. Chatter Vibrations of Lathe Tools. June 1955. Paper 55-SA22. Trans. A.S.M.E. Vol.78, 1956, p.1127.

6. N.I. Tashlickii. Initial source of the Excitation Energy of Self-Induced Vibration in Cutting. Vestnik Maschinostroenija 2/1960.

7. W.N. Holken. Untersuchungen von Ratternschuringungen an Drehbanken. Diss T.A. Aachen, 1957.

8. S.A. Tobias. The Vibrations of Vertical Milling Machines Under Test and Working Conditions. Proc.Inst.Mech. Vol.173, No.18, 1959, p.174.

9. M.E. Merchant. Basic Mechanics of the Metal Cutting Process. Trans. A.S.M.E. Applied Mech. Div. A-168 1944.

10. W.B. Palmer and P.L.B. Oxley. The Mechanics of Orthogonal Machining. Proceedings of the Institution of Mech.Engineers. Vol. 173, p.623.

11. W.B. Heginbotham and S.L. Gogia. Metal Cutting and the Built Up Nose. Proceedings of the Institution of Mechanical Engineers. Published 18th April 1961.

12. E.R.G. Eckert. Introduction to the Transfer of Heat and Mass. McGraw-Hill p.43.

13. E.R.G. Eckert. Introduction to the Transfer of Heat and Mass McGraw-Hill p.51.

14. Milton C. Shaw. Metal Cutting Principles. M.I.T. 3rd Edition.

Further Bibliography.

Chatter.

J.P. Gurney and S.A. Tobias. A Graphical Analysis of Regenerative Machine Tool Instability. Trans. A.S.M.E., Series B, Feb. 1962. p.103.

S.A. Tobias and W. Fishwick. The Vibrations of Radial Drilling Machines under Test and Working Conditions. Proceedings I. Mech.E., Vol. 170., 1956, p.232.

W. Fishwick and S.A. Tobias. Machine Tool Chatter, Effect of Flexibility in Machine and Foundation. Engineering, Vol. 185, 1958, p.568.

J. Tlusty. Die Berechnung des Rahmens der Werkzeugmaschine. 1955., Schwerindustrie der T schechoslowakei, No.1, p.8.

R.S. Hahn. On the Theory of Regenerative Chatter in Precision Grinding Operation. 1954 Trans. A.S.M.E., Vol.76, p.593.

R.S. Hahn. Metal Cutting Chatter and Its Elimination. 1953, Trans. A.S.M.E., Vol.75, p.1073.

R.S. Hahn. Vibrations of Flexible Precision Grinding Spindles. 1959, Trans. A.S.M.E. Series B., Vol.81, No.3., p.201.

F. Eisele and M. Sadowy. Rattern und Dynamische Steifigkeit von Werkzeugmaschinen. 1955. 2 - FoKoMa - Paper p.151. Vogel-Verlag, Weurzburg.

H. Lysen. Statische und Dynamische Stabiliteat der Werkstoff Formung. 1955, 2-FoKoMa. p.175. Vogel-Verlag, Weurzburg.

N.H. Cook. Self-Excited Vibrations in Metal Cutting. Trans. A.S.M.E. Series B., Vol.81, No.2. p.183.

General Metal Cutting.

E.G. Leowen and M.C. Shaw. On the Analysis of Cutting Tool Temperatures. Trans. A.S.M.E. Vol.76, 1954, p.217.

D.R. Olberts. A Study of the Effects of Tool Flank Wear on Tool Chip Interface Temperature. Trans. A.S.M.E. 1959, Series B. Vol.81, No.2., p.183.

P. Albrecht. An Explanation of the Formation of Groove Wear on Cutting Tools. 1956., Microteonic, Vol.10, No.3., p.144.

G.S. Reichenbach. Experimental Measurement of Metal Cutting Temperature Distributions. 1958., Trans. A.S.M.E. Vol.80,p.525.

M. Kronenberg. Analysis of Initial Contact of Milling Cutter and Work in Relation to Tool Life. 1946, Trans. A.S.M.E. Vol.68, p.217.

D. Kececioglu and A.S. Sorensen. Comparative Effect of Land and Crater Wear on Tool Life When Dry Cutting, Mist Cooling and Flood Cooling. Trans. A.S.M.E. Series B, Feb. 1962., p.49.

Life Tests of Carbide Tools. A.S.A. Standard No.B5.34-1956. Published by A.S.M.E. 1956.

S. Kobayashi and E.G. Thomsen. The Role of Friction in Metal Cutting. Trans. A.S.M.E. Series B, Vol.82, 1960. p.324.

A.G. MacDonald, S. Kobayashi and E.G. Thomsen. An Application of Plastic Flow Analysis to Orthogonal Metal Cutting. University of California. I.E.R. Report No.117, Issue No.4 May 1960.

S. Kobayashi and E.G. Thomsen. Some Observations on the Shearing Process in Metal Cutting. Trans.A.S.M.E. Series B, Vol.81, 1959, p.251.

M.C. Shaw, N.H. Cook and I. Finnie. The Shear-Angle Relationship in Metal Cutting. Trans. A.S.M.E. Vol.75, 1953, p.273.

M.E. Merchant. Mechanics of the Metal Cutting Process. 1945. Journal Appl. Physics, Vol.16, pp.267, 318.

R.S. Hahn. Some Observations on Chip Curl in the Metal Cutting Process under Orthogonal Cutting Conditions. 1953, Trans. A.S.M.E., Vol. 75, p.581.

Int. J. Mach. Tool Des. Res. Vol. 1, pp. 283–292. Pergamon Press 1961. Printed in Great Britian

THE DYNAMIC CUTTING OF METALS

J. D. SMITH* and S. A. TOBIAS†

INTRODUCTION

IT HAS been observed by S. Doi and S. Kato [1] that when oscillating a lathe tool normal to the cut surface, the normal thrust component variation lags the chip thickness variation (tool displacement). This observation, which was confirmed subsequently by W. Hölken [2] and N. I. Tashlickii [3], is of great importance from the point of view of machine tool chatter analysis since it means that the cutting process by itself is unstable.

There is a considerable amount of experimental evidence which leads to the contradictory conclusion that under the conditions described the cutting thrust should lead the tool displacement. This evidence originates from investigations concerned with regenerative machine tool chatter. These showed (for instance S. A. Tobias [5]) that chatter arises only in a limited number of speed bands and that very low speeds are stable. The explanation of this fact is that the cutting thrust acting on an oscillating tool is dependent not only on the chip thickness but also on the feed velocity. It is easily shown that the postulation of such a dependence is equivalent to the postulation of an inherent phase lag effect, and it is to be expected that the indirect evidence from the field of chatter analysis should confirm Doi and Kato's observation. However, this is not so, since the stability of low machining speeds leads to the conclusion that the cutting force must lead the chip thickness variation.

The present paper summarizes experimental work done by previous investigators and work in progress which aims to resolve the above-mentioned contradiction.

PREVIOUS EXPERIMENTAL RESULTS

The apparatus used by Doi and Kato [1] is shown in Fig. 1. The workpiece is attached to a long flexible shaft held in a chuck and supported at the free end by a steady which

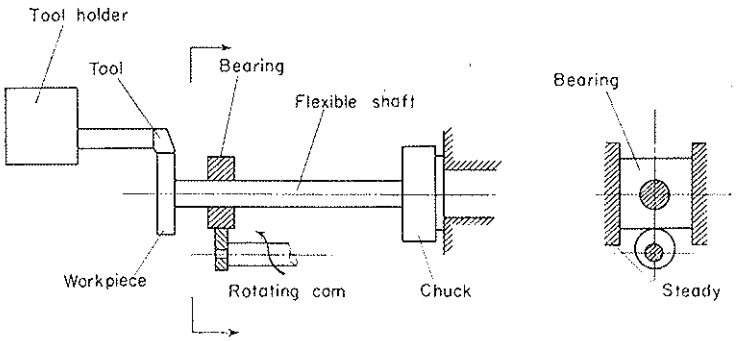

FIG. 1. Sketch of apparatus used by Doi and Kato [1].

* Staveley Research Department, Clapham, Bedford; formerly Department of Mechanical Engineering, University of Birmingham.
† Professor of Mechanical Engineering and Head of Department, University of Birmingham.

prevents vertical motion of the workpiece but allows a rotating cam to oscillate the workpiece horizontally. The fixed cutting tool then cuts a chip with an approximately sinusoidal thickness variation. The surface cutting speed for these tests was 3·4 ft/min. The cam oscillated the workpiece and hence varied the chip thickness at 1·5 c/s. The small elastic deflections of the tool were measured optically to give the normal and tangential cutting forces.

Results obtained from this rig are given in Fig. 2, which shows a record of the chip thickness variations, the normal cutting force and tangential cutting force variations while oscillating the workpiece. The figure indicates that the maximum values of the forces at point D and D′ do not occur at the same time as the maximum value of chip thickness at point A. The time interval between A and D or D′ is referred to as the inherent time lag of the normal or tangential cutting force respectively.

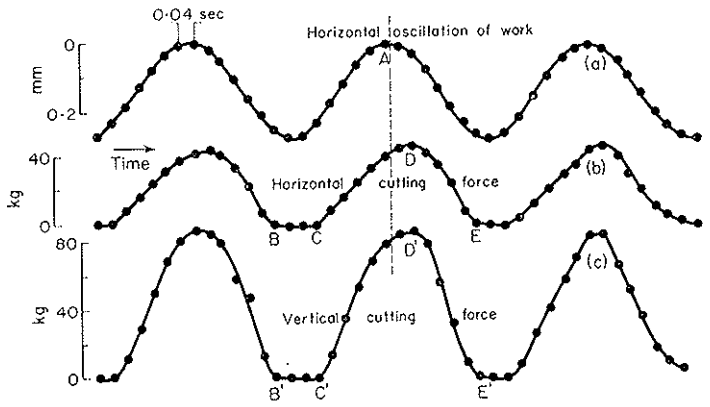

FIG. 2. Horizontal oscillations of workpiece and resulting variation of horizontal and vertical cutting forces, after Doi and Kato [1].

The derived values for this inherent time lag are given in Figs. 3(a) and (b), plotted as functions of the cutting angle and the chip thickness. The observed time lag increases with chip thickness and cutting angle.

Similar Russian work by N. I. Tashlickii [3] was carried out at higher cutting speeds but low frequencies using a rigidly mounted tool and an eccentrically mounted workpiece. Results obtained from this rig are shown in Fig. 4 which is again a plot of the cutting forces and chip thickness during vibration.

A typical result obtained by W. Hölken [2] is shown in Fig. 5. The figure represents the variation of chip thickness, normal force and tangential force as a function of time. These results, like those of Tashlickii, confirm Doi and Kato's observations of a time lag of force relative to chip thickness.

In their work on regenerative chatter S. A. Tobias and W. Fishwick [4] treat phase effects in a completely different manner. Their theory is based on the assumption that the cutting force is a function of feed velocity as well as of chip thickness, and it is easily shown that this is mathematically equivalent to postulating a lag or lead of force relative to displacement.

Evidence concerning the sign of the phase angle between chip thickness and thrust variations is derived from the form of stability charts, describing the stability of, say, a

face milling process (Tobias [5]). A chart of this type shows those speed ranges at which a certain depth of cut (or chip width) is stable or unstable. It can be obtained experimentally or theoretically and its form for drilling and face milling is well established. The stability chart is divided into two regions by the stability band envelope. For values of chip width less than the value given by this envelope the cutting process is unconditionally stable. In the region above the envelope the cutting process may be stable or unstable, depending on the rotational speed of the tool.

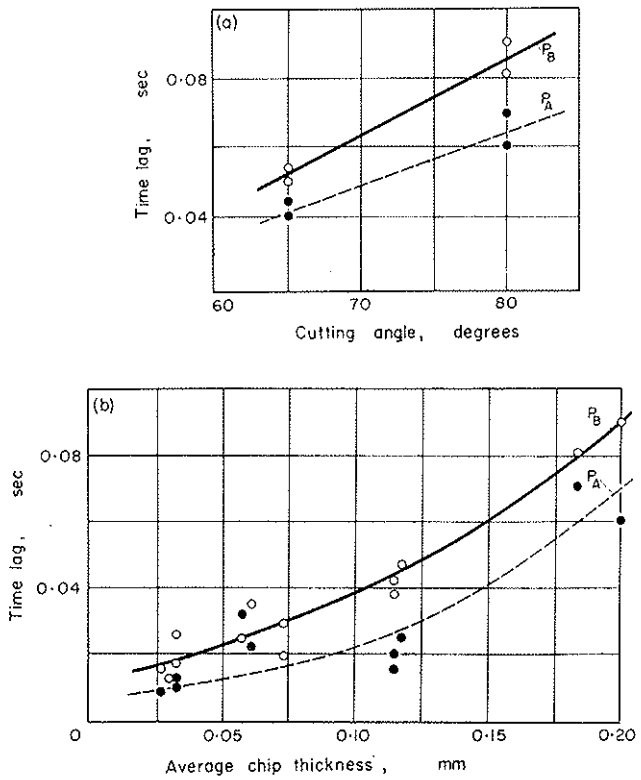

FIG. 3. Lag of cutting forces behind the workpiece displacement.
P_A normal thrust, P_B tangential thrust. (a) Lag of thrust components as a function of average chip thickness, (b) lag of thrust components as a function of cutting angle, after Doi and Kato [1].

It can be shown that the shape of the stability envelope is an indication of the phase relationship between cutting force and chip thickness variation. When the cutting force lags the displacement (in accordance with Doi and Kato's observation) then the shape of the envelope is of the form indicated by curve A in Fig. 6. A leading cutting force results in an envelope of the type of curve C, curve B being the transitional case when force and displacement are in phase.

An experimentally determined stability chart is shown in Fig. 7. In that figure unstable combinations of the depth of cut and the rotational speed are marked by circles, dots or half-filled circles. Comparing this figure with Fig. 6, it is clear that the form of the stability

envelope leads to the conclusion that the cutting force must have been leading the dynamic displacement.

Since general conclusions derived from face milling or drilling tests do not necessarily apply also to observations made when turning, Doi and Kato's experiment was repeated with a specially designed test rig.

EXPERIMENTAL APPARATUS

Although lathe turning was being investigated, it was found more convenient to carry out the experiment by mounting the specimens on the arbor of a rigid horizontal milling machine and the cutting tool with its associated suspension, damping, measuring and

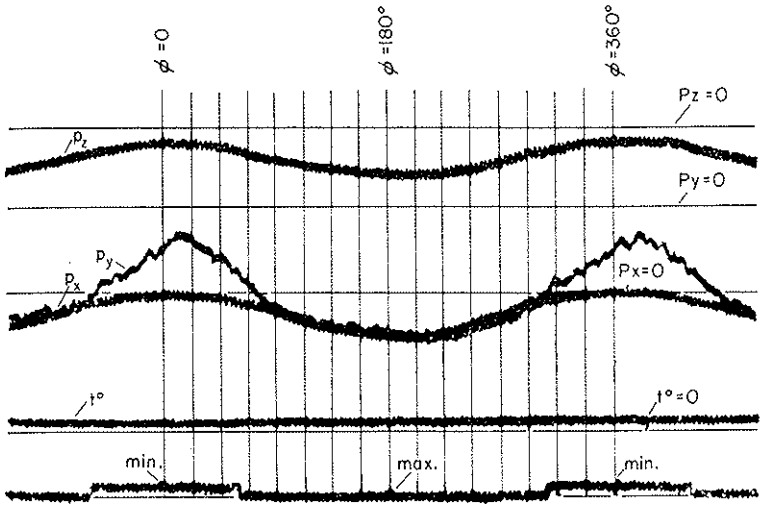

FIG. 4. Lag of cutting forces behind the chip thickness variation.

Experiments were carried out with an eccentrically mounted workpiece, the position for the minimum and maximum chip thickness values removed by the tool being shown on the bottom trace. The variation of the tangential thrust P_z, the normal thrust P_y and the feed thrust P_x during one workpiece revolution is shown, while the chip thickness varies from a minimum value, through a maximum to the next minimum. Lag of cutting forces can be seen by considering their variation in relation to $\varphi = 0°$ and $\varphi = 360°$ which fixes the position of minimum chip thickness. Tool-chip interface temperature t° was not affected by the process. After Tashlickii [3].

excitation systems on the miller table. A sketch of the apparatus is shown in Fig. 8.

The cutting tool is held on the dynamometer by straps, which for clarity are not shown in the sketch. The dynamometer is supported by vertical leaf springs which allow it to move horizontally but not vertically. This horizontal movement of the dynamometer and tool will give a chip thickness variation but will not allow any vertical movement which would alter the surface cutting speed. The movement of the dynamometer relative to the miller bed is measured by fitting strain gauges on the supporting vertical leaf springs.

Under these conditions, since the mechanical damping was low, violent chatter occurred at nearly all cutting conditions. It was found in practice impossible to use any passive damping system such as a dashpot, rotary silicone damper or eddy current method, since the combination of high frequency, low amplitude and large forces made any passive system inoperative. An active system was finally adopted, using a standard velocity pick up, the

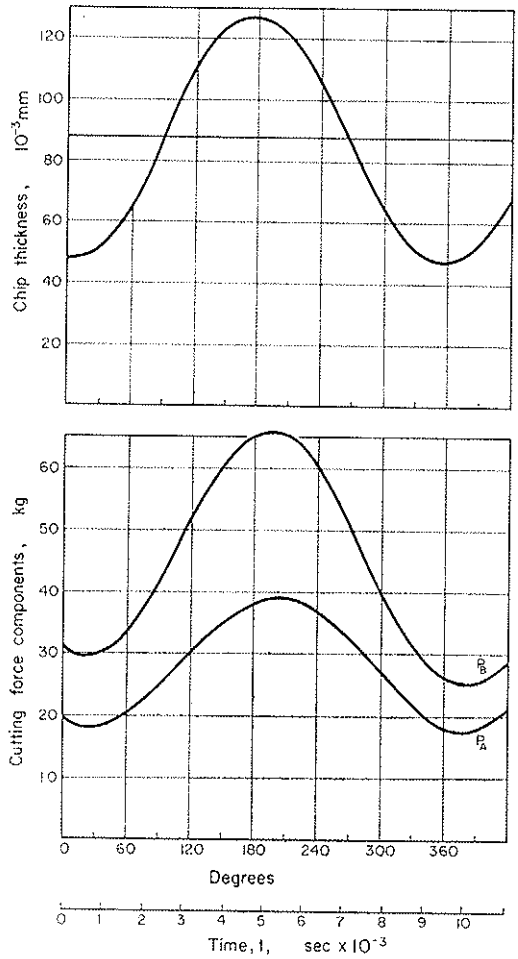

FIG. 5. Lag of cutting forces according to Hölken [2].

Top figure shows the variation of chip thickness around average value. Lower figure presents resulting variation of cutting forces. P_A normal thrust, P_B tangential thrust.

signal of which was amplified and fed into electromagnetic vibrators arranged to oppose the motion. This system is, of course, a servo power loop in which care must be taken to prevent instability. An additional signal from a separate oscillator is fed in to force the test vibration required. This composite system in which the vibration generators both damp out chatter and force the required oscillations requires far less power than two separate systems. The circuits are arranged so that any level of damping can be switched in or out

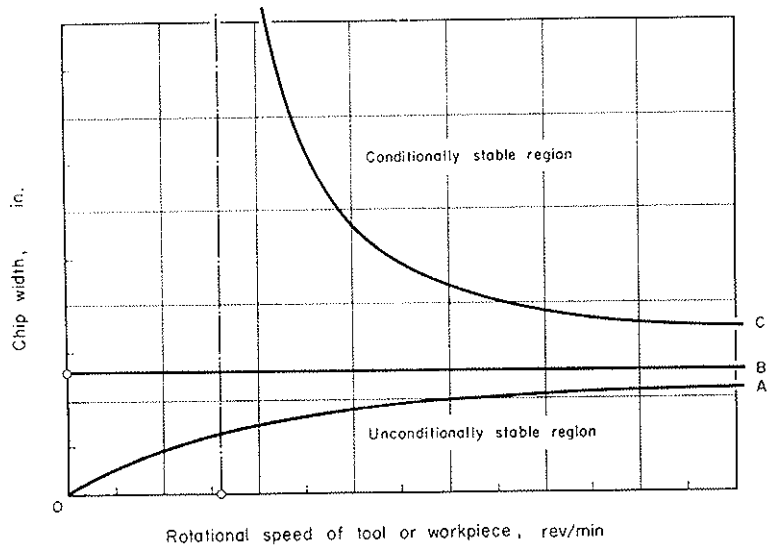

FIG. 6. The stability band envelope divides the stability chart into the regions of conditional and unconditional stability.

The conditionally stable region contains one or more unstable speed bands, separated by stable speeds. Curve A: corresponds to conditions when cutting force variation lags chip thickness variation, Curve B: cutting force variation in phase with chip thickness variation, Curve C: cutting force variation leads chip thickness variation.

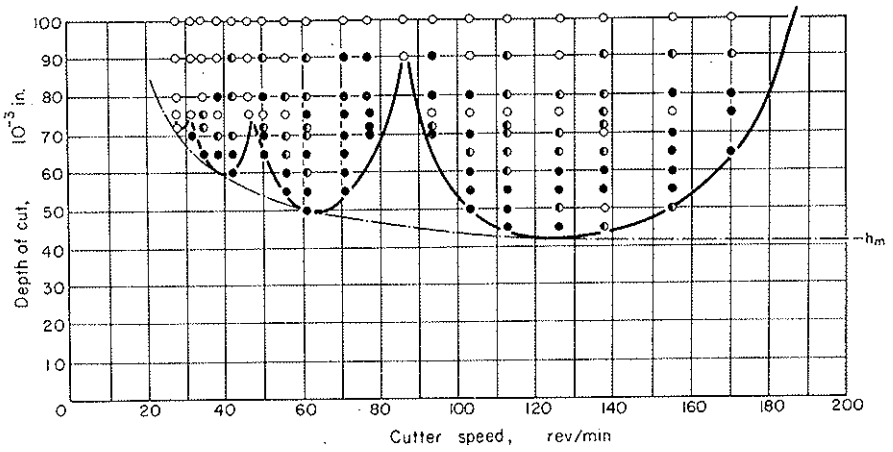

FIG. 7. Experimentally determined stability chart.

Points marked with dots, circles and half-filled circles represent cutting conditions in which chatter arose. Unstable speeds fall into bands lying above the stability band envelope h_m. Shape of stability band envelope corresponds to a cutting force variation leading the chip thickness variation. After Tobias [5].

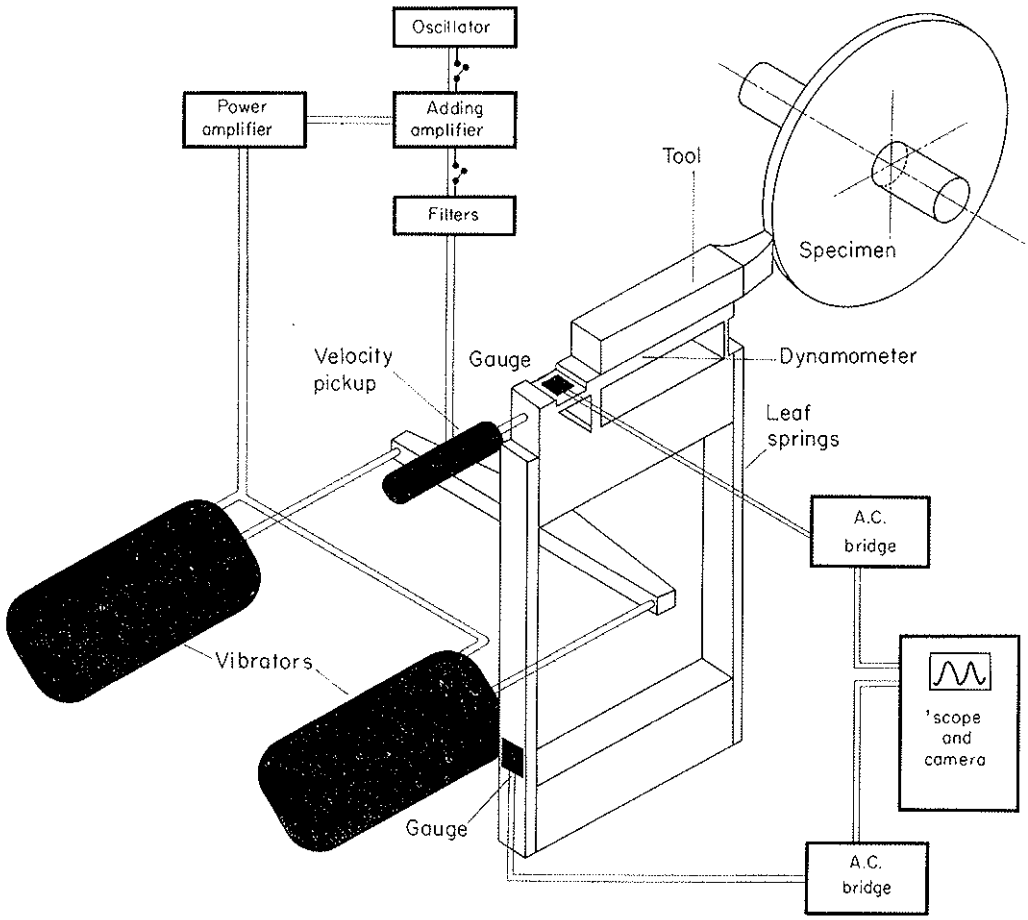

FIG. 8. Sketch of experimental rig.

instantaneously during a test run and the required oscillation can similarly be switched during a run. The normal range of frequencies used during test was from 5 c/s to 400 c/s, though this range could be extended. The amplitude of vibration possible over most of this range was greater than 0·010 in. peak to peak.

For the majority of the tests a lightweight strut dynamometer was used for force measurement. The cutting forces act on short struts which are in compression: two vertical struts take the tangential cutting force and the single horizontal strut carries the normal force. Standard wire strain gauges on the struts measure the strut strains and hence the forces. The gauge strains are measured by a sensitive a.c. strain gauge bridge. The dynamometer allows measurement of a force of less than 1 lb though the capacity of the dynamometer is nearly a ton. The combination of very short struts of high stiffness and a tool and support of low mass gives the system a natural frequency of above 6000 c/s.

Normal phasemeters are unsuitable for cutting force and displacement measurements since they are affected by noise or amplitude variations and require considerable time to reach the correct reading: an accuracy of $\pm 1°$ at small phase angles is difficult to obtain with such phasemeters. To overcome this problem the force and displacement signals are fed to matched amplifiers driving an oscilloscope and the oscilloscope traces are filmed. Phase and amplitude are measured from these records by the method shown in Fig. 9 or by filming the traces as Lissajous ellipses as shown in Fig. 10.

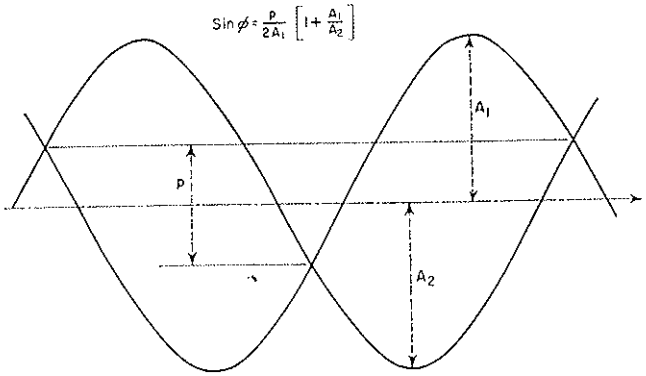

FIG. 9. Method used for the determination of small phase angles.

Oscilloscope traces of force and displacement variation, having amplitudes of A_1 and A_2 respectively. Traces are approximately 180° apart. Phase angle φ is found by the formula given in the figure.

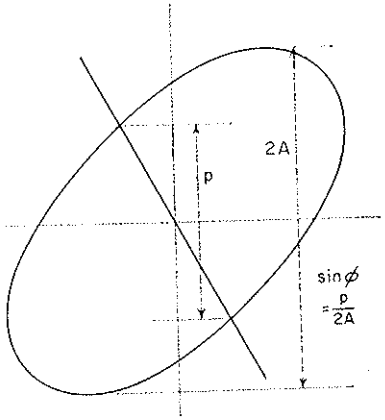

Fig. 10. Method used for the determination of phase angles.

Force is displayed horizontally and displacement of tool (i.e. chip thickness variation) vertically. The straight line is the trace obtained when not cutting, i.e., it gives the dynamometer head inertia force and is the "zero" for the cutting force. Phase angle φ is found by the formula stated in the figure.

EXPERIMENTAL RESULTS

Some of the experimental results are shown in Fig. 11. The phase angle between the chip thickness variation (radial oscillation of the tool) and the corresponding force variation is plotted as a function of frequency while the chip size and cutting speed are constant. At low frequencies the results confirm those of Doi and Kato as the cutting forces lag behind the chip thickness. However, as the frequency of oscillation of the tool rises, the lag of the cutting force with respect to the chip thickness decreases to zero, changes sign and becomes a phase lead. Above 40 c/s, i.e. in the frequency range which is of importance for chatter of most machine tools, the observed lead of the cutting force confirms the evidence deduced from regenerative chatter analysis.

In this chatter frequency range it was also observed that the phase lead of the cutting force decreases with increase of surface cutting speed. This result is also to be expected from regenerative chatter evidence.

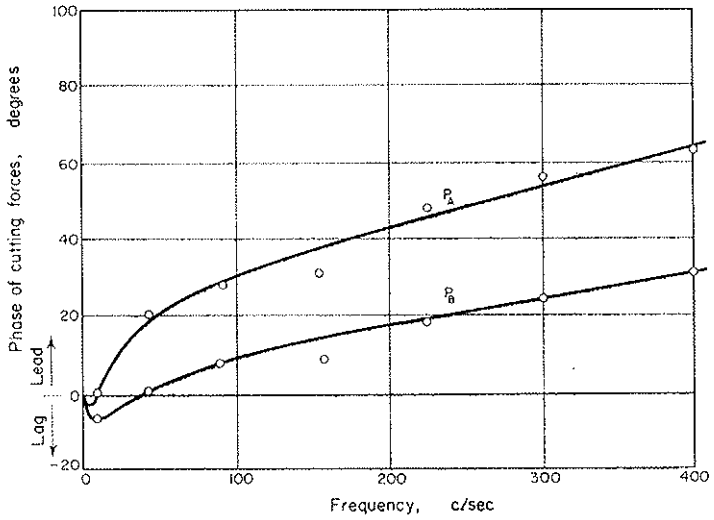

FIG. 11. Typical experimental results concerning phase relation between normal thrust P_A and tangential thrust P_B and the chip thickness variation, as a function of the frequency of oscillation. Material: mild steel, cutting speed: 400 ft/min, average chip thickness: s = 0·005 in., chip width: b = 0·075 in., amplitude of chip thickness variation: ds = 0·002 in., tool: carbide, top rake angle: 10°.

CONCLUSIONS

The preliminary results of an investigation in the dynamic cutting of metals have been summarized in this paper. The measurements so far carried out show that the use in any chatter investigation of the assumption that force is simply proportional to chip thickness will give very inaccurate results, since the effect of the observed phase changes can dominate chatter behaviour. For normal chatter frequencies the phase changes are such as to increase the damping and hence the stability of the system. This, of course, may very greatly increase the cutting capacity of a machine. The phase lags observed at very low frequencies will decrease the stability of a machine at these frequencies.

Explanation of the observed phase changes is not possible by any one simple hypothesis.

Several explanations are being considered, but none of these is satisfactory. It appears that an exact explanation will involve at least five different effects.

REFERENCES

[1] S. DOI and S. KATO, *Trans. Amer. Soc. Mech. Engrs.* **78,** 1127 (1956).
[2] W. H. HÖLKEN, *Untersuchungen von Ratterschwingungen an Drehbänken.* Diss. T. H., Aachen (1957).
[3] N. I. TASHLICKII, *Vestnik mashinostroenija*, No. 2 (1960).
[4] S. A. TOBIAS and W. FISHWICK, *Trans. Amer. Soc. Mech. Engrs.* **80,** 1079 (1958).
[5] S. A. TOBIAS, *Proc. Instn. Mech. Engrs, Lond.* **173,** 474 (1959).